

Editor-in-Chief B.E.Paton

Editorial board:

Yu.S.Borisov	V.F.Khorunov
A.Ya.Ishchenko	I.V.Krivtsun
B.V.Khitrovskaya	L.M.Lobanov
V.I.Kirian	A.A.Mazur
S.I.Kuchuk-Yatsenko	
Yu.N.Lankin	I.K.Pokhodnya
V.N.Lipodaev	V.D.Poznyakov
V.I.Makhnenko	K.A.Yushchenko
O.K.Nazarenko	A.T.Zelnichenko
I.A.Ryabtsev	

International editorial council:

N.P.Alyoshin	(Russia)
U.Diltey	(Germany)
Guan Qiao	(China)
D. von Hofe	(Germany)
V.I.Lysak	(Russia)
N.I.Nikiforov	(Russia)
B.E.Paton	(Ukraine)
Ya.Pilarczyk	(Poland)
P.Seyffarth	(Germany)
G.A.Turichin	(Russia)
Zhang Yanmin	(China)
A.S.Zubchenko	(Russia)

Promotion group:

V.N.Lipodaev, V.I.Lokteva
A.T.Zelnichenko (exec. director)

Translators:

O.S.Kurochko, I.N.Kutianova,
T.K.Vasilenko, V.F. Orets
PE «Melnik A.M.»

Editor

N.A.Dmitrieva
Electron galley:
I.S.Batasheva, T.Yu.Snegiryova

Address:

E.O. Paton Electric Welding Institute,
International Association «Welding»,
11, Bozhenko str., 03680, Kyiv, Ukraine

Tel.: (38044) 287 67 57

Fax: (38044) 528 04 86

E-mail: journal@paton.kiev.ua

http://www.nas.gov.ua/pwj

State Registration Certificate
KV 4790 of 09.01.2001

Subscriptions:

\$324, 12 issues per year,
postage and packaging included.
Back issues available.

All rights reserved.

This publication and each of the articles
contained herein are protected by copyright.
Permission to reproduce material contained in
this journal must be obtained in writing from
the Publisher.

Copies of individual articles may be obtained
from the Publisher.

CONTENTS

SCIENTIFIC AND TECHNICAL

- Makhnenko V.I. and Kvasnitsky V.V.* Stress-strain state of assemblies of the cylindrical shape in diffusion bonding 2
- Nesterenko N.P., Senchenkov I.K., Chervinko O.P. and Menzheres M.G.* Simulation of temperature fields and stresses in polyethylene pipes in hot-tool welding 7
- Getskin O.B., Erofeev V.A. and Poloskov S.I.* Simulation of the process of electrode metal transfer in short-circuiting arc welding 11
- Shlepakov V.N. and Naumejko S.M.* Peculiarities of desulphurisation of weld metal in flux-cored wire welding 16
- Lazorenko Yu.P., Shapovalov E.V., Melnik E.S., Lutsenko N.F. and Dolinenko V.V.* Efficiency of method for automatic recognition of electrode imprints in spot welding of three-layer honeycomb structures 19

INDUSTRIAL

- Sidlin Z.A.* Current status of welding consumables production in Russia 23
- Barvinko A.Yu., Barvinko Yu.P. and Golinko V.M.* To the 60th anniversary of industrial application of the technology of manufacturing cylindrical tanks from coiled blanks 26
- Skulsky V.Yu. and Gavrik A.R.* Effect of carbon on phase composition of weld metal of welded joints in martensitic steel with 9 % Cr 28
- Khaskin V.Yu.* Application of laser-arc cladding for filling up narrow cavities in aluminium alloy items 31

BRIEF INFORMATION

- Makarenko N.A., Chigarev V.V., Granovsky N.A., Bogutsky A.A. and Kushchy A.M.* Device for igniting arc of double-anode plasmatron 35
- Tsykulenko K.A.* On the role of contact resistances in electroslag cladding process 37
- News 40

NEWS

- International Conference «Welding and Related Technologies into the Third Millennium» 42
- International Forum on Nanotechnologies 44
- Developed at PWI 15, 34, 41, 43, 45



STRESS-STRAIN STATE OF ASSEMBLIES OF THE CYLINDRICAL SHAPE IN DIFFUSION BONDING

V.I. MAKHNENKO¹ and V.V. KVASNITSKY²

¹E.O. Paton Electric Welding Institute, NASU, Kiev, Ukraine

²National Technical University of Ukraine «Kiev Polytechnic Institute», Kiev, Ukraine

The stress-strain state of assemblies of the sleeve-flange type, made from dissimilar materials by diffusion bonding, and regularities in formation of this state were studied by finite element computer modelling, allowing for the effect of plastic strains.

Keywords: diffusion bonding, sleeve-flange assembly, dissimilar materials, stress-strain state, computer modelling, plastic strains

Components of a cylindrical shape, made from dissimilar materials by diffusion bonding, are often used in machine building. Study [1] considers the stress-strain state (SSS) of assemblies of the cylinder-cylinder and sleeve-sleeve types in diffusion bonding. It is shown that under force and thermal loading the level of stresses within the bond zone dramatically changes even when the parts bonded have the same diameters. Bonding the sleeve-flange type cylindrical parts of different diameters leads to formation of a stress raiser in the sleeve-to-flange transition zone, which may have a substantial effect on SSS of the bond and its formation.

The purpose of this study was to investigate SSS of the sleeve-flange assemblies within the bond zone in diffusion bonding.

Modelling of SSS was carried out allowing for the effect of plastic strains. It is reported [2] that plastic strains can be subdivided into time-independent strains (instantaneous plasticity) and time-dependent ones (creep). The present study investigates instantane-

ous plasticity strains. Modelling of SSS within the elasticity theory frames is considered in study [3].

Investigations were conducted by the computer modelling method using software package ANSYS. Mises condition $\sigma_{eq} = \sigma_y$, where σ_{eq} are the equivalent (reduced) stresses, and σ_y is the yield stress, was taken as a criterion of formation of plastic strains. Results of the present study were compared with those obtained in study [4] dedicated to modelling of SSS in diffusion bonding of cylindrical parts containing no design stress raiser.

The investigations were carried out on the sleeve-flange bond samples and computation model (Figure 1). Variants of the combinations of materials properties are given in the Table. The strengthening modulus in plastic deformation for all materials was assumed to be equal to zero, except for model 1, where it was assumed to be equal to $1 \cdot 10^3$ MPa to provide stability of the solution.

The results of solving the plastic problems were compared with those of solving the elastic problems.

In model 1, loading was applied according to the classic scheme of diffusion bonding, i.e. uniform com-

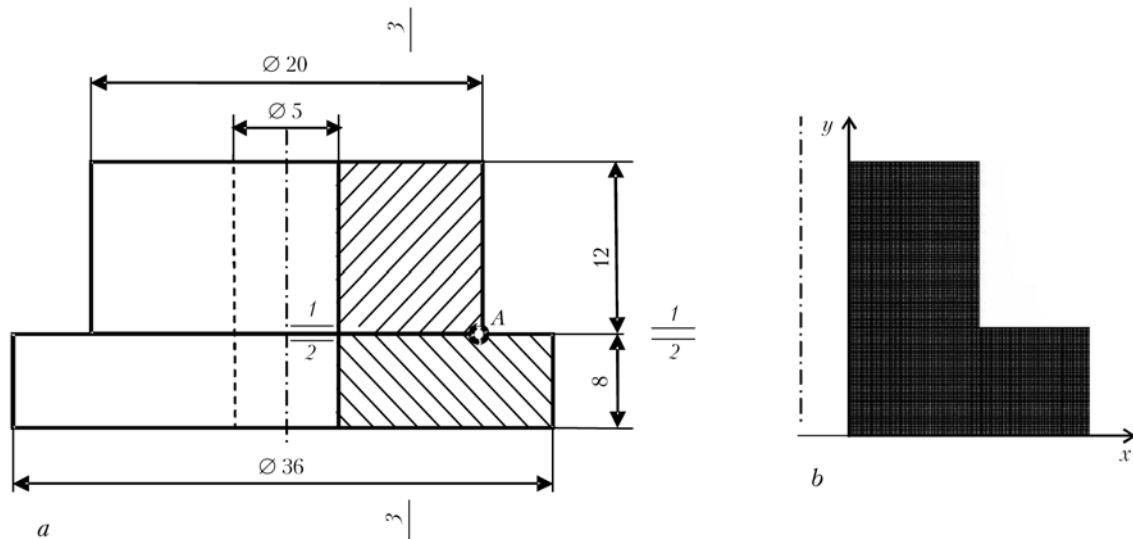


Figure 1. Schematic of the sleeve-flange assembly bond (a) and sections of finite element model (b)



Investigated variants of loading and combinations of properties of bonded materials in the assembly (computation models 1-5)

Variant No.	LTEC·10 ⁶ , 1/deg		Loading <i>p</i> , MPa	<i>T</i> , °C	σ _y , MPa	
	Sleeve	Flange			Sleeve	Flange
1 _p	10	10	40	0	39	39
1 _{p,s}	10	10	40	0	39	80
1 _{p,f}	10	10	40	0	80	39
2 _p ^h	10	20	0	+100	60	60
	20	10	0	-100		
2 _p ^c	10	20	0	-100	60	60
	20	10	0	+100		
3 _{p,s} ^h	10	20	0	+100	60	120
	20	10	0	-100		
3 _{p,s} ^c	10	20	0	-100	60	120
	20	10	0	+100		
3 _{p,f} ^h	10	20	0	+100	120	60
	20	10	0	-100		
3 _{p,f} ^c	10	20	0	-100	120	60
	20	10	0	+100		
4 _p ^h	10	20	40	+100	80	80
	20	10	40	-100		
4 _p ^c	10	20	40	-100	80	80
	20	10	40	+100		
5 _{p,s} ^h	10	20	40	+100	80	160
	20	10	40	-100		
5 _{p,s} ^c	10	20	40	-100	80	160
	20	10	40	+100		
5 _{p,f} ^h	10	20	40	+100	160	80
	20	10	40	-100		
5 _{p,f} ^c	10	20	40	-100	160	80
	20	10	40	+100		

Note. Superscripts «h» and «c» stand for heating and cooling, respectively, and subscript «p» --- stands for the plastic solution; the subscript also comprises symbols designating materials of different strength values, i.e. less strong (with lower yield stress) material of the sleeve as «s» and flange as «f»; LTEC is the linear thermal expansion coefficient.

pression with the axial force at a constant temperature. Comparison of the stress fields with corresponding fields in the elastic solution shows that with formation of plastic strains the character of the stressed state as a whole hardly changes, the level of the concentration of stresses at a sleeve-to-flange transition point on the external surface of the bonded assembly remains high (point *A* in Figure 1), but the level of stresses in this region and its size do change. Variants of the identical (low) strength of both materials, 1_p, and lower strength of the sleeve material, 1_{p,s}, have almost identical stress fields. The stressed state in a variant with lower strength of the flange material, 1_{p,f}, hardly differs from the elastic solution. Thus, plastic strains in the sleeve exert a higher effect on the assembly stress fields. This is attributable to the fact that the region

of plastic strains in the sleeve exceeds that in the flange (Figure 2).

Plastic strains in variants 1_p and 1_{p,s} are concentrated in the sleeve far from the bond and close to the stress concentration point, their values in the sleeve far from the stress concentration point growing with distance from the bond (Figure 2, *a, b*). Plastic strains in variant 1_{p,f} develop only in the flange within a very narrow zone close to the stress concentration point (Figure 2, *c*). Diagrams of plastic strains prove the absence of the latter in a larger part of the bond both on the side of the sleeve (Figure 3, *a*) and on the side of the flange (Figure 3, *b*) in all the variants of combinations of strength of the materials. Plastic strains reach their maximal value at the stress concentration point.

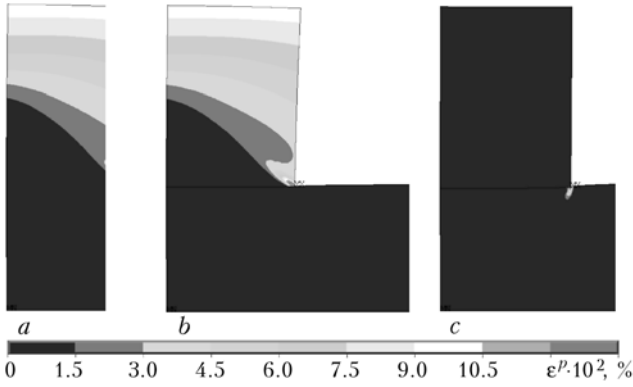


Figure 2. Fields of plastic strains ϵ^p in model 1, variants 1_p (a), $1_{p.s}$ (b) and $1_{p.f}$ (c)

Plastic strains in the upper (opposite to the bond) edge of the sleeve amount to 0.1 % in variants 1_p and $1_{p.s}$. Far from the bond, they are absent only in a variant with lower strength of the flange material.

Therefore, analysis of the results of the plastic solution shows that the variants of application of a constant compressive load do not provide development of plastic strains within the bond zone. Hence, they do not create conditions for formation of a sound bond. At the same time, in the cases where the sleeve material has lower strength than the flange material, and where the sleeve and flange materials have identical strength, the conditions are created for formation of plastic strains far from the bond, this leading to increase in total strains in the bonded assembly.

In models 2 and 3, loading was applied according to the scheme of diffusion bonding with a varied temperature and without the axial force compression after adhesion of the surfaces. Analysis of the stress and

strain fields shows that in heating and cooling the fields of equivalent stresses and plastic strains fully coincide with each other (Figure 4, a, b), and the axial stress fields differ only in signs. The character of the stressed state in formation of plastic strains hardly changes, compared with the elastic variant, the difference being seen only in the immediate proximity to the bond and in the stress concentration zone. The character of distribution of stresses along the bond both in the sleeve and in the flange with formation of plastic strains becomes more uniform, and the presence of plastic strains causes decrease in peaks of all the stresses at the stress concentration point.

All plastic strains both in heating and in cooling are concentrated within a very small region located near the bond surface. In variants 2_p^h and 2_p^c they are concentrated more on the sleeve side, in variants $3_{p.s}^h$ and $3_{p.s}^c$ --- fully on the sleeve side, and in $3_{p.f}^h$ and $3_{p.f}^c$ --- on the flange side. The zone of plastic strains on the flange side is much narrower and occupies only part of the bond close to its external surface (Figure 4). Diagrams of plastic strains show the presence of the latter in the entire bond, but they are distributed non-uniformly both along the bond and between the sleeve and flange (Figure 3, a, b).

In model 2, plastic strains reach their maximal values on the sleeve side, at the bond edge close to the stress concentration point. Here they amount to 8 %, but in the flange their value is much lower. Inside the bond, in the sleeve, they gradually decrease down to a minimal value (0.05 %) at a distance of about 1.5 mm (0.2 of the sleeve thickness) from the internal

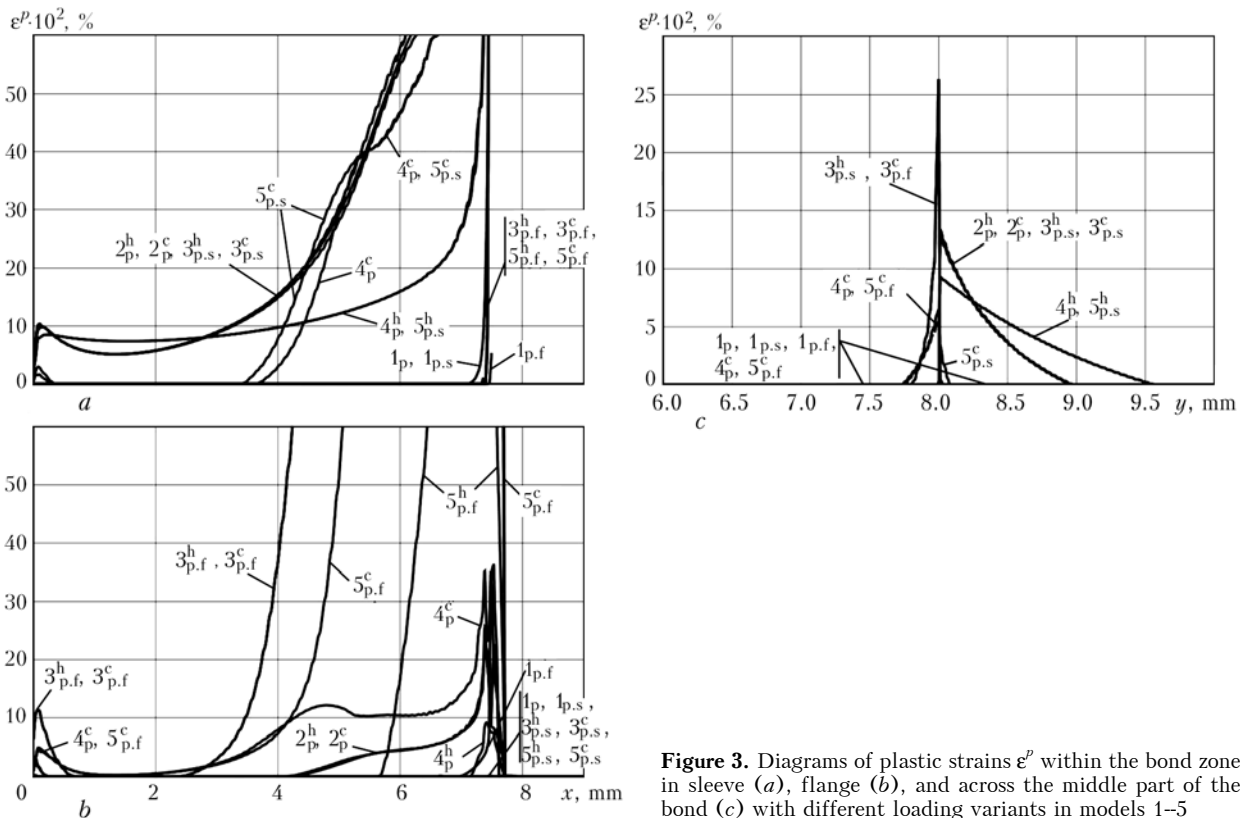


Figure 3. Diagrams of plastic strains ϵ^p within the bond zone in sleeve (a), flange (b), and across the middle part of the bond (c) with different loading variants in models 1-5

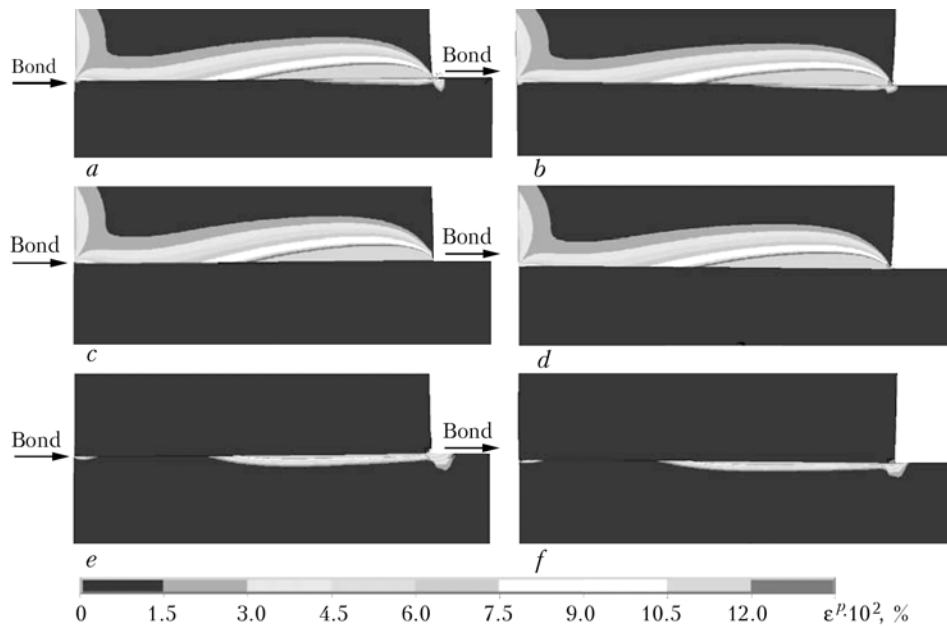


Figure 4. Fields of plastic strains within the bond zone in sections of the sleeve–flange assembly; variants 2_p^h (a), 2_p^c (b), $3_{p,s}^h$ (c), $3_{p,s}^c$ (d), $3_{p,f}^h$ (e) and $3_{p,f}^c$ (f)

surface of the sleeve. They again grow to some extent (up to 0.1 %) towards the internal surface of the sleeve. Plastic strains in the flange are concentrated mostly in the internal half of the bond. They are absent in the rest of the bond, and some low strains (0.03 %) appear only in a small region close to the internal surface of the sample.

In a major part of the bond, except for the stress concentration point, in a direction of the sample axis (across the bond), these strains in the sleeve act as shortening in heating and elongation in cooling, and visa versa in the radial and circumferential directions. Plastic strains very rapidly decrease with distance from the bond, and at a distance of about 1 mm their value becomes equal to zero (Figure 3, c).

In variants $3_{p,s}^h$ and $3_{p,s}^c$, on the sleeve side, the values of distribution of plastic strains both in heating and in cooling remain unchanged (see Figure 3, a). At lower strength of the flange material, plastic strains in the sleeve are absent along the entire bond, and appear only in a very narrow zone at the stress concentration point.

The diagrams of plastic strains on the flange side change with decrease in strength of both sleeve and flange (Figure 3, b). Plastic strains are absent in the flange with decrease in strength of only the sleeve material. In variants $3_{p,f}^h$ and $3_{p,f}^c$, these strains increase, and non-uniformity of their distribution along the bond increases as well. They reach their maximal value (over 7 %) at the stress concentration point. Plastic strains gradually decrease to zero in the internal part of the bond. As a result, they are absent in the zone where tangential stresses are close to zero (at a distance of 0.5 to 2.5 mm from the internal surface of the sleeve). Then they again grow to some extent towards the internal surface of the sleeve.

With distance from the bond, the values of plastic strains very rapidly decrease and become equal to zero at a distance of 0.2 mm from the bond (see Figure 3, c).

Therefore, analysis of the plastic solution for bonding materials with different LTEC, and either identical or different strength, proves the conclusion derived with the elastic solution that variations in temperature (in heating or cooling) create favourable conditions for localisation of plastic strains particularly within the bond zone. In this case, plastic strains have a non-uniform distribution both along the bond and between the parts bonded. The minimal value of plastic strains was fixed at a point located at a distance of 0.2 of thickness of the sleeve from its internal surface, and the maximal value --- at the external surface of the sleeve.

In models 4 and 5, loading was applied by compression with the axial force and varying the temperature. The following variants were considered: identical strength of the sleeve and flange materials (4_p^h and 4_p^c), lower strength of the sleeve material ($5_{p,s}^h$ and $5_{p,s}^c$), and lower strength of the flange material ($5_{p,f}^h$ and $5_{p,f}^c$). As shown by comparison of the results with those of the elastic solution, the character of the stressed state in formation of plastic strains changes but slightly. However, the level of stresses close to the bond and at the stress concentration point decreases.

Plastic strains are concentrated near the bond, mostly on one side of the bond, i.e. in variants 4_p^h , 4_p^c , $5_{p,s}^h$ and $5_{p,s}^c$ --- primarily in the sleeve, and in variants $5_{p,f}^h$ and $5_{p,f}^c$ --- in the flange. Their values rapidly decrease with distance from the bond (Figure 5). When heating is replaced by cooling, the

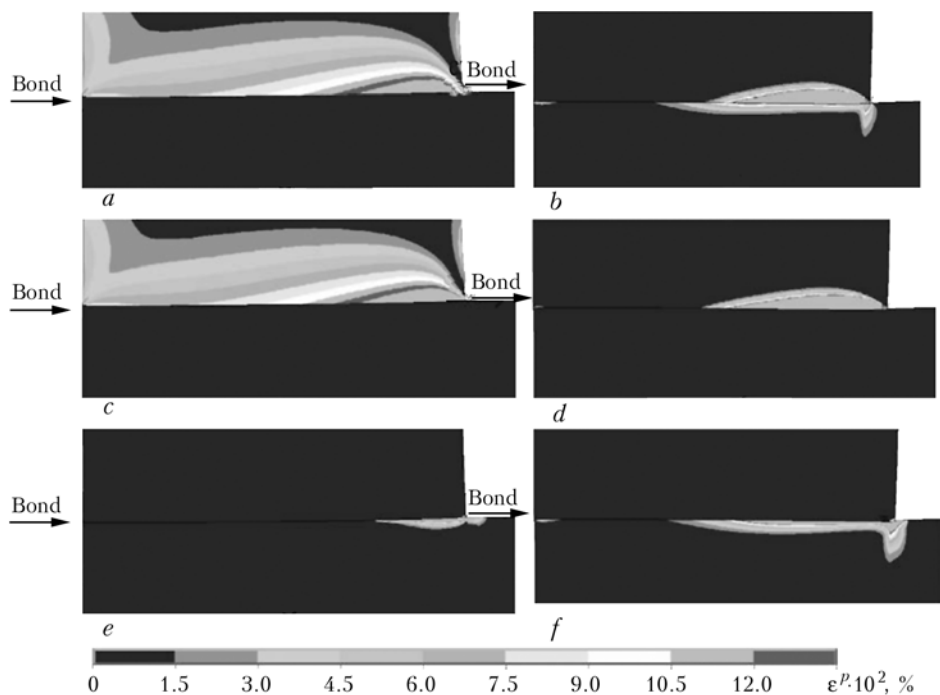


Figure 5. Fields of plastic strains within the bond zone in sections of the sleeve–flange assembly; variants 4_p^h (a), 4_p^c (b), $5_{p,s}^h$ (c), $5_{p,s}^c$ (d), $5_{p,f}^h$ (e) and $5_{p,f}^c$ (f)

region of plastic strains in the sleeve substantially decreases, and that in the flange increases.

In variants 4_p^h and $5_{p,s}^c$, the distribution of plastic strains along the bond in the sleeve is more uniform than in heating without compression (see Figure 3, a). The maximal values of plastic strains are fixed at the stress concentration point, where they amount to 4 %, whereas in the major part of the bond they are at a level of 0.07–0.20 %. The opposite situation takes place in cooling (variants 4_p^c and $5_{p,s}^h$): the uniformity decreases, and there are no plastic strains almost in half of the bond (in its internal part).

In the flange, on the contrary, plastic strains in heating are absent almost in the entire bond, except for the stress concentration point, while in cooling their values are close to zero at the point with zero tangential stresses (at a distance of 0.2 of thickness of the sleeve from its internal surface). In the rest of the bond they change from 0.05 % to several percent at the stress concentration point (see Figure 3, b).

In a variant with lower strength of the flange material, plastic strains both in heating and in cooling are absent along the entire length of the bond, except for the stress concentration point (see Figures 3, a and 5, e, f). In the flange, plastic strains appear both in heating and in cooling. However, in heating they are concentrated only in a small part of the bond adjoining the external surface (see Figures 3, b and 5, e), and in cooling they are distributed almost along the entire bond (Figures 3, b and 5, f).

Plastic strains forming within the bond zone very rapidly diminish with distance from the bond surface (see Figure 3, c).

Therefore, analysis of the derived solution shows that the combination of compression with heating and cooling in a bond of the sleeve–flange type, where the

sleeve material have lower LTEC than the flange material, also creates favourable conditions for localisation of plastic strains particularly within the bond zone. However, plastic strains in this case are distributed along the entire length of the bond only on the sleeve side (material with lower LTEC) in heating, and on the flange side (material with higher LTEC) in cooling. In the case of the reverse combination of LTEC of the sleeve and flange materials (higher LTEC in the sleeve, and lower LTEC in the flange) with respect to SSS, the heating and cooling stages change places.

The combination of compression with heating, where the sleeve material has lower LTEC and strength than the flange material, does not only create favourable conditions for localisation of plastic strains within the bond zone on the sleeve side, but also provides a more uniform distribution of plastic strains along the bond. This is also true for the case of compression with cooling, where the flange material has lower LTEC.

The combination of compression with cooling, where the sleeve material has lower LTEC and strength than the flange material, creates favourable conditions for localisation of plastic strains particularly within the bond zone on the sleeve side, but does not provide the distribution of plastic strains along the entire bond. This is also the case of compression and heating, if the flange material has lower LTEC.

The combination of compression with heating in the sleeve–flange bond, where the sleeve material has lower LTEC but higher strength than the flange material, does not provide conditions for development of plastic strains along the entire bond both on the sleeve and flange sides. The same is also true for compression and cooling, where the flange material has lower LTEC.



The combination of compression with cooling in the sleeve–flange bond, where the sleeve material is characterised by lower LTEC and higher strength than the flange material, provides conditions for localisation of plastic strains within the bond zone on the flange side, which is also the case of the combination of compression with heating, if the flange material has lower LTEC.

CONCLUSIONS

1. The regularities in the effect of the loading scheme in diffusion bonding, established earlier for assemblies of the cylinder–cylinder and sleeve–sleeve types, are also true in general for the sleeve–flange assemblies.

2. The geometry of parts within the bond zone has a substantial effect on the character of SSS. Transition from a small diameter (sleeve) to a large one (flange) dramatically shifts the zone of action of plastic strains to the sleeve.

3. For plastic strains to form in the bond on the flange side, the sleeve material should be much stronger than the flange one. When designing billets for bonding of parts of the materials that have close strength values, it is necessary to avoid, where possible, changes in diameters of the assemblies within the bond zone.

1. Makhnenko, V.I., Kvasnitsky, V.V., Ermolaev, G.V. (2008) Effect of physical-mechanical properties of the materials joined and geometry of parts on distribution of stresses during diffusion bonding in vacuum. *The Paton Welding J.*, **1**, 2–8.
2. Makhnenko, V.I. (1976) *Computational methods for investigation of the kinetics of welding stresses and strains*. Kiev: Naukova Dumka.
3. Kuznetsov, V.D., Kvasnitsky, V.V., Ermolaev, G.V. et al. (2007) General principles of formation of the stressed state in diffusion bonding of parts of the cylindrical shape. *Transact. of National Shipbuilding Univ.*, **417(6)**, 62–73.
4. Makhnenko, V.I., Kvasnitsky, V.V., Ermolaev, G.V. (2008) Stress-strain state of diffusion bonds between metals with different physical-mechanical properties. *The Paton Welding J.*, **8**, 2–6.

SIMULATION OF TEMPERATURE FIELDS AND STRESSES IN POLYETHYLENE PIPES IN HOT-TOOL WELDING

N.P. NESTERENKO¹, I.K. SENCHENKOV², O.P. CHERVINKO² and M.G. MENZHERES¹

¹E.O. Paton Electric Welding Institute, NASU, Kiev, Ukraine

²S.P. Timoshenko Institute of Mechanics, NASU, Kiev, Ukraine

The paper deals with the features of formation of thermal and mechanical fields in the joint zone in butt welding of polyethylene pipes by a hot tool inserted into the butt. It is shown that the magnitude and spatial distribution of residual stresses depend not only on the main parameters of the welding mode, but also on ambient temperature. A procedure of calculation of the temperature field in welded samples is proposed for correction of heating time.

Keywords: hot-tool welding, polyethylene pipes, thermomechanical processes, residual stresses, simulation, viscous-flow state temperature, welded joint quality

Welding is the main technological process which determines the operational reliability and speed of construction of polyethylene pipelines. Hot-tool welding is mostly used for joining pipes and parts. Activation (heating) of the surfaces being welded is performed as a result of their physical contact with the heated tool. Direct nature of heating predetermines the intermittent nature of the process, as the tool has to be removed from the welding zone and then the parts have to be pressed together in order to join the heated surfaces. In such a process three stages can be conditionally singled out: heating of the surfaces being welded, technological pause required for removal of the heated tool from the welding zone; upsetting of the parts being welded by applying pressure and their holding under pressure for a certain time determined by the cooling rate and relaxation processes in the welded joint [1].

The main parameters of the technological process are heater temperature θ_h ; time of surface melting t_m ; heating t_h ; technological pause t_{pause} and upsetting t_{up} ; pressure at melting P_m , heating P_h and upsetting

P_{up} . Additional parameters of the welding mode include ambient temperature θ_{am} , geometry of the surfaces to be welded, thermophysical properties of the material, etc.

The interrelation and values of the above parameters determine not only the possibility of producing a sound welded joint, the technological process efficiency, but also the material structure in the weld zone, which essentially influences its performance [2–4]. Here, impact bending strength, long-term strength, crack resistance, corrosion resistance, etc. are used as parameter optimization criteria, alongside the short-term strength at tension or bending of welded samples.

A large number of the noted criteria and the respective kinds of testing were the reason for development of a multitude of normals, nomograms with recommendations on optimization of the main parameters of the technological process. Here, as a rule, averaged parameter values are given without indication of the optimization function. This, probably, accounts for the fact that the developed recommendations are contradictory or cardinally different from each other.

Thermomechanical processes realized in the joint zone were studied mainly for thermal resistor welding

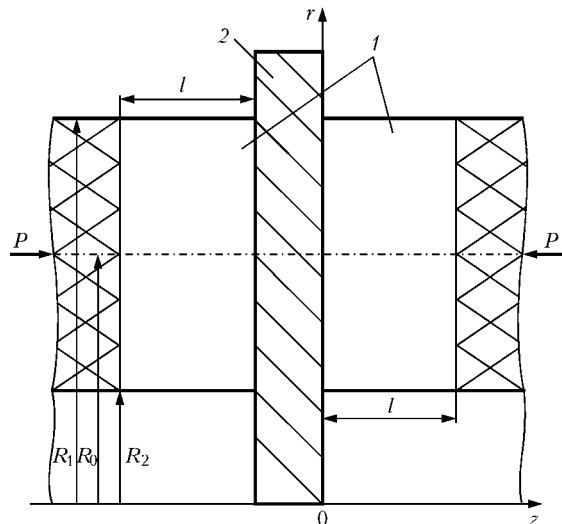


Figure 1. Calculation procedure of polyethylene pipe welding: 1 — initial billets; 2 — hot tool

[5, 6]. Available theoretical developments in the field of simulation of thermal and mechanical condition of the weld zone in hot-tool butt welding of polymers mostly are of a qualitative nature, as they do not take into account the dependence of mechanical and thermophysical characteristics of the material on temperature, as well as the rheological processes of residual stress formation in the weld.

This paper deals with mathematical simulation of temperature fields and stress-strain state of polyethylene pipes of 110 mm diameter in hot-tool butt welding, allowing for temperature dependence of material properties and process prehistory. Solving such problems allows a rational selection of the main parameters of the mode of hot-tool welding at different ambient temperatures.

In the cylindrical system of co-ordinates $0rz\varphi$ definition of the problem of axisymmetric quasistatic thermomechanical condition of polyethylene pipes in hot-tool butt welding includes the following relationships: equilibrium equation

$$\frac{\partial \sigma_{rr}}{\partial r} + \frac{1}{r} (\sigma_{rr} - \sigma_{\varphi\varphi}) + \frac{\partial \sigma_{rz}}{\partial z} = 0, \tag{1}$$

$$\frac{\partial \sigma_{rz}}{\partial r} + \frac{1}{r} \sigma_{rz} + \frac{\partial \sigma_{zz}}{\partial z} = 0;$$

equation of heat conductivity

$$c(\theta) \frac{\partial \theta}{\partial t} = \frac{1}{r} \frac{\partial}{\partial r} \left[\lambda(\theta) r \frac{\partial \theta}{\partial r} \right] + \frac{\partial}{\partial z} \left[\lambda(\theta) \frac{\partial \theta}{\partial z} \right]; \tag{2}$$

kinematic equations

$$\varepsilon_{rr} = \frac{\partial u_r}{\partial r}, \quad \varepsilon_{zz} = \frac{\partial u_z}{\partial z}, \quad \varepsilon_{\varphi\varphi} = \frac{1}{r} u_r, \tag{3}$$

$$\varepsilon_{rz} = \frac{1}{2} \left(\frac{\partial u_z}{\partial r} + \frac{\partial u_r}{\partial z} \right).$$

Governing equations are taken in Nutting's form:

$$s_{ij}(t) = \frac{E(t, \theta)}{2[1 + \nu(\theta)]} e_{ij}(t), \quad i, j, k = r, z, \varphi, \tag{4}$$

$$\sigma_{kk}(t) = \frac{E(t, \theta)}{3[1 - 2\nu(\theta)]} [\varepsilon_{kk}(t) - 3\alpha(\theta)(\theta - \theta_0)].$$

Equations (1)–(4) are complemented by the following boundary conditions:

at $r = R_1, R_2$

$$-\lambda(\theta) \frac{\partial \theta}{\partial r} = \gamma(r, z)(\theta - \theta_{am}), \quad \sigma_{rr} = 0, \quad \sigma_{rz} = 0;$$

at $z = 0$

$$u_z = 0, \quad \sigma_{rz} = 0, \quad \theta = \theta_h, \quad 0 < t < t_m + t_h,$$

$$\sigma_{zz} = 0, \quad \sigma_{rz} = 0, \quad -\lambda(\theta) \frac{\partial \theta}{\partial r} = \gamma(r, z)(\theta - \theta_{am}),$$

$$t_m + t_h < t < t_m + t_h + t_{\text{pause}},$$

$$u_z = 0, \quad \sigma_{rz} = 0, \quad \frac{\partial \theta}{\partial z} = 0, \quad t > t_m + t_h + t_{\text{pause}};$$

at $z = l$

$$-\lambda(\theta) \frac{\partial \theta}{\partial z} = \gamma(r, z)(\theta - \theta_{am}), \quad \sigma_{zz} = \sigma_{zn}(t), \quad \sigma_{rz} = 0,$$

as well as initial condition $\theta(r, z) = \theta_0$ at $t = 0$.

Here $u_i, \varepsilon_{ij}, \sigma_{ij}$ are the components of the vector of displacements, tensors of strains and stresses; s_{ij}, e_{ij} are the components of deviators of tensors of stresses and strains; $s_{ij} = \sigma_{ij} - \frac{1}{3} \sigma_{kk} \delta_{ij}$; $e_{ij} = \varepsilon_{ij} - \frac{1}{3} \varepsilon_{kk} \delta_{ij}$; δ_{ij} is the Kronecker symbol; $E(t, \theta)$ is the relaxation function at uniaxial tension; $c(\theta), \lambda(\theta)$ are the coefficients of bulk heat capacity and heat conductivity; $\alpha(\theta)$ is the coefficient of linear thermal expansion; θ_0 is the reference temperature; γ — is the coefficient of heat emission; $\sigma_{zn}(t)$ is the stress of end face pressing up of pipes, the time dependence of which is given in [2]; θ_h is the heater temperature.

Experimental concretization of the governing equations of polyethylene in terms of Nutting relaxation equation at uniaxial tension yields the following relationship:

$$\sigma = E_0(\theta) t^{m(\theta)} \varepsilon^{n(\theta)}. \tag{5}$$

For generalization of relationship (5) for the case of a multiaxial stressed state it is assumed that Poisson's coefficient ν is independent on time, but depends only on temperature ($\nu = \nu(\theta)$), i.e. bulk creep is absent. Coefficients $m(\theta)$ and $n(\theta)$ were determined by analyzing the published data [7]. Calculation procedure of the process is given in Figure 1.

Problem (1)–(4) was solved by finite difference method. Simulation was conducted for a polyethylene pipe $2R = 0.11$ m. During calculation the values of ambient temperature $\theta_{am} = \theta_0 = -15, 0, 20, 30$ °C, as well as duration of the technological pause in the working cycle $t_{\text{pause}} = 3, 5, 10$ s were varied, and heating temperature was taken to be equal to $\theta_h = 210$ °C.

Figure 2, a shows variation of temperature and stresses at $\theta_{am} = \theta_0 = -15$ °C, $t_{\text{pause}} = 5$ s in the midpoint $r = R_0 = (R_1 + R_2)/2$ at the pipe edge $z = 0$. It is seen that at the stage of $0 < t < t_1, t_1 = t_m + t_h + t_{\text{pause}}$, not only axial σ_{zz} , but also radial σ_{rr} and circumferential $\sigma_{\varphi\varphi}$

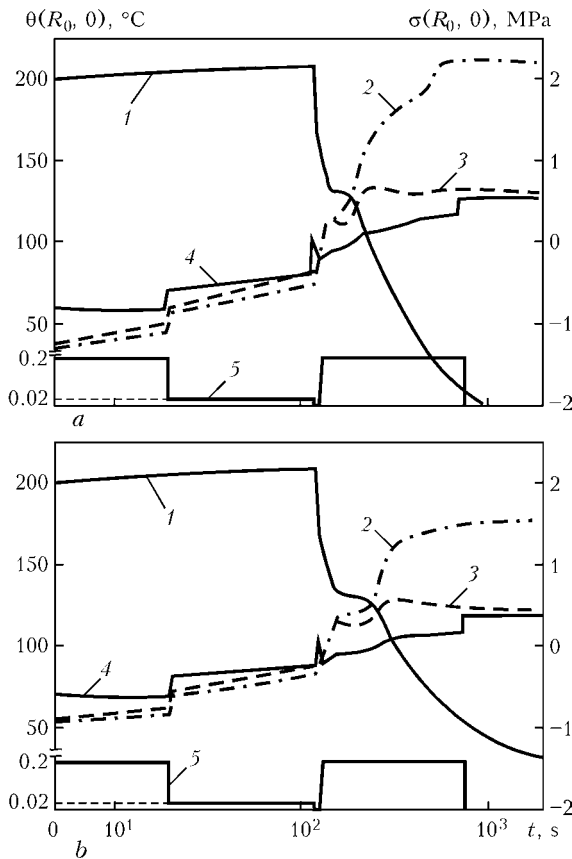


Figure 2. Dependence of temperature and stresses at $\theta_{am} = 15$ (a) and 30 (b) $^{\circ}\text{C}$; $t_{\text{pause}} = 5$ s in point $z = 0$ and $r = R_0$ for $t = 10^3$ s; 1 — θ ; 2 — $\sigma_{\phi\phi}$; 3 — σ_{rr} ; 4 — σ_{zz} ; 5 — σ_{zn}

stress components are compressive: axial component — as a result of pressing up, and the other — as a result of compression of the material expanding at heating. During cooling components σ_{rr} and $\sigma_{\phi\phi}$ start rising and at $t > t_1$ all the components become tensile, and their value exceeds 2.2 MPa, which is more than 15 % of the base material yield point. Axial stresses are practically zero. The above stresses can be conditionally regarded as residual, although they will relax very slowly. Calculations conducted under the condition $\theta_{am} = \theta_0 = 30$ $^{\circ}\text{C}$ (Figure 2, b) show that σ_{ij} does not exceed 1.5 Pa. Thus, welding of polyethylene pipes at below zero temperatures leads to higher residual stresses, which may essentially affect the welded joint performance.

Temperature and stress distributions along axial coordinate z in the median section of the pipe by thickness, $r = R_0 = 0.05$ m, for moment of time $t = 10^3$ s are shown in Figure 3. These data correspond to the following values of cycle parameters: $\theta_0 = \theta_{am} = 20$ $^{\circ}\text{C}$ (Figure 3, a), $\theta_0 = \theta_{am} = -15$ $^{\circ}\text{C}$ (Figure 3, b), $t_{\text{pause}} = 5$ s. Selected time corresponds to the start of the process of slow relaxation of stresses, which yields, essentially, an estimate of residual stresses. In this distribution axial stresses are practically absent, and radial and circumferential ones are approximately equal, being tensile on the welding surface. They become compressive at distance $z \approx 0.01$ m (Figure 3, a). At $z \geq 0.05$ m, i.e. at distance from the butt joint of $z \approx 5h$, $h = R_1 - R_2$, stresses due to welding, disappear. It is seen that in welding at below zero temperatures the tensile and compressive

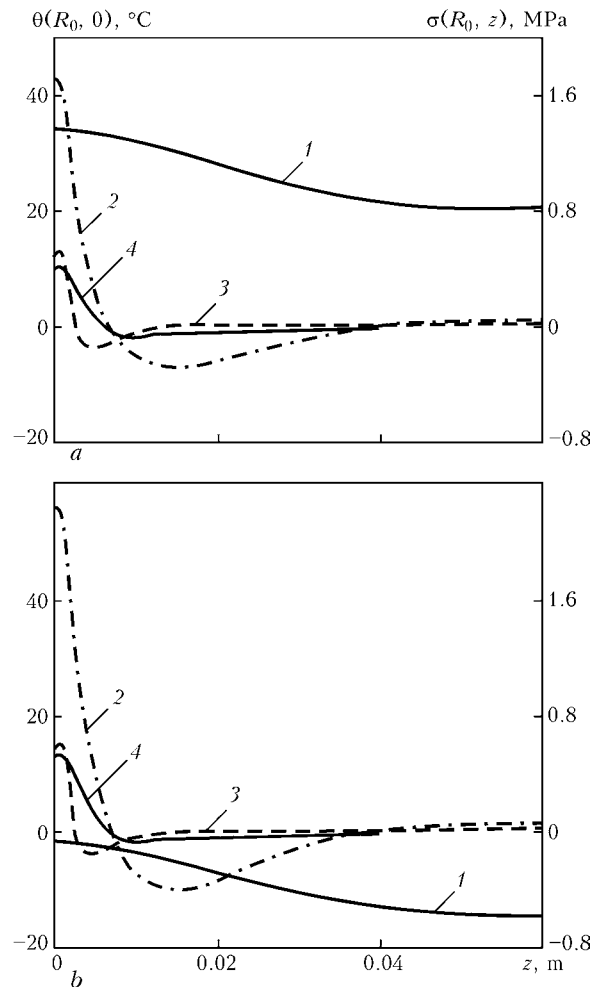


Figure 3. Distribution of residual stresses along the pipe axis at $\theta_{am} = 20$ (a) and -15 (b) $^{\circ}\text{C}$; $t_{\text{pause}} = 5$ s for $t = 10^3$ s (for designations see Figure 2)

stresses are higher by absolute values, than in welding at above zero temperatures (Figure 3, b).

As was noted above, one of the main process parameters of the mode of hot-tool butt welding is the time between the end of heating and start of upsetting of welded pipes (technological pause). In this time interval the surface-melted edges, being in contact with air, oxidize under the impact of oxygen and cool down due to convective heat exchange and heat removal inside the pipe, thus essentially affecting the welded joint quality. Melt cooling rate determines initiation and growth of crystalline formations in the weld, type of resultant supermolecular structure, and, consequently, strength properties of the welded joint. In addition, the butt cooling rate and duration of the technological pause determine the temperature and melt flow index at the moment of upset start. At a non-irrational proportion of these values realization of rheological processes in the joint zone decreases markedly and the possibility of producing a welded joint as such is eliminated. Therefore, it is of interest to consider the issues related to the influence of technological pause duration on the temperature of surfaces being welded, taking into account the external temperature factors.

Figure 4 shows the dependence of the temperature of pipe edges being welded on the duration of the

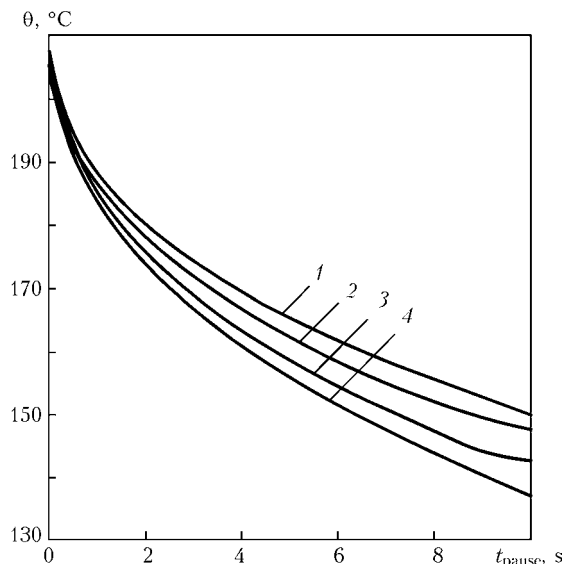


Figure 4. Dependence of pipe edge temperature on technological pause duration: 1 --- $\theta_0 = \theta_{am} = 30$; 2 --- 20; 3 --- 0; 4 --- -15 °C

technological pause for different values of ambient temperature $\theta_{am} = \theta_0 = -15, 0, 20$ and 30 °C. It is seen that intensive cooling of the edges being welded occurs at this stage of the welding process. That is, in 10 s the temperature of the pipe edge drops from 210 to 150 °C (at $\theta_{am} = 30$ °C), and in welding under the conditions of below zero temperatures ($\theta_{am} = -15$ °C) --- to 137 °C.

In keeping with the normative documents (SNiP 3.05.02-88, Russia) in welding pipes of 63-110 mm diameter ($\theta_{am} = 20$ °C) the technological pause should not exceed 5 s, thus providing favourable temperature conditions for formation of permanent joints. Therefore, as follows from Figure 4, in pipe welding at below zero temperatures it is necessary to correct the technological process parameters recommended for $\theta_{am} = 20$ °C. As the time of the technological pause is determined by the time of heater removal from the welding zone and time required for abutment of the pipe edges to be welded, it is difficult to minimize it. More efficient is increase either of the heater temperature, or the time of heating of the edges to be welded. However, as shown by plastographic investigations, increase of the heater temperature may lead to polymer thermal destruction, defect formation, and, consequently, to lowering of strength properties of welded joints. Therefore, in our opinion, it is rational to increase the time of pipe edge heating at fixed values of heater temperature and technological pause duration. The value of penetration depth should correspond to the value recommended for welding pipes at ambient temperature of 20 °C.

The graph given in Figure 5 can be used to correct the heating time in welding of polyethylene pipes under the conditions of negative temperature. It shows isolines of plastic transition temperature ($\theta_m = 120$ °C) of polyethylene at the ambient temperature $\theta_{am} = -15$ °C. As shown by calculations, at $\theta_{am} = 20$ °C, the temperature of transition into the plastic state at 0.002 m distance from the pipe edge, is achieved after 80 s, and at temperature $\theta_{am} = -15$ °C --- after 120 s (Figure 5). Therefore, to provide the specified temperature conditions in the joint zone in welding pipes at $\theta_{am} = -15$ °C, the heating time should be increased by 40 s at

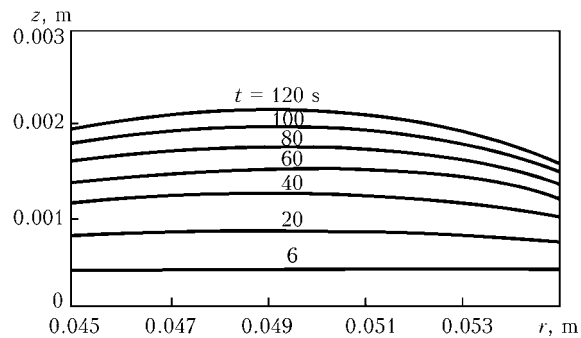


Figure 5. Kinetics of isolines of polymer plastic transition in polyethylene pipe welding ($\theta_m = 120$ °C; $\theta_{am} = \theta_0 = -15$ °C)

the minimum. The developed procedure allows plotting similar dependencies for arbitrary values of ambient temperatures.

Conducted testing of welded joints made in welding under the conditions of specified ambient temperatures (-15 -- $+30$ °C) with heating time correction by the proposed procedure, showed that plastic fracture of samples occurs outside the weld zone. Several criteria were used to assess the quality of pipe welded joints: nature of sample fracture to SNiP 3.05.02-88 and stress cracking resistance at accelerated testing of the welded joint in a surfactant solution.

Analysis of the results of simulation of temperature and mechanical fields in the joint zone in hot-tool welding of polyethylene pipes at different temperature conditions leads to the following conclusions:

- axial, radial and circumferential components of mechanical stresses are compressive at the stages of surface melting, heating and technological pause, and during cooling of the butt joint they become tensile;
- values and spatial distribution of residual stresses depend not only on the main parameters of the welding mode, but also on ambient temperature;
- in welding at below zero ambient temperatures residual stresses are higher by their absolute value than in welding at above zero temperatures and may reach 15-20 % of base metal strength;
- to ensure the specified quality of welded joints in welding at below zero ambient temperatures, it is necessary to increase the time of heating of the pipe edges being welded. To correct the heating time, it is recommended to use the developed procedure for calculation of the temperature field in the samples being welded.

1. Komarov, G.V. (2006) *Joints of polymer material parts: Manual*. St.-Petersburg: Professiya.
2. Nesterenko, N.P., Senchenkov, I.K., Chervinko, O.P. (2007) Modeling of temperature fields and stresses in hot-tool welding of plastic pipes at below zero temperatures. In: *Proc. of Sci.-Techn. Seminar on Ensuring the Service Reliability of Pipeline Transport Systems*. Kiev: PWI.
3. Starostin, N.P., Amosova, O.A. (2007) Flash-butt welding of polyethylene pipes at low ambient temperatures. *Svarochn. Proizvodstvo*, 4, 17-20.
4. Kajgorodov, G.K., Kargin, V.Yu. (2001) Influence of cooling rate of polyethylene weld on its strength. *Truboprovody i Ekologiya*, 2, 13-14.
5. Sokolov, V.A., Krasnikov, M.A. (2004) Problems of quality evaluation of polyethylene pipes using sleeves with embedded heaters. *Ibid.*, 2, 7-98.
6. Makhnenko, V.I., Velikoivanenko, E.A., Rozyuka, G.F. et al. (1991) Mathematical modeling of deformation processes in welding of polyethylene pipes. *Avtomatich. Svarka*, 4, 1-6.
7. Piven, A.A., Grechanaya, N.A., Chernobylsky, I.I. (1976) *Thermophysical properties of polymer materials*. Kiev: Vyshcha Shkola.



SIMULATION OF THE PROCESS OF ELECTRODE METAL TRANSFER IN SHORT-CIRCUITING ARC WELDING

O.B. GETSKIN¹, V.A. EROFEEV² and S.I. POLOSKOV³

¹RPC «Tekhnotron», Cheboksary, Russia

²Tula State University, Tula, Russia

³REC «Welding and Control» at N.E. Bauman MSTU, Moscow, Russia

The physical-mathematical model of drop transfer phenomena in consumable electrode welding with short-circuiting of the arc gap is considered, which allows for conditions of electrode metal transfer and interaction of the arc with electric parameters of the power source. The software realizing the numerical solution of the model equations makes it possible to study the phenomena occurring in welding and justifiably determine not only the technological parameters of the process, but also the technological requirements to design of various types of consumable-electrode arc welding equipment.

Keywords: arc welding, consumable electrode, shielding gas, drop transfer phenomena, virtual process, power source, arc, arc gap, short-circuiting, physical-mathematical model, controlled drop transfer

Making stationary butt joints involves certain objective problems of ensuring a stable transfer of electrode metal drops into the weld pool. This transfer is achieved in the most effective manner in welding with short-circuiting (SC) of the arc gap and additional impact on the drop at its transition into the pool. Different variants of such impact on electrode metal drops were developed already in 1960–1970s [1–3]. However, effective realization of the proposed welding processes with the controlled drop transfer (CDT) of electrode metal became possible only in the middle of 1990s [4, 5], owing to improvement of microprocessor devices and development of powerful transistor keys [6], allowing fast switching of current by a complex control algorithm.

Many questions of practical realization of CDT and establishing the technological requirements to welding equipment are still insufficiently studied so far. This is related to the fact that studying the fast processes in consumable-electrode arc welding by experimental methods requires considerable funds for research, and experimental result processing proper is characterized by a high labour consumption. Therefore, the most effective method of obtaining the necessary quantitative characteristics of the process with CDT is simulation of the above impacts and welding techniques. Simulation of any object (system, process, or phenomenon) is usually understood to be reproduction and study of another object, similar to the original, with subsequent transfer of the obtained results on the simulated object. Simulation should allow both for physical phenomena in welding, and for mathematical dependencies at their description.

The purpose of the work was to study control algorithms and determine the parameters of welding with CDT of electrode metal based on simulation of phenomena in the phases of SC, electrode melting and drop formation.

Work of many authors presented in review [7], led to development of an «ideal» cycle of welding with SC, in which the individual cycle phases are controlled by their own algorithm (Figure 1). The following stages of microcycle of electrode metal drop transfer across the arc gap are singled out: t_1 — electrode melting and drop formation; t_2 — drop stabilization; t_3 — SC and start of the drop flowing over into the pool; t_4 — end of flowing over; t_5 — breaking up of the melt bridge between the electrode and the pool and arc excitation. Stages t_1, t_2 form arcing phase t_a , and t_3 – t_5 — SC phase of duration $t_{s,c}$.

Determination of the moments of completion of each of the above phases during the welding process is a problem. The most readily accessible experimental parameters of the process are values of arc current and voltage measured during drop transfer into the pool.

Duration of stage t_1 and current I_a determine the drop size, and in the simplest case they are assigned depending on electrode diameter and feed rate. The moment of completion of phase t_2 is readily recorded by lowering of the arc voltage below the sum of the arc anode and cathode voltage drops. The most complicated problem is determination of the moment of completion of stage t_3 , as in this microcycle there exist two bridges, one in the zone of drop–pool contact,

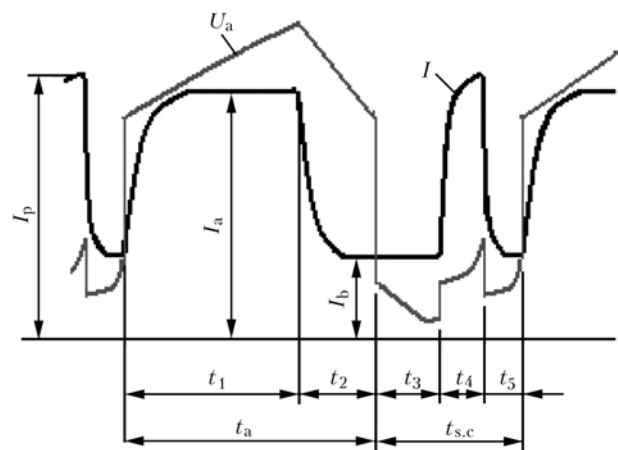


Figure 1. Oscillogram of arc current and voltage in pulsed arc welding with SC (for designations see the text)



the second in the drop-wire zone. It is believed [8] that the moment, from which the arc gap resistance (or voltage) starts rising, can be taken as the start of stage t_4 . It is not obvious, however, the change of which of the bridges causes it. Even more complex is determination of the moment of completion of stage t_4 , i.e. the moment of applying current pulse I_p to accelerate the drop transfer. A fast increase of the arc gap resistance (or voltage above 8–10 V) is an indication of the start of bridge disruption in the drop-wire zone. The above CDT stages are realized by different control algorithms [9], including stabilization of current or voltage in the phase of drop formation, with or without applying the current pulse in SC phase from a separate or main source.

This study is a comparative analysis of the above control variants based on simulation of the physical processes involved.

Physico-mathematical model. The model is based on equations describing electrode wire melting by the arc allowing for heating of electrode extension [10, 11]. The main distinctive feature of the developed model is the possibility of visual reproduction and comparative analysis of different algorithms of pulsed control of drop transfer at SC of the arc gap.

Electric processes. Description of electric processes allowed for inductance L , resistance R of the source and arc power circuit, as well as resistance of electrode wire extension $R(T)$.

Arc current I_a was determined by its volt-ampere characteristic (VAC) allowing for dependence of arc voltage U_a and its length l_a

$$U_a(I_a, l_a) = U_e + l_a \text{grad } U \left(1 - \frac{I_{s.c.}}{I_a} \right), \quad (1)$$

where U_e is the sum of arc anode and cathode voltage drops; $\text{grad } U$ is potential gradient in the arc column; $I_{s.c.}$ is the value of current at which the arc voltage is minimum (SC current).

Electrode extension resistance was determined by temperature distribution in the extension:

$$R(T) = \frac{4}{\pi d_f^2} \int_0^{l_e} \rho_e(T_f(z)) dz, \quad (2)$$

where d_f is the electrode wire diameter; l_e is the length of electrode wire extension from the edge of the current-conducting nozzle to the arc; $\rho_e(T_f)$ is the dependence of specific resistance of electrode material on its temperature T_f ; z is the ordinate of axial displacement of electrode wire and drop into the pool.

Metal temperature in the extension is determined allowing for arc current variation in time:

$$T_f = \frac{16}{c\rho(\pi d_f^2)^2} \int_{t-\tau}^t \rho_e(T_f) I_a^2(\tau) d\tau, \quad (3)$$

where $\tau = l_e/v_f$ is the time of metal displacement from the current-conducting tip for distance l_e from its edge;

ρ is the density of electrode material; c is the specific heat content; t is the time of the cycle of transfer of one electrode metal drop, consisting of microcycles $t_a + t_{s.c.}$.

Electric processes in the arc power circuit are described by an equation, which correlates the current and voltage in the source with the arc energy parameters by switching conditions:

$$I_a = \frac{1}{L} \int_0^t (U_{o.c.} - U_k - R \max(I_p, I_b)) dt, \quad (4)$$

where $U_{o.c.}$ is the specified open-circuit voltage of the source; U_k is the voltage of key K ; I_b is the specified base current.

Key voltage changes in each stage (microcycle) of drop transfer into the pool:

$$U_k = \begin{cases} 0 & \text{at } t \in (t_2, t_3) \cup t \in t_5, \\ U_a & \text{at } t \in t_1 \cup t \in t_4. \end{cases} \quad (5)$$

Voltage in the arc gap in the arcing phase is determined by its VAC, and in SC phase — by voltage drop in the electrode extension and in the bridges of drop-pool and drop-wire zones. Total bridge resistance R_{dr} is calculated in keeping with the change of voltage drop and is described as a function of coordinate Z_{dr} of the drop center of gravity:

$$R_{dr} \approx \rho_{dr} \frac{D}{d_f \sqrt{(D - 2Z_{dr})(D + d_f - 6Z_{dr})}}, \quad (6)$$

where ρ_{dr} is the melt specific resistance; D is the current drop diameter.

Wire melting and drop formation. Drop size is determined by electrode metal melting rate v_f , dependent on heat transfer from the arc to the drop. Arc thermal power increases the average drop temperature at the rate equal to

$$\frac{dT_{dr}}{dt} = \frac{U_e I_a - \lambda \frac{\pi d_f^2}{D} (T_{dr} - T_L)}{c\rho \frac{\pi D^3}{6}}, \quad (7)$$

where λ is the electrode metal heat conductivity; T_L is the melting temperature; T_{dr} is the current average temperature of the drop.

At the same time a thermal flow of the following power forms in the drop-electrode wire zone:

$$P_f = \pi d_f^2 \frac{2\lambda}{D} (T_{dr} - T_f). \quad (8)$$

This thermal flow causes additional melting of the electrode wire with increase of the current drop volume V_{dr} at the rate of

$$\frac{dV_{dr}}{dt} = \frac{P_f}{c\rho(T_L - T_f) + H_L}, \quad (9)$$

where H_L is the specific melting heat.

Current drop diameter is determined by its volume



Table 1. Assigned values of parameters of welding with SC for different control algorithms

No	Control algorithm	$U_{o.c.}$, V	I_a , A	$I_{s.c.}$, A	τ_1 , ms	τ_5 , ms	I_b , A
1	With set source voltage and complete limitation of SC current	35	--	--	20	0.5	40
2	With set source voltage and pulse at SC	35	--	--	20	0.5	40
3	With set values of melting pulse currents and SC	--	250	350	--	--	--
4	Uncontrolled transfer of electrode metal drop	30	--	--	--	0	0

$$D = \sqrt[3]{\frac{6}{\pi}} V_{dr}. \tag{10}$$

Formation of arc gap. Length of arc gap l_a was determined by the minimum distance between the surfaces of the weld pool and electrode drop. As parameter l_a depends on the rate of electrode feed v_f and drop diameter D , the following relationship is valid:

$$\frac{dl_a}{dt} = - \frac{dD}{dt} - v_f. \tag{11}$$

Drop transfer. Duration of stage t_1 of the drop transfer microcycle is set, and t_2 is determined by the value of arc length, which is equal to zero at the moment of SC and is determined by location of the drop center of gravity. Location of drop center of gravity Z_{dr} depends on its shape and is given by the following equation:

$$\frac{d^2 Z_{dr}}{dt^2} = \frac{m_{dr}}{F_\sigma + F_I + m_{dr}g}, \tag{12}$$

where $m_{dr} = \frac{1}{6} \pi D^3 \rho$ is the drop weight; $F_\sigma = \pi D \sigma (1 - Z_{dr}/Z_2)$ is the surface tension force; $F_I \approx k I_a^2 (Z_{dr}/Z_1 - 1)$ is the axial component of the electromagnetic force, the direction and magnitude of which depends on the drop shape and pool surface curvature at their coalescence.

Simultaneous solution of the system of equations (1)–(12) allows virtual reproduction of melt drop transfer from the electrode into the pool at SC. For a numerical solution, equations (1)–(12) were transformed into a system of ordinary differential equations of the first order, solved for the derivatives. Solution of all the equations of this system was performed in the common time cycle with a step of not less than $dt = 10^{-5}$ s, thus allowing a detailed reproduction of fast processes at drop transfer from the electrode into

the weld pool, from the initial contact of the electrode and item up to achievement of a steady state.

Simulation results. Simulation was performed for the case of CO₂ welding with 1.2 mm wire at wire feed rate of 120 mm/s at power supply from a power source with VAC slope of 0.08 V/A with welding circuit inductance of 4 mH, which corresponds to parameters of UAST-1 system for automatic orbital welding of the main pipelines [12]. It allowed determination of variation of parameters of the process of drop transfer into the pool at the stages of SC, electrode melting and drop formation at different algorithms of drop transfer control.

Process parameters in different control variants (power source open-circuit voltage $U_{o.c.}$, base current I_b , melting current pulse duration τ_1 and duration of current switching-on delay τ_5 after SC start) are given in Table 1. Table 2 gives the main results of calculation of process characteristics at different control algorithms. Control variants correspond to control algorithms, given in Table 1.

Figures 2–5 show the results of simulation in the form of graphs of variation of arc current, voltage and length during several periods of electrode metal transfer into the weld pool (electrode wire diameter was 1.2 mm, feed rate --- 120 mm/s at power supply from a source with VAC slope of 0.08 V/A, pulse duration was 0.02 s).

Obtained results showed that at pulsed control of the process the arc current, period of drop transfer from the electrode into the weld pool, drop size and maximum arc length are significantly greater than in a continuous mode in the absence of control (see Table 2). However, average values of arc current differ only slightly. An essential increase of the drop size and maximum arc length is observed. This is due to increase of arc current in the phase of drop formation, which is the result of large values of power source open-circuit voltage at pulsed control. Increase of the period of drop transfer and SC duration is a direct

Table 2. Parameters of the process obtained at simulation of the process of electrode metal transfer with CDT

Control variant	I_{max} , A	I_{av} , A	l_a^{max} , mm	l_a^{av} , mm	$t_{s.c.}$, ms	Drop transfer period, ms	D , mm	T , °C	T of extension heating, °C
1	270	172	0.90	0.48	5.6	33	1.65	1780	330
2	265	185	0.90	0.47	5.4	33	1.65	1750	370
3	350	184	0.94	0.50	5.2	32	1.64	1737	400
4	210	198	0.62	0.19	4.0	16	1.25	1680	372

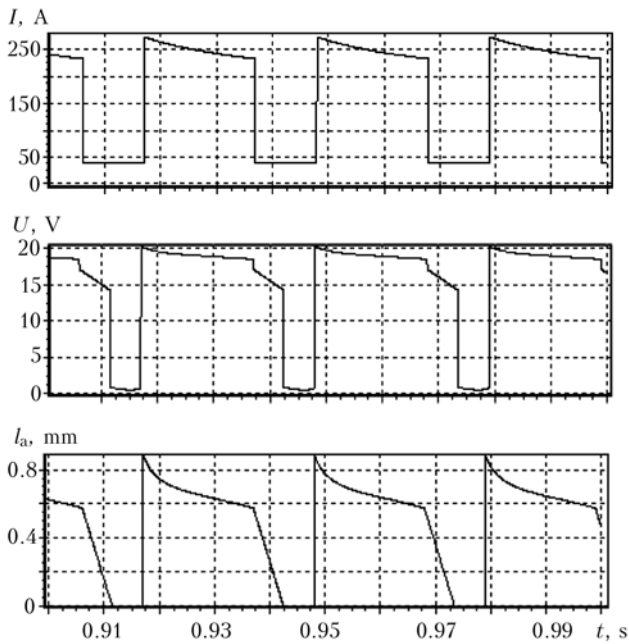


Figure 2. Results of simulation of welding with SC at setting of the power source open-circuit voltage and complete limitation of SC current ($U_{o-c} = 35$ V)

result of increase of the maximum arc length, drop weight and diameter. At limitation of current for the entire period of the SC, the short-circuit duration is somewhat greater than at feeding of the current pulse at the SC final stage.

Analysis of the technological features of the process of welding with CDT. The main disadvantage of an uncontrolled process of arc welding with SC is a very narrow range of process parameters, in which a stable process of electrode metal transfer into the weld pool is realized [13]. At pulsed control, the duration of drop formation is assigned, thus allowing control of the drop formation process by adjustment

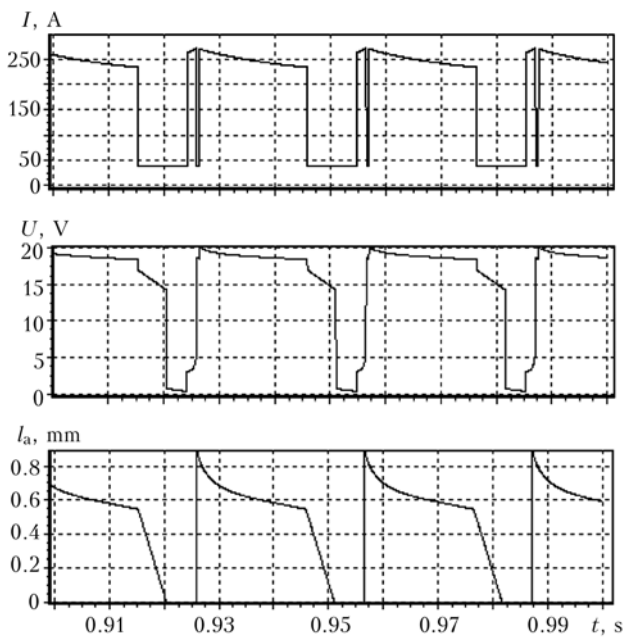


Figure 3. Result of simulation of the process with SC at setting of open-circuit voltage of the power source and applying the current pulse in SC final stage (0.0005 s delay of current pulse after SC)

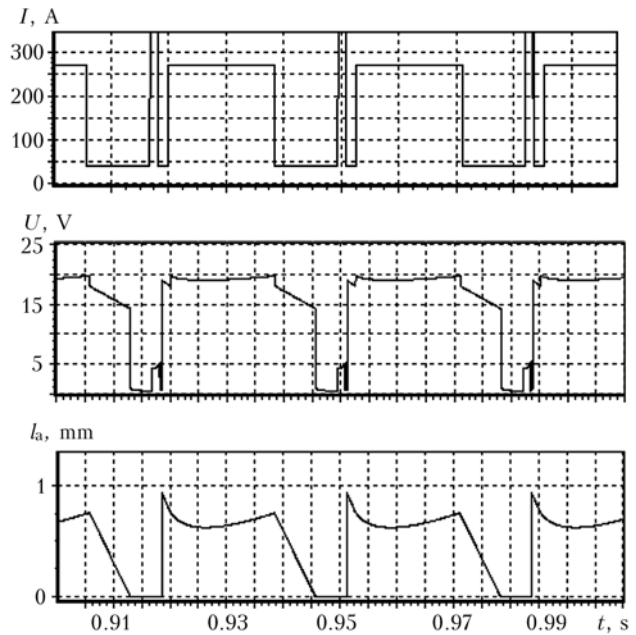


Figure 4. Result of simulation of welding with SC at setting of current in the phase of drop formation and current in SC final phase (current pulse amplitude at the stage of drop formation is 260 A, at stabilization stage — 40 A, at SC — 350 A)

of the current pulse. It is possible to use the effect of self-regulation of the arc by setting not the pulse current, but arc power source voltage. This ensures an automatic change of current at the change of the electrode wire feed rate, and also weakens the influence of instability of electrode wire characteristics on arc length and drop size and repetition period. The latter, in its turn, improves the stability of welded joint formation and their quality.

The above advantages widen the range of parameters, in which the process of welding with periodical SC is realized. The maximum drop size, at which the drop is retained on the electrode, limits the duration

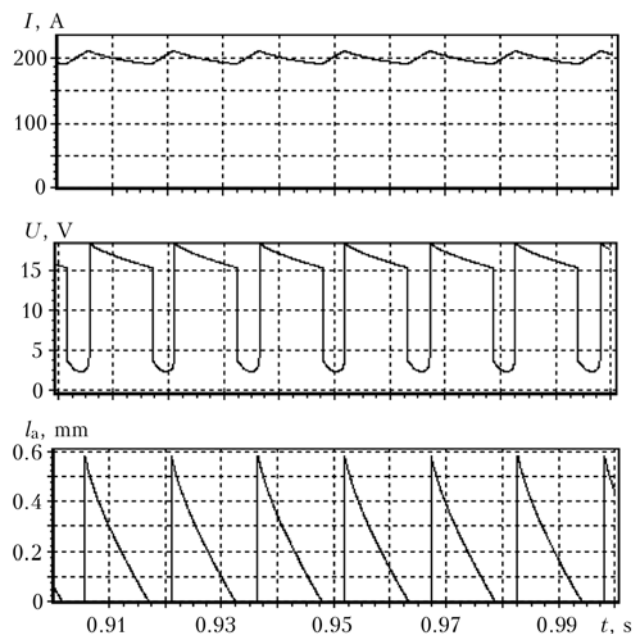


Figure 5. Result of simulation of uncontrolled process of arc welding with periodical SC ($U_{o-c} = 30$ V)



and amplitude of pulse current in the drop formation phase. Maximum value of power source voltage is unlimited, and minimum current of the pilot arc is limited only by the condition of maintaining the formed drop in the molten state.

CONCLUSIONS

1. In order to study the control algorithms and determine the parameters of electrode metal CDT a physical-mathematical model of the process of gas-shielded arc welding was developed in the power source-arc system, which allows for fast phenomena in the phases of SC, electrode melting and drop formation in consumable-electrode arc welding.

2. Implementation of the model in the form of a computer program for virtual reproduction of fast phenomena in the phases of SC, electrode melting and drop formation in consumable-electrode welding allows a substantiated determination not only of the technological parameters of the process, but also technological requirements to design of various kinds of equipment for mechanized and automatic consumable-electrode arc welding.

1. Tavrovsky, V.P. (1969) Automatic pulsed arc welding of position butts of steam pipes. *Energet. Stroitelstvo*, **10**, 28–32.

2. Paton, B.E., Shejko, P.P., Pashulya, M.P. (1971) Automatic control of metal transfer in pulsed arc welding. *Avtomatich. Svarka*, **9**, 1–3.
3. Paton, B.E., Potapievsky, A.G. (1973) Types of shielded-gas welding processes with stationary and pulsed arc (Review). *Ibid.*, **9**, 1–8.
4. Stava, E.K. (1999) New surface transfer tension process speeds pipe welding. *Pipe Line and Gas Industry*, **82(9)**, 55–57.
5. Wang, F., Hou, W.K., Hu, S.J. et al. (2003) Modelling and analysis of metal transfer in gas metal arc welding. *J. Phys. D: Appl. Physics*, **36**, 1–19.
6. Grabovetsky, G.V., Kharitonov, S.A., Preobrazhensky, E.B. et al. (2001) Some tendencies in development of apparatuses and devices of power electronics. *Khimiya v Interesakh Ust. Razvitiya*, **9(7)**, 921–928.
7. Lankin, Yu.N. (2007) Automatic control of the MAG welding process with periodic short-circuiting of arc gap (Review). *The Paton Welding J.*, **1**, 2–8.
8. Yamamoto, T., Ohji, T., Miyasaka, F. et al. (2002) Mathematical modeling of metal active gas arc welding. *Sci. and Technol. of Welding & Joining*, **7(4)**, 260–264.
9. Lebedev, V.K. (2004) Tendencies in development of power sources and control systems (based on materials of US patents). *The Paton Welding J.*, **1**, 37–45.
10. Getskin, O.B., Poloskov, S.I., Erofeev, V.A. et al. (2008) Physico-mathematical model of the «power supply-arc» system for consumable-electrode shielded-gas welding. *Tyazh. Mashinostroenie*, **6**, 18–20.
11. Getskin, O.B., Poloskov, S.I., Erofeev, V.A. et al. (2008) Simulation of specifics of drop transfer control in short-circuiting arc welding. *Tekhnologiya Mashinostroeniya*, **10**, 25–29.
12. Getskin, O.B. (2008) Development of automatic machine of modular configuration for orbital welding of the main pipelines. *Svarka i Diagnostika*, **6**, 19–23.
13. Getskin, O.B., Poloskov, S.I., Erofeev, V.A. et al. (2008) Process stability of consumable-electrode welding with short-circuiting of the arc gap. *Tyazh. Mashinostroenie*, **9**, 20–23.

PULSED-ARC MIG/MAG WELDING OF ENAMELED PRODUCTS USING CONTROLLABLE CONDITIONS OF HEATING AND COOLING

At the present time the products with enameled internal surface have found a wide spreading in heat power engineering and oil production industry. Enameling provides a reliable protection of the product from corrosion in operation in aggressive media and 4–5 times increases the inter-repair period of service. For example, the application of enameled pipes in central heating systems makes it possible to extend the inter-repair period of service of pipelines up to 20–25 years.

However, the problems arise in welding such products, especially pipes, caused by a low resistance of enamels to thermal action of the arc. It burns out at heating up to the temperature above 1000 °C and the temperature of about 800 °C is insufficient for its quality heat treatment. Traditional methods of arc welding cannot provide conditions of heating and cooling of joints, at which the enamel is subjected to the quality heat treatment without burning out.

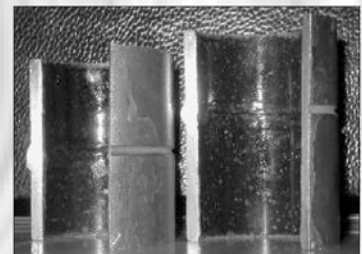
The offered technology of a pulsed-arc consumable-electrode shielded-gas welding guarantees the high accuracy of heating and cooling control. Here, enamel under weld is subjected to the temperature action for a short time, that does not only lead to its burning out, but also provides the reliable heat treatment.

This technology is realized in standard welding equipment, which is completed with the control systems, developed at the E.O. Paton Electric Welding Institute.

Purpose. It can be used in heat power engineering, oil production industry and other branches where the products and pipelines with enamel protection of the inner surface are manufactured and used, and also in repair of the mentioned products.

Proposals for co-operation. Development, manufacture, delivery of equipment, implementation of technology, training of personnel.

Contacts: Prof. Savitsky M.M.
E-mail: savitsky@paton.kiev.ua





PECULIARITIES OF DESULPHURISATION OF WELD METAL IN FLUX-CORED WIRE WELDING

V.N. SHLEPAKOV and S.M. NAUMEJKO

E.O. Paton Electric Welding Institute, NASU, Kiev, Ukraine

Metallurgical methods intended to decrease the sulphur content of the weld metal in flux-cored wire welding were studied. The possibility of decreasing the content of sulphur in metal by using magnesium- and calcium-containing master alloys is shown. The prospects for improvement of mechanical properties of welded joints through decreasing the sulphur content of the deposited metal are considered.

Keywords: arc welding, flux-cored wire, low-alloyed weld metal, desulphurisation, weld pool stage, droplet stage, thermodynamics of desulphurisation reactions, calcium- and magnesium-containing master alloys, mechanical properties, structure of weld metal.

In ferrous metallurgy, the sulphur content of steel can be substantially decreased by processing the melts with desulphurising fluxes [1, 2], this improving ductility of the steel and its tough and brittle fracture resistance. In fusion electric arc welding, the sulphur content of the weld metal in a welded joint is controlled in view of the need to prevent formation of defects (hot cracks) and provide required mechanical properties of the welded joints [3–5].

The methods for decreasing the sulphur content of the deposited metal include interaction of metal with slag and gaseous phase, as well as employment of the base materials with low sulphur content.

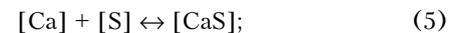
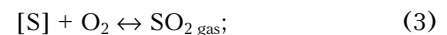
The purpose of this study was to investigate peculiarities of desulphurisation of the deposited metal by controlling the content of the metal phase through the flux-cored wire core.

In welding of some grades of steels, silicocalcium was added to the composition of flux-cored wires to ensure the required physical-mechanical and service properties of the welded joints. However, that provided only the insignificant decrease in the sulphur content. Note that silicocalcium is inapplicable for welding of low-silicon steels. Because of the high silicon content of the weld metal, it is important to try and use other desulphurising agents based on calcium and magnesium. One of the alternatives is the use of alumocalcium and alumomagnesium master alloys in wires of the basic type. As reported in [2], in out-of-furnace treatment of steels by using flux-cored wire with granulated aluminium and calcium, recovery of the latter is 29 %, and in treatment with the silicocalcium wire it is 11 %. However, it is a known fact that out-of-furnace treatment of steel is characterised by a long time of existence of the melt.

The process of fusion arc welding features a short time of existence of the melt. Desulphurisation with this welding method occurs both at a stage of the weld pool and at a stage of a droplet. Compared with the weld pool stage, the droplet stage is characterised by

a higher temperature (above 2500 K) and presence of a substantial specific interfacial area. These peculiarities of the droplet stage make it possible to effectively influence the desulphurisation process due to interaction of sulphur dissolved in the droplet with the gaseous phase formed in melting of components of the flux-core wire core.

In terms of thermodynamics, in arc welding of steel the most probable reactions are those occurring as follows:



Calculations of Gibbs energy ΔG_T^0 at temperature $T = 1800\text{--}2500$ K by the entropy method were made by using the following formulae:

$$\Delta H_T^0 = \Delta H_{298}^0 + \sum [n_i(H_T^0 - H_{298}^0)_i]; \quad (7)$$

$$\Delta S_T^0 = \Delta S_{298}^0 + \sum [n_i(S_T^0 - S_{298}^0)_i]; \quad (8)$$

$$\Delta G_T^0 = \Delta H_T^0 - T\Delta S_T^0, \quad (9)$$

where ΔH_{298}^0 is the standard enthalpy, kJ/mol; ΔS_{298}^0 is the standard entropy, J/mol; $n_i(H_T^0 - H_{298}^0)_i$ is the high-temperature constituent of enthalpy of the i -th component, kJ/mol; and $n_i(S_T^0 - S_{298}^0)_i$ is the high-temperature constituent of entropy of the i -th component, kJ/mol.

Thermodynamic data required to calculate ΔG_T^0 were taken from studies [6–8]. Variation in the Gibbs energy with temperature for reactions (1) through (6) is shown in Figure 1.

Equilibrium constants K_{eq} were calculated from the following formula:

$$K_{\text{eq}} = e^{-\Delta G_T^0/RT}, \quad (10)$$

where R is the universal gas constant, J/kmol.

The values of equilibrium constants K_{eq} for reactions (1) through (6) at temperatures of 2000 and



Table 1. Equilibrium constants

Reaction	2000 K	2500 K
$[\text{Fe}] + [\text{S}] \leftrightarrow [\text{FeS}]$	$4.125 \cdot 10^{-2}$	--
$[\text{Mn}] + [\text{S}] \leftrightarrow [\text{MnS}]$	$4.278 \cdot 10^{-3}$	--
$[\text{Ca}] + [\text{S}] \leftrightarrow [\text{CaS}]$	$2.127 \cdot 10^{-4}$	$1.211 \cdot 10^{-2}$
$[\text{S}] + \text{O}_2 \leftrightarrow \text{SO}_2_{\text{gas}}$	$4.310 \cdot 10^{-4}$	$6.817 \cdot 10^{-3}$
$[\text{S}] + 6\text{F} \leftrightarrow \text{SF}_6$	$2.910 \cdot 10^{-4}$	$1.380 \cdot 10^{-4}$
$[\text{Mg}] + [\text{S}] \leftrightarrow [\text{MgS}]$	$1.181 \cdot 10^{-5}$	$1.387 \cdot 10^{-6}$

2500 K, which are characteristic of the weld pool and droplet stages, are given in Table 1.

It can be seen from variations in the Gibbs energy and equilibrium constants at the droplet stage ($T \geq 2500 \text{ K}$) that the best desulphuriser is calcium, which is capable of actively removing sulphur into the gaseous phase and fluorine. As the value of the equilibrium constant for formation of calcium sulphide at $T = 2500 \text{ K}$ is much higher than that for formation of sulphur oxide and fluoride and magnesium sulphide, it is the interaction of calcium and sulphur at the droplet stage that plays the decisive role in the desulphurisation process, whereas the reaction of fixation of sulphur to form manganese sulphides starts developing in solidification of metal.

Experimental verification was conducted to prove the calculation results. Flux-cored wire of the fluoride-oxide type was chosen as an investigation object. Welding was performed in air by using 1.6 mm diameter experimental wires of a tubular design at the

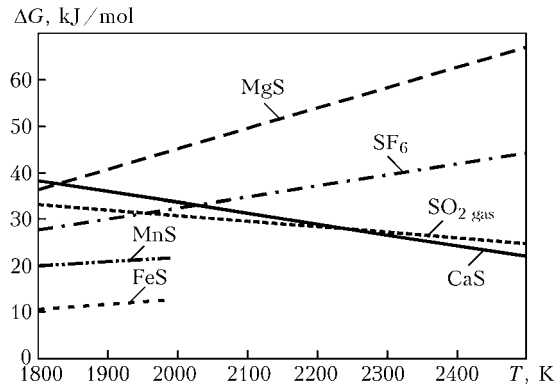


Figure 1. Variation in Gibbs energy ΔG in formation of sulphur oxide and fluoride, and sulphides with temperature

straight polarity direct current: $I_w = 250\text{--}260 \text{ A}$, $U_a = 21\text{--}22 \text{ V}$, electrode extension --- 20 mm. Welding was carried out by using semi-automatic device PDGO-510 (produced by SELMA Company), having a continuously adjustable wire feed speed, and arc power supply VS-600 with a step adjustment of open-circuit voltage. Samples for chemical analysis were made in six layers by using copper plates for pre-forming the side surfaces of the bead. Chemical composition of the deposited metal was determined by spectral and chemical analysis. The effect by the sulphur content on structure and mechanical properties of metal of the multilayer welds in flat position was investigated. Steel St3sp (killed) 20 mm thick was used as a base metal for the test butt joints. The level of alloying of the deposited metal with C-Si-Mn-Ni, produced by using all the types of the wires, was kept unchanged. Welding of the butt joints for mechanical

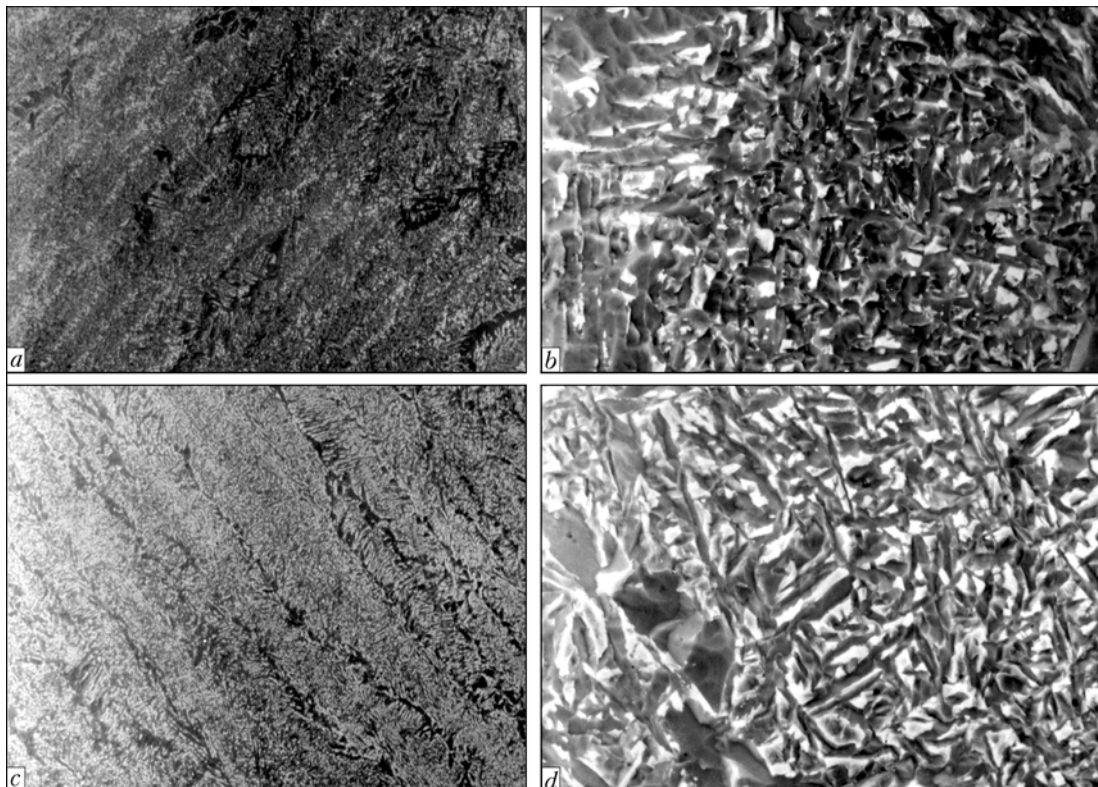


Figure 2. Microstructure of deposited metal of the weld with sulphur content of 0.003 (a, b) and 0.020 (c, d) wt.%; a, c --- $\times 100$; b, d --- $\times 1000$

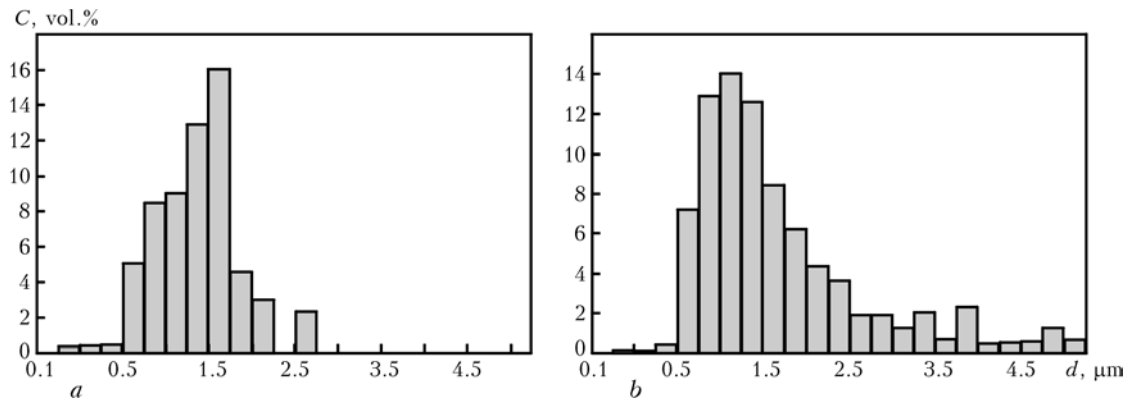


Figure 3. Size distribution of non-metallic inclusions in deposited metal with sulphur content of 0.003 (a) and 0.020 (b) wt.%; C — content of non-metallic inclusions

Table 2. Effect of sulphur content of deposited metal on mechanical properties of the weld

S, wt.%	σ_t , MPa	σ_y , MPa	δ , %	KCV, J/cm ² , at temperature, °C			
				+20	-20	-40	-60
0.003	635	525	23.3	140.0	68.1	57.5	52.5
0.008	590	480	22.1	90.0	65.5	45.1	--
0.020	500	400	21.0	85.2	42.8	35.2	--

tests was carried out in compliance with GOST 26271-91. Metallographic analysis of structure of the weld metal was conducted after etching in 4 % HNO₃ solution in alcohol by using microscope «Neophot-302» and scanning electron microscope JSM-840. Volume content of non-metallic inclusions was determined by using quantitative analyser «Omnimet».

Data on the methods of adding calcium- and magnesium-containing master alloys to the wire core, as well as on the sulphur content of the deposited metal are given below.

Desulphurisers (form of addition), wt.%	S, wt.%
0	0.020
2.0 Mg	0.009
1.75 Mg (1.0 Mg, 1.5 AlMg)	0.008
1.25 Mg (3.5 AlMg)	0.005
1.4 Ca (3.5 AlCa)	0.002
0.8 Ca, 0.75 Mg (1.5 AlMg, 2.0 AlCa)	0.003

The effect of the sulphur content of the deposited metal on structure is shown in Figure 2, and mechanical properties of the weld metal are given in Table 2.

The content of non-metallic inclusions at a 0.003 wt.% S content of the deposited metal is 0.3 vol.%, and that at S = 0.02 wt.% is 0.85 vol.%. At the same time, it can be seen from Figure 3 that at a low sulphur content (0.003 wt.%) of the deposited metal the content of dispersed non-metallic inclusions is higher than at S = 0.020 wt.%.

Therefore, calcium-base master alloys are the most active desulphurising agents. This is attributable to the fact that calcium fixes sulphur to form calcium sulphide CaS, which is insoluble in iron. By assimilating with neutral slag, it decreases the content of iron sulphide in the weld pool, and reduces the content and size of non-metallic inclusions in the weld metal,

thus exerting the positive effect on mechanical properties of the welded joints.

CONCLUSIONS

1. In flux-cored wire welding the important role in desulphurisation of metal is played by the processes occurring at the droplet stage. These processes result in formation of volatile sulphur fluorides and oxides, as well as sulphides insoluble in iron. The efficiency of desulphurisation of the weld metal at the droplet stage is higher in the case of using calcium-containing master alloys.

2. Fluorine and manganese actively interact with sulphur at the weld pool stage.

3. Active desulphuring agents, based on master alloys of the type of alumocalcium, added to the composition of the flux-cored wire core lead to increase of ductility, decrease of the content and size of non-metallic inclusions, and improvement of tough-ductile properties of the weld metal.

- Vikhlevshchuk, V.A., Kharakhulakh, V.S., Brodsky, S.S. (2000) *Ladle final treatment of steel*. Dnepropetrovsk: System. Tekhnologii.
- Onishchuk, V.P., Kirilenko, V.V., Dyudkin, D.A. et al. (2000) Out-of-furnace treatment of molten steel with flux-cored alumocalcium wire. *Metall i Litio Ukrainy*, 1/2, 20-23.
- Pidgaetsky, V.V. (1970) *Pores, inclusions and cracks in welds*. Kyiv: Tekhnika.
- Pokhodnya, I.K., Gavrilyuk, Yu.A., Orlov, L.N. (1989) Desulphurisation of metal in flux-cored wire welding. *Automatich. Svarka*, 11, 47-50.
- Pokhodnya, I.K., Suptel, A.M., Shlepakov, V.N. (1972) *Flux-cored wire welding*. Kiev: Naukova Dumka.
- Kireev, V.A. (1975) *Methods for practical calculations in thermodynamics of chemical reactions*. Moscow: Khimiya.
- Vladimirov, L.P. (1970) *Thermodynamic calculations of equilibrium of metallurgical reactions*. Moscow: Metallurgiya.
- (1981) *Thermodynamic properties of individual materials*: Refer. Book. Vol. 3: Elements B, Al, Ca, Th, Ti, Be, Ba and their compounds. Book 2. Tables of thermodynamic properties. Moscow: Nauka.



EFFICIENCY OF METHOD FOR AUTOMATIC RECOGNITION OF ELECTRODE IMPRINTS IN SPOT WELDING OF THREE-LAYER HONEYCOMB STRUCTURES

Yu.P. LAZORENKO, E.V. SHAPOVALOV, E.S. MELNIK, N.F. LUTSENKO and V.V. DOLINENKO
E.O. Paton Electric Welding Institute, NASU, Kiev, Ukraine

Methods for automatic recognition of the electrode imprints on digital images in spot welding of the three-layer honeycomb structures — correlation, statistical, and neuron network ones — have been investigated. The algorithms for recognition of the electrode imprints on surface of a three-layer honeycomb structure using an optical sensor system have been developed. High efficiency of the developed algorithms has been demonstrated.

Keywords: spot welding, arc welding, three-layer structures, technical vision, recognition of specimens, statistical recognition, geometrical adaptation, welding tool, neuron network, processing of images

Three-layer honeycomb welded structures, which usually have a cylindrical shape, are widely used in different branches of industry. Basis of these structures constitute volumetric metal elements of the honeycomb type to which from external and internal sides metal sheets are welded. Such three-layer honeycomb welded structures are characterized by significant strength at a relatively small mass. Welding of external layer of the mentioned structures is performed using resistance spot welding and does not cause special difficulties. The problem occurs at welding of the last layer, because in this case positioning of the welding head is performed relatively positions of the electrode imprints on external layer of the structure. At present such positioning is performed manually using special templates. The operator performs mating of the template, rigidly connected with the welding head, and imprints of the electrode on external side of the cylinder, whereby the welding head on internal side of the cylinder is installed into the position necessary for performing of the welding. Mentioned method of the welding head positioning takes long time, and because of this reason welding of large-sized three-layer structures may last for dozens of working

shifts. In addition, accuracy of the welding head positioning depends to a significant degree upon the operator. Improvement of quantity and quality parameters of this welding process may be achieved due to use of the automation means. In development of automated welding systems good prospects has application of the technical vision.

Purpose of this article is investigation of efficiency of the methods for automatic recognition of the electrode imprints on digital images of the external layer surface of the three-layer honeycomb structures.

Preliminary processing of initial images. Electrode imprints on initial gray scale digital images of the structure external layer surface produced using a television video sensor have round shape and brightness lower than that of the base metal area (Figure 1, *a*). At change of the filming conditions on initial digital images change such characteristics as general level of brightness and its range, contrast range of the electrode imprint contours, and presence of patches of light. In connection with this for correct recognition of the electrode imprints first preliminary processing of initial digital images is performed which includes three procedures: singling out of the object contours; linear contrasting; binarization.

Singling out of the object contours is performed using the «Laplacian of Gaussian» filter [1, 2]. After processing using this filter the background area has

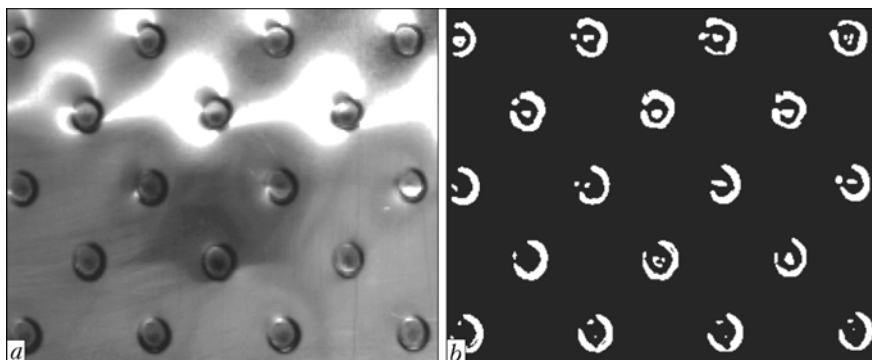


Figure 1. Preliminary processing of digital images of external layer surface of structures with imprints (*a*) and binary electrode initial produced as a result of preliminary processing (*b*)



brightness value close to zero, and the electrode imprints are characterized by high level of brightness. Linear contrasting normalizes brightness of the image by means of linear expansion of its dynamic range up to full dynamic range.

Procedure of the binarization consists in marking-out of the digital image points (pixels) into two groups: imprints of the electrodes and the base metal area. The digital image points, to which correspond imprints of the electrodes, are marked by 1, and the points, to which corresponds the base metal area, are marked by 0.

The result of such marking is a binary (a two-level) image. In this work procedure of binarization was performed by means of the threshold processing which consisted in comparison of the assigned point brightness with a certain threshold value. If brightness values of the image point are higher than this value, it is assigned mark 1, while if it is lower than this value — mark 0. Value of the brightness threshold T for the assigned digital image is calculated according to formula

$$T = M + k\sigma, \quad (1)$$

where M is the mean arithmetic value of the digital image brightness; k is the regulation parameter; σ is the mean square deviation of the image brightness. Example of the binary image is presented in Figure 1, b , where imprints of the electrodes are marked by white color, and the base metal area — by black color. Subsequent recognition of the required objects is carried out using the binary image.

Methods for recognition of electrode imprints.

Besides electrode imprints on binary images, frequently different noises are erroneously singled out, which occur in connection with the fact that on surface of a three-layer honeycomb structure cracks, dark spots and patches of light are present. Task of recognition of the electrode imprints is brought down to separation of singled out on the binary image objects into two classes — the electrode imprint and the noise. The recognition algorithm should also determine center of the found electrode imprint.

In this work three methods for recognition of the electrode imprints on surface of a three-layer honeycomb structure were investigated: correlation, statistical, and neuron network ones.

Correlation method for recognition of specimens [1–3] is based on comparison of the object being recognized with the reference objects using analysis of the mutual correlation function. In the developed correlation algorithm recognition of the required objects is performed by means of the detected object comparison with the reference image of the electrode imprint. As the reference one of the electrode imprint images was used, which was brought by means of preliminary processing to the binary form. In this algorithm a normalized correlation function was used which was calculated for the reference image of the electrode imprint and the assigned rectangular fragment of the

binary image containing the object being recognized. Normalized function of correlation R is calculated by formula

$$R = \frac{\sum_{j=0}^{N-1} \sum_{i=0}^{M-1} I(i, j)E(i, j)}{\left[\sum_{j=0}^{N-1} \sum_{i=0}^{M-1} I^2(i, j) \right]^{1/2} \left[\sum_{j=0}^{N-1} \sum_{i=0}^{M-1} E^2(i, j) \right]^{1/2}}, \quad (2)$$

where M and N are respectively the width and the height of the image fragment I being analyzed and of the reference image of the spot welding zone E ; i, j are respectively the line and the column indices.

Decision in relation to the fact if the object being recognized is the electrode imprint image is made on basis of the value of the mutual correlation function in the point of its local maximum. If this value exceeds a certain assigned threshold value, the object is classified by the recognition algorithm as the electrode imprint, otherwise — as the noise. According to the developed algorithm, center of the electrode imprint is located in the point of the local maximum of the mutual correlation function.

In statistical method of recognition classification of the singled out at the binarization stage objects (the electrode imprint and the noise) is performed on basis of analysis of the values of informative signs calculated for the binary images. The classification consists in the task of division of the space of the signs into two areas that correspond to two specified classes of the objects. For solution of this task the Bayesian classifier [4, 5] was used which ensured the minimum recognition error and in which initial data for making decision are conditional densities of distribution of probability of the informative signs for each class of the objects. In case when classification is performed for two classes ω_0 (the noise) and ω_1 (the electrode imprint), the object, described by vector of the signs \mathbf{x} , is classified as belonging to the class ω_1 if the condition

$$p(\mathbf{x} | \omega_1)P(\omega_1) > p(\mathbf{x} | \omega_0)P(\omega_0), \quad (3)$$

where $p(\mathbf{x}, \omega_i)$ is the conditional density of probability distribution of the vector of signs \mathbf{x} for class ω_i ; $P(\omega_i)$ is the prior probability that the object detected belongs to class ω_i . If condition (3) is not fulfilled, the decision is made that the object belongs to class ω_0 . In this investigation an assumption was made that densities of probability had normal distribution.

In the developed statistical algorithm of recognition the following three signs were used: area of the object S (number of pixels from which consists the object on the binary image), the biggest length of the object L_{\max} , and coefficient of similarity with the circumference K_R which is calculated from the formula

$$K_R = \frac{N_{R \max}}{S}, \quad (4)$$



where $N_{R_{max}} = \max N_R(x, y)$; $N_R(x, y)$ is the number of points (pixels) of the object located at distance $R \pm \pm K_1 R$ from the point with coordinates $(x, y \in \in W_R)$; coefficient $K_1 \ll 1$; R is the radius of the circumference with which the object is compared; W_R is the square area of the image of $R_0 \times R_0$ size, center of which is in geometrical center of gravity of the object; R_0 is the mean radius of the electrode imprint the value of which is determined as mean arithmetic value of radii of the imprints from the instructing plurality; $N_R(x, y)$ is calculated for all values R that are within the range $R_0 \pm K_2 R_0$ where coefficient $K_2 \ll 1$. Center of the found electrode imprint is determined by the algorithm as lying in the point (x, y) with maximum value $N_R(x, y)$ in area of the W_R image, for which coefficient K_R is calculated (4). Respectively for vector of sings \mathbf{x} the following structure is selected:

$$\mathbf{x} = \begin{bmatrix} S \\ L_{max} \\ K_R \end{bmatrix}$$

For building of conditional densities of the probability distribution a set of binary images of imprints of the electrodes and the noises was used. Conditional densities of distribution of probabilities $p(\mathbf{x} | \omega_0)$ and $p(\mathbf{x} | \omega_1)$ for the objects (imprints of the electrode and the noises) with area $S = 120$ points are presented in Figure 2.

In the neuron network method of the electrode imprint recognition a multiplayer artificial neuron network [5–8] with direct propagation of the signal is used. To the neuron network input image of the object being recognized is fed, while at the output it evaluates probability of the fact that the object being recognized is the electrode imprint. If this probability is bigger than a certain threshold value, the decision is made that this object is the electrode imprint.

Input vector of the neuron network is formed on basis of a binary image of the object. Images fed to the network input have a fixed size 17×17 pixels. Average size of the spot welding zones for different initial images may significantly vary, that's why before recognition of the object scaling of its binary image up to the size 17×17 pixels is performed.

The neuron network used in the developed algorithm for recognition of the spot welding zones consists of three layers of neurons: input I , hidden H , and output O ones (Figure 3). The input layer which has $17 \times 17 = 289$ neurons ($I_1 - I_{289}$) fulfills function of connection of the input signals with neurons of the hidden layer and transmits input signals without transformation. The hidden layer consisting 10 neurons $H_1 - H_{10}$ performs non-linear transformation of the input signals according to the activation function. Sigmoid function was used as the activation function. The output layer of the neuron network consists of one neuron O_1 that forms the output signal.

For ensuring correct work of the neuron network it is necessary to correctly set values of the neuron

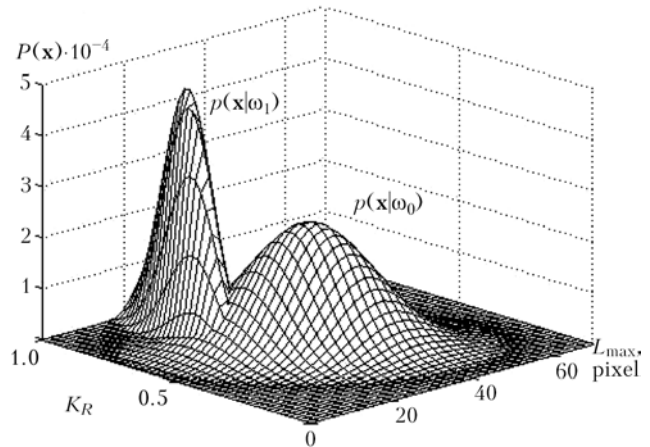


Figure 2. Conditional densities of distribution of probability $p(\mathbf{x} | \omega_0)$ and $p(\mathbf{x} | \omega_1)$

weights, for which purpose using method of reverse propagation of the errors [7] instructing on the sample was performed, which represented a set of binary images of the electrode imprints.

Investigation of efficiency of the recognition methods. Efficiency of the investigated methods of recognition of the electrode imprints was estimated experimentally by their check on the test images. A set of nine digital images, which significantly differed from each other by general level and range of brightness, were used as test specimens. Their characteristic feature was distortion of brightness because of patches of light and low contrast range of contours of the required object. The investigated algorithms were implemented in the form of a program module in programming language C++. As criterion of the recognition efficiency percentage of the errors was used equal to the ratio of number of the recognition errors to general number of objects on the test images.

As a result of check of the developed recognition algorithms on test images it was established that they were characterized by rather high efficiency. Spatial positions of the required objects were determined sufficiently accurately using the suggested algorithms. In recognition of the test images using the developed algorithms 4–9 % of errors were made. The most efficient turned out to be the recognition algorithm using an artificial neuron network (4 % of errors). Somewhat less efficient was algorithm of statistical recognition

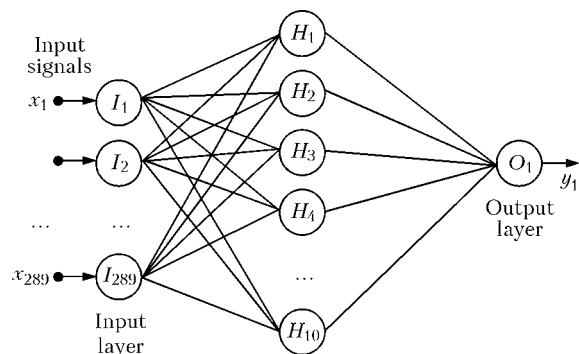


Figure 3. Multilayer artificial neuron network with direct propagation of signal

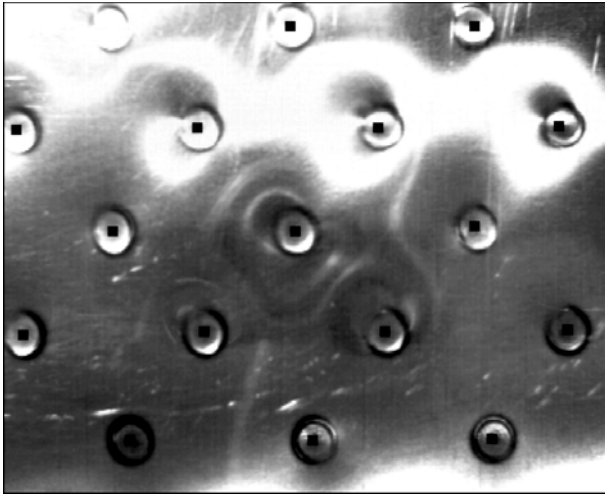


Figure 4. Result of recognition of electrode imprints using statistical method (black squares — centers of electrode imprints)

(6 % of errors). The least efficient was correlation algorithm (9 % of errors). As a rule the errors occurred in recognition of low-contrast objects, contours of which were poorly singled out against background of the base metal. Reason of the errors was imperfection of the equipment for producing initial images. In Figure 4 the digital image is presented on which electrode imprints were recognized using the statistical method.

Algorithm for correction of recognition errors.

For correction of the electrode imprint recognition errors the algorithm was developed which detected noises that were erroneously assumed as electrode imprints and determined coordinates of the imprint centers not detected during recognition. Principle of action of this algorithm is based on aprioristic data on character of mutual arrangement of the electrode imprints on surface of a three-layer structure (Figure 5).

So, the considered methods of automatic recognition of the electrode imprints are sufficiently efficient. Using means of geometrical adaptation implemented on basis of suggested methods of recognition of the electrode imprints it is possible to significantly in-

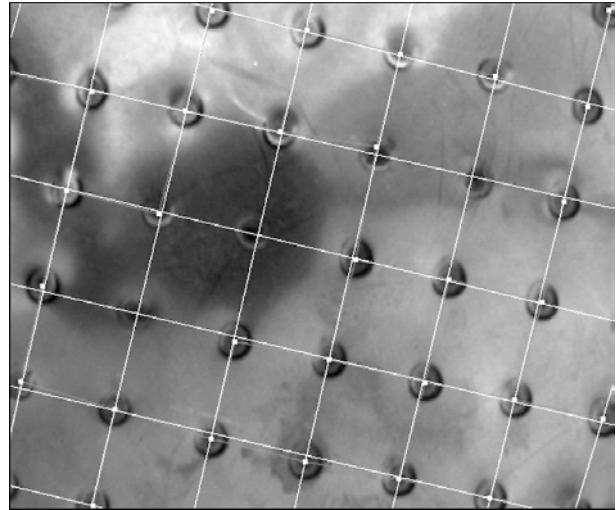


Figure 5. Determination of coordinates of electrode imprint centers using algorithm for correction of recognition errors (in nodes of mesh consisting of white lines are centers of required electrode imprints)

crease rate and accuracy of the welding head positioning in welding of three-layer honeycomb structures. Results of this work may be used for development of automated systems for spot welding of three-layer structures.

1. Gonsales, R., Woods, R. (2006) *Numerical image processing*. Moscow: Tekhnosfera.
2. Prett, U. (1982) *Numerical image processing*. Moscow: Mir.
3. Gruzman, I.S., Kirichuk, V.S., Kosykh, V.P. et al. (2000) *Numerical image processing in information systems: Manual*. Novosibirsk: NGU.
4. Fukunaga, K. (1979) *Introduction in statistic theory of pattern recognition*. Moscow: Nauka.
5. Michie, D., Spiegelhalter, D., Taylor, C. (1994) *Machine learning, neural and statistical classification*. New York: Ellis Horwood.
6. (2003) *Neurocomputers in image processing systems*. Ed. by A.I. Galushkin. Book 7. Series Neurocomputers and Their Applications. Moscow: Radiotekhnika.
7. Kalan, R. (2003) *Main concepts of neuron neural nets*. Moscow: Williams.
8. Forsait, D.A., Pons, J. (2004) *Computer vision. Current approach*. Moscow: Williams.



CURRENT STATUS OF WELDING CONSUMABLES PRODUCTION IN RUSSIA

Z.A. SIDLIN

TEKHPRM Ldt, Moscow, Russia

The current status of welding consumables production in Russia is considered. Positive tendencies in this economic sector over the recent years are noted. Alongside, there are also problems associated with falsification in welding consumables market, with ensuring the stable quality of consumables, service personnel qualifications, and need to improve the raw materials quality.

Keywords: *welding industry, welding consumables, coated electrodes, positive factors, quality, raw materials*

Production of welding consumables in Russia, first of all of coated electrodes, has a sufficiently good progress. It is well known that application of welding consumables correlates with steel consumption. However, according to the last indicator, as Russia is significantly (more than 2 times) behind the economically developed countries, it is necessary to properly evaluate perspectives of the domestic market of steel and welding consumables [1].

According to Rosstat data, production of welding consumables increased by 10.2% in 2007 in comparison with 2006, and made up 183,600 t. Electrodes still constitute the main portion of welding consumables (approximately 78%), which complies with the level of mechanization of welding processes in India. Welding wire production (apart from that included in electrode composition) makes up 35,000 t, fluxes — 17,000 t, and flux-cored wire — 5,000 t. It is seen that the relationship of portions of different welding consumables is far from the modern level of development of the welding industry. It can be noted that the portion of manual arc welding in developing China has reduced already to 63.4% [2]. The situation with welding fluxes becomes better owing to organization of their production at ESAB-SVEL plant in St.-Petersburg, as well as planned start of the second line of production of ceramic fluxes at Chelyabinsk Tube-Rolling Mill in 2009 with bringing flux throughput up to 14,000 t per year. The output of copper-coated welding wire increased by 11,000 t per year owing to a line launched at Oryol plant «Severstal-metiz» in 2008. According to the estimate by consulting company «Frost and Sullivan», the main sector of the welding industry market in Russia is welding consumables, which in value terms make up 65% of its volume [3].

The leading electrode manufacturers situated in different regions of the country (Table) demonstrate positive dynamics of growth of electrodes production. Total output of these manufacturers makes up 93–96% of national one. What is especially good is that the growth is taking place regardless closing of the series of continuously working electrode manufacturers, including large ones (10,000–60,000 t per year) in recent

years. Most of the closed manufacturers were highly expensive, technically outdated and manufactured low quality bulk products, the demand for which permanently decreased. However, the available facilities, including the newly launched and modernized, are quite enough to meet the current demand for electrodes. The portion of imported electrodes in the Russian market is not large, and made up 13,600 t (8.2%) in 2006 [4].

At the same time, consolidation of a number of medium-capacity facilities (with output of up to 10,000 per year), which are characterized by a high mobility and possibility of diversification of production (Sychevsk Electrode Plant, St.-Petersburg Electrode Plant, Mezhhgosmetiz-Mtsensk, SZSM, Volgondsk Electrode Plant, etc.) as well as of small-size factories manufacturing special electrodes (Welding Consumables Plant in Berezovsk, «Electrode Service» in Moscow region, etc.), which are continuously upgrading their production, took place.

In the recent time, a weight-average diameter of the produced and used electrodes, as well as of alloyed welding wire for mechanized welding (the share of 0.8–1.6 mm wire is 64%) has significantly decreased.

The positive factor promoting improvement of quality of the produced welding consumables was transfer of highly skilled and experienced personnel from higher education institutions and research and development institutes directly to production: ZSM (group of candidates of technical sciences under the leadership of A.N. Balin, LEZ (Prof. Yu.M. Belov), LOEZ (candidate of technical sciences I.S. Ioffe), etc.

Other positive tendencies seen in the domestic Russian market include improvement of the production accuracy, quality of dressing of end-faces, appearance and packing of electrodes, their apiece marking, increase in output of welding copper-coated wire on eurocassettes with a series layer winding, etc.

Undoubtedly, increase of a range of power sources and improvement of their characteristics, extending technological capabilities of the existing range of electrodes, is very important as well.

All the above-stated provide today the domination of products of Russian manufacturers in the domestic market, the import quota being sufficiently low. However, the problems accumulated in consumables production partially transferred from the earlier times,

Output of electrodes in Russia in regions, thou t

Region	2005	2006	2007	2007/2006, %
Russia, total, including	158.1	166.6	183.6	110.2
Moscow	31.6	36.4	43.9	120.5
Oryol region	26.3	33.3	31.8	95.3
St.-Petersburg	15.7	18.4	23.1	125.4
Rostov region	12.5	16.7	17.6	105.7
Chelyabinsk region	13.4	12.1	13.1	108.4
Kostroma region	6.0	8.0	10.0	124.2
Tyumen region	10.0	9.9	9.3	93.6
Smolensk region	5.2	5.7	6.6	114.3
Sverdlovsk region	5.6	4.2	5.8	136.6
Nizhegorodskaya region	3.8	4.9	4.8	97.5
Penza region	3.8	3.7	3.9	104.3
Kurgan region	3.4	3.2	2.9	89.8
Moscow region	2.5	2.4	2.6	106.1

and also the new ones, need some time to be effectively solved in order to maintain a national manufacturer.

For electrodes manufacturers and customers, one of the most serious points is identification of a product to reveal and/or prevent falsification. In the welding industry, different electrodes are mainly identified from their marking, which is established by technical documents of developing (manufacturing) organizations. In the former USSR and in the post-Soviet area, a letter designation of electrode grades in a coded and legally unprotected form, as a rule, stands for the name of a developing organization, which in most cases is not a manufacturer. According to the existing legislation, normative-technical documents are transferred from a developer to manufacturer mostly free of charge, i.e. «as a technical assistance». Therefore, at present ANO, MR, OZS, OZL, TsT, EA etc. series electrodes are produced, as a rule, without supervision of a developer. Moreover, there are the cases where documents for electrodes, sometimes even in the form of collections, are distributed by outside organizations and natural entities on a market basis. Besides, modernization of electrode grades carried out by manufacturing organizations, without a developing organization knowing about it, is aimed mainly at reduction of the cost value of electrodes, and often to the detriment of their quality characteristics. As a result, as well as due to a significant difference in technical level of different manufacturers, which nominally produce electrodes of the same grade, the electrodes that have the same grade designation, but are produced by different manufacturers, could significantly differ in their properties. Although up to now part of these trade marks has been patented in Russia (and Ukraine) (moreover, far from always by authors or their legal representatives), this has had no effect on the manufacturers' practice [5].

In order to distinguish their products among the similar ones, a range of enterprises introduce now

double grade designations, supplemented by plant designations. Also, a civilized process of emergence of the true trade marks is taking place.

Electrode manufacturers face in their practice with falsification of the supplied raw materials and welding wire (change of grades and trade marks, falsification of certificates of quality and origin, etc.). Also, electrode manufacturers themselves can supply false electrodes from commercial considerations (using cheaper ilmenite in the guise of rutile, with significantly changed composition of coating in comparison with that characteristic of the grade, or produced on a wire that does not correspond to the regulatory documents, etc.) As applied to the electrodes, which are an important type of products, providing reliability and safety of parts to be welded, such falsification is not allowable. Moreover, at enterprises which do not have specialists of a required qualification and necessary checkout-and-testing equipment, changes in the known grades are introduced through orientation to purely external characteristics, and only to some of the indicators of their welding-operational characteristics. The problem of falsification is characteristic of the entire Russian market and CIS countries as a whole, and it is necessary to fight against it first of all legislatively at the government level.

At the same time, falsification should not be confused with «substitute products». For example, the electrodes with ilmenite coating are valid products, which successfully replace rutile electrodes in some applications, but their markings, certificates, shipping and information documents should indicate their original name, and their price should correspond to quality and origin.

According to data of the above-mentioned consulting company «Frost and Sullivan», Russian consumables are just a bit inferior to foreign ones in their welding-operational characteristics and design, but their lower price is the key competitive advantage at RF market, which is highly sensitive to price (Russian manufacturers and customers themselves consider this difference more significant). However, this advantage is lost due to a significant increase in prices, and primarily in the price of metal. Thus, since April 2008, the Russian leading metallurgical companies, such as Severstal, Mechel, Magnitogorsk and Novolipetsk metal industrial complexes, again increase prices for metal rolled stock (on average by 35–40 %), referring to increase in prices of raw materials. Meanwhile, most of Russian metallurgical companies, which are vertically integrated structures, have in their own significant iron ore resources. Thus, NLMK has 96 %, and Evraz and Severstal have 80 % of their ore demand [6].

«Metallurgical factor» may have the most negative influence on a state of the Russian economy as a whole, including consumables. In such cases, the country has the right and is obliged to interfere and take the control of situation. The effectiveness of such interference can be seen at a well known example of Mechel.

Naturally, welding consumables manufacturers were forced to raise the prices. However, the price policy of different manufacturers is significantly different. Thus, analysis of the prices of the three leading plants shows increase of 27, 24 and 16 % in prices for



general-purpose electrodes, a price for high-alloy electrodes (following nickel price) reduced approximately by 6 % at the two plants, and at the third plant — an increase of 23 %.

Sometimes it is stated that disadvantages of domestic electrodes are related to «outdated covering formulas», i.e. covering compositions [7]. In our opinion, this is true only for narrow-purpose electrodes, for example, for welding of the root layers in butt joints on main pipelines. Providing that the time-proved compositions and manufacturing technologies are kept to, Russian electrodes, according to the quality indicators, are sufficiently competitive. In particular, successful work of the ESAB-SVEL enterprise (St.-Petersburg) in Russia with 100 % Swedish capital proves this fact, producing Russian electrode of the UONI, OZS and other grades alongside with the OK grade electrodes, and developing its output.

The main problem for providing electrodes competitiveness is related to their quality consistency. Namely, quality inconsistency, which is peculiar to products of many plants and related, generally, to their low technical level, dramatically reduces competitiveness of domestic electrodes. It is well known that the electrodes manufacturing technology has a direct and often decisive influence on physical and metallurgical processes taking place during weld formation, and therefore, on weld quality and welding-operational characteristics of electrodes. Positive properties of any good electrode grade could come to nothing if the problems of their commercial manufacturing technology are not satisfactorily solved. Proper solution of these problems at present is more important than rarely justifiable «invention» of infinite number of new electrode grades or «modernization» of the existing ones [8]. This statement is true in our time as well.

Among the characteristics that determine the technical level of production, the level of qualification of workers of the main specialities, as well as of technicians and engineers, is very significant. This is especially painful for welding consumables production, where under the Soviet time, as well as now, training of the personnel has been performed only directly at a plant at the absence of modern literature. To some extent, publication of monograph «Production of Electrodes for Arc Welding» will help to reduce acuteness of this problem [9].

Even with highly qualified personnel, the influence of a human factor could be minimized only through reasonable automation of control of working operations control and a technological process as a whole. At the present level of development of electrode plants and their financial condition the one-stage integrated automation of the whole production seems to be irrational even for large plants. The process approach to production automation, according to one of the fundamental principles of ISO 9000, is more effective. Automation of separate processes in the technology, i.e. local processes, in addition to «pluses» obtained from the possibility to control and manage

them in real time, significantly increases stability of parameters and quality of products. Such step-by-step approach, taking into account tasks and current possibilities of a specific enterprise, and creating conditions for production automation as a whole, makes it possible to actively receive a real profit from introduction of particular stage [10].

Practical implementation of most of the technological operations with a high level of reliability requires a significant improvement of quality the feed stock or technology of its prior preparation at a factory manufacturing welding consumables. However, the task of supplying necessary quality raw materials and ferroalloys is a many years' problem. This is due to a general situation in the field of raw materials and manufacturing sectors [11], as well as to small ranges of application of components, increased requirements to them imposed by welding consumables manufacturers, absence of unified approaches employed by different electrode manufacturers, most of which follow the line of the least resistance and agree to use low-quality materials. Most of electrode manufacturing enterprises use the wait-and-see attitude and make no investments in investigations of new materials and their implementation. The successive work on the expansion of sources of raw materials in welding consumables production is carried out, perhaps, only by Central R&D Institute of Structural Materials «Prometej» [12, 13].

Without solving the problem of raw materials, neither stable quality assurance nor increase of a general level of welding-operational characteristics of electrodes, according to which Russian electrodes (like the CIS ones as a whole) are inferior to the best commercial products, is possible. So, the efforts on increasing and stabilizing the welding-operational characteristics become the central task of domestic welding consumables manufacturers.

1. Sidlin, Z.A. (2005) Electrode production in Russia. *Svarochn. Proizvodstvo*, **10**, 35–37.
2. Bernadsky, V.N., Makovetskaya, O.K. (2007) *SVESTA-2007*. Kyiv: PWI.
3. (2006) Russian and Ukrainian markets of welding technique according to estimation of Frost and Sullivan Company. *Svarshchik*, **49**(3), 4.
4. Bunakova, O., Khazanov, L. (2008) Jewellers of wire products. *Metallosnabzhenie i Sbyt*, **1**, 86–88.
5. Sidlin, Z.A. (2007) To problem of quality of current national electrodes for manual arc welding. *Svarochn. Proizvodstvo*, **12**, 32–34.
6. Maleev, V. (2008) Bright future is postponed. *Izvestiya*, April 8.
7. Ioffe, I.S., Gavrilin, Yu.M. (2004) Increase in competitiveness of Russian electrodes. *Svarochn. Proizvodstvo*, **4**, 50–51.
8. Sokolov, E.V. (1950) Electrodes with quality coatings for arc welding. *Avtogennoe Delo*, **11**, 26–30.
9. Sidlin, Z.A. (2008) *Production of electrodes for arc welding*. Kiev: PWI.
10. Sidlin, Z.A., Goldinbert, P.I., Vetrov, D.V. (2008) Automation of welding consumable production — increase in quality stability. *Svarochn. Proizvodstvo*, **2**, 37–39.
11. Leontiev, L.I., Yusfin, Yu.S., Malysheva, T.Ya. et al. (2007) *Source of raw materials and fuel of ferrous metallurgy*. Moscow: Akademykniga.
12. Nikolae, A.I., Gerasimova, L.G., Petrov, V.B. et al. (2004) Titanium and titanium rare-mineral raw materials of Kolsky peninsula as a source of traditional and new welding consumables. *Svarochn. Proizvodstvo*, **9**, 45–49.
13. Nikolae, A.I., Petrov, V.B., Pleshakov, Yu.V. et al. (2008) Characteristics of raw material source in Murmansk region, components of electrode coatings and fluxes for welding. *Ibid.*, **5**, 32–36.

TO THE 60th ANNIVERSARY OF INDUSTRIAL APPLICATION OF THE TECHNOLOGY OF MANUFACTURING CYLINDRICAL TANKS FROM COILED BLANKS

A.Yu. BARVINKO, Yu.P. BARVINKO and V.M. GOLINKO
E.O. Paton Electric Welding Institute, NASU, Kiev, Ukraine

The historical aspect of introduction and development of the method and technology of construction of vertical cylindrical tanks with application of large-sized coiled blanks is considered. The advantages, disadvantages and prospects for further application of the method are described.

Keywords: *coiled blank, welded tanks, site weld, angular deformations, geometrical shape of the wall*

60 years ago the first vertical cylindrical tank of volume $V = 240 \text{ m}^3$, the bottom and wall of which were assembled from coiled blanks by their forced deployment in site was constructed in a tank farm in Kiev. The idea of assembling the tank wall and bottom from coiled blanks with overall dimensions suitable for railway transportation, was proposed by Prof. G.V. Raevsky at PWI in 1944 [1] and successfully implemented under production conditions in 1948 at construction of a tank in Kiev (Figure 1). In view of the obtained results, machines of a rather simple design for making coiled blanks by one-sided automatic submerged-arc welding were constructed in Kujbyshev and Saratov (Russia), which allowed already in 1952 mounting 152 tanks by the coiling method [2] (a new method of tank construction). Specialists of PWI, Ministry of Oil Industry and Minmontazhspejsstroj of the USSR participated in development of this process and its broad introduction into production. In 1958 A.E. Ignatchenko, G.V. Raevsky (Work Supervisor), E.K. Alekseev, V.M. Didkovsky, O.M. Ivantsov, V.S.

Kornienko, V.S. Laykhov, B.V. Popovsky received the Lenin award for development and introduction of the industrial process of construction of tanks for oil storage from flat panels, rolled up into coils.

The country's post-war need to rebuild the destroyed industry in the shortest term promoted an intensive introduction of the coiling method. Tank farms for storage of oil and petroleum products were established practically from scratch. Under the conditions of an acute shortage of qualified welders and climbing cranes, when it was impossible to conduct welding and mounting operations in winter because of weather conditions, deployment of a coiled wall (or its part) and bottom directly in the construction site was a considerable step forward.

Performance of the operations of assembly and welding of the main structures in the plant with application of automatic submerged-arc welding, allowed an essential improvement of their quality and shortening the manufacturing time. Erection organizations successfully mastered construction of up to $5,000 \text{ m}^3$ tanks inclusive with up to 10 mm wall thickness from coiled blanks [3].

In 1960–1970s the coiling method was developed further in connection with an abrupt increase of the volumes of transportation of Siberian oil into the European part of the Soviet Union. The government of the country set the task of construction of oil processing plants and the main pipelines for its transportation in the shortest term, and in all these enterprises it was necessary to mount large tank farms of the volume of $V = 5,000, 10,000, 20,000$ and $50,000 \text{ m}^3$. Manufacturing coiled blanks with application of steels of increased and high strength of up to 17 mm thickness required development of a new generation of mills for their welding and coiling, as well as development of the technology of mounting tank walls of a considerable thickness.

In the newly built mills the operations of sheet feeding and panel assembly were fully mechanized. Technology of two-sided automatic welding with the total pneumatic pressing down of the edges ensured a good quality of the welds at up to 17 mm sheet



Figure 1. First welded tank of 240 m^3 volume built by the coiling method in Ukrneftesnab oil tank farm in Kiev in 1948

© A.Yu. BARVINKO, Yu.P. BARVINKO and V.M. GOLINKO, 2009

thickness inclusive without edge preparation [3]. Just in one plant fitted with such mills, it was possible to manufacture coiled blanks for 240 tanks of $V = 10,000 \text{ m}^3$ during one year (Figure 2), thus allowing mounting of practically all the tanks of up to $50,000 \text{ m}^3$ capacity inclusive by the coiling method.

In 1970–1980s during intensive construction of large-volume tanks from coiled blanks with application of steels of increased and high strength, the insufficient scope of research on operational reliability of coiled tank wall during the guaranteed service life (20 years) became obvious. As a result, fatigue cracks started initiating in the vertical site butt joints of the wall in many tanks ($V = 20,000$ and $50,000 \text{ m}^3$) after 10–12 years of operation. The main causes for their development were considerable angular deformations [4] and low-cycle loading of the wall. For tanks of $V = 20,000 \text{ m}^3$ special guidelines were developed for reinforcement of the site butt welded joints of the wall at initiation of cracks in them [5]. It was proposed to perform local reinforcement of the wall by welding horizontal stiffeners in the butt joints. However, under the conditions of low-cycle loading this quite often led to fracture of fillet welds, which were used to attach the stiffeners to the wall, so that the recommendations of the above guidelines were soon rejected.

Angular deformations in the butt joint result from the presence of rectilinear sections of the wall along the vertical edges of the coil panels. Ensuring their curvature close to that of the design curvature of the tank wall along the entire height turned out to be a quite complicated task in site. The necessary engineering solutions were sought, which allow making site butt joints with admissible angular deformation [6]. Today, however, there is no acceptable technology for making the vertical site butt joints on coiled blanks, taking into account the currently valid standards [7, 8], for more than 10 mm ring thickness without application of additional structural elements.

Considering the availability of a large number of coiled tanks ($V = 10,000$, $20,000$ and $50,000 \text{ m}^3$) in the country's tank farms, in 1987/1988 PWI upon the assignment of USSR Minnefteprom performed investigations to assess the residual life of vertical site butt joints of the wall from steels VSt3sp5, 09G2S-12 and 16G2AF in the presence of angular deformations in them (deflection f is up to 20 mm at template length of 500 mm). The obtained results were entered as the recommended ones into the codes for mounting tanks from coiled blanks [9]. Investigation results demonstrated an essential reduction (particularly for 09G2S and 16G2AF steels) of the number of loading cycles up to initiation of fatigue cracks at increase of the deflection. At the change of values f from 5 to 10 mm for 09G2S steel and from 2 to 4 mm for 16G2AF steel, the number of loading cycles up to initiation of a visually observable crack decreased from $10 \times 1 \cdot 10^3$ to $5 \times 1 \cdot 10^3$. Obtained results were used in development of new codes for tank mounting [7, 8].

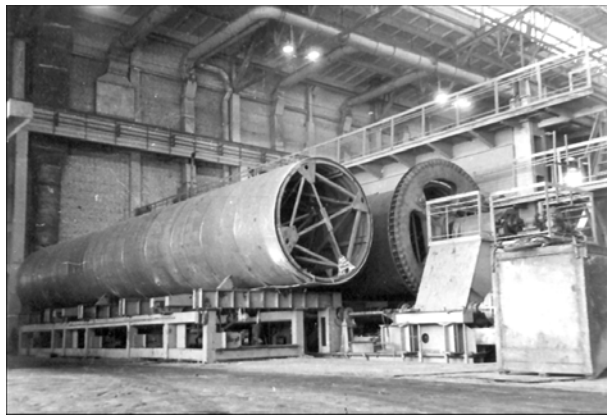


Figure 2. Mill for manufacturing large welded coiled panels built at Novokuznetsk Plant of Tank Metal Structures in 1974

Achievement of the design geometrical shape of the tank wall at application of coiled blanks is influenced by one more factor, alongside the angular deformations. After assembly and welding of panels of up to $18 \times 32 \text{ m}$ size and up to 50 t weight in the bench, they have the geometrical shape close to a rectangle. After positioning the coils in a vertical position, a local sagging of the coil base occurs under the action of its weight. With decrease of the coil weight at its deployment, sagging of the base under it will also become smaller (Figure 3). Considering the tolerance on difference in foundation marks of up to 15 mm [10], during deployment the panel lower edge takes on a curvilinear shape. Such a change of the geometrical shape of the edge leads to development on the lower thicker rings of extensive shallow protrusions and dents, the depth of which in most cases does not exceed the admissible value. The upper thinner rings form horizontal folds (corrugations) and dents, which abruptly change their shape at filling/discharging of the product through «popping-out», which may lead to wall rupture.

The above drawbacks, as well as requirements of the new Ukrainian codes [7] to wall thickness and its geometrical shape, led to the fact that now in Ukraine practically all the tanks with the lower ring thickness of 10 mm and more are made of separate sheets. Application of sheets of up to $8.0 \times 2.5 \text{ m}$ size essentially



Figure 3. Construction of a tank of $50,000 \text{ m}^3$ volume from welded coiled blanks (1974)



reduces the volume of welding operations in the construction site. Here the actual deviations of the wall geometrical shape often are 2 to 1.5 times smaller than the norms.

As in 2000 most of the tanks of the capacity of $V = 20,000$ and $50,000 \text{ m}^3$ built with application of coiled blanks have operated for their specified service life (20 years) under the conditions of low-cycle loading, and all the vertical site welded joints of the wall have practically exhausted their design operating life, PWI developed the technology of replacement of site butt joints along the entire wall height [11]: wall sections with a vertical weld are sequentially cut out and special inserts are welded in instead of them. Geometrical shape of the inserts prepared for welding allows for the wall pre-stress and features of welding performance under the conditions of a rigid contour. After welding in the inserts the vertical site joints become a regular section of the wall with shifted vertical welds within the ring or enlarged inserts, and meet the requirements of the codes [7, 8].

The advantages of the coiling method enabled its acceptance also in modern fabrication. This is a large tank park with the maximum wall thickness of up to 10 mm with volume $V \leq 5,000 \text{ m}^3$. In addition, coiled blanks with sheet thickness of up to 6 mm inclusive are used successfully for mounting bottoms of large-volume tanks.

In connection with the fact that the same tank wall thickness was preserved in the new Russian norms [8], the coiling method is currently also used in this

country alongside construction of tanks from individual sheets. The site butt joint is made not as one line, but in the form of a «comb» with shifting of vertical joints in the adjacent rings for distance $8t$ (where t is the greatest of sheet thicknesses in the adjacent rings). To increase the rigidity of the sections of the wall upper rings adjacent to the site weld, additional structural elements are mounted in some cases.

1. Raevsky, G.V. (1952) *Producing steel vertical cylindrical tanks by method of coiling*. Moscow; Leningrad: Gostoptekhizdat.
2. (1962) *Coiling of sheet structures*. Ed. by L.L. Zilberberg. Moscow: TsBTTI.
3. Biletsky, S.M., Golinko, V.M. (1983) *Industrial production of outside welded sheet structures*. Kiev: Naukova Dumka.
4. Barvinko, Yu.P., Biletsky, S.M., Golinko, V.M. et al. (1991) About tolerances on angular deformations of vertical welded butt joints in tanks of 10–50 thou m^3 capacity. *Avtomatich. Svarka*, 4, 20–23.
5. RD-39-30-1331–85: Instructions on reinforcing of vertical site butt joints of walls of RVS-2000 tanks. Introd. 01.01.86.
6. Popovsky, B.V., Ritchik, G.A. (1986) Ensuring the geometrical shape of the coiled tank walls in zones of site butt joints. *Montazh. i Spets. Raboty v Stroitelstve*, 11, 11–15.
7. VBN V.2.2.-58.2–94: Vertical steel tanks for storage of petroleum and petroleum products. Valid from 01.10.94.
8. PB 03-605–2003: Rules for installation of vertical cylindrical steel tanks for petroleum and petroleum products. Introd. 09.07.03.
9. VSN 311–89: Erection of steel vertical cylindrical tanks for petroleum and petroleum products from 10,000 up to 50,000 m^3 . Introd. 01.01.90.
10. SNiP 3.03.01–87: Load-carrying and frame structures. Valid from 01.06.88.
11. Makhnenko, V.I., Barvinko, A.Yu., Barvinko, Yu.P. et al. (2002) Estimation of stressed state of the wall of coiled vertical cylindrical tanks in welding-in of sheet inserts. *The Paton Welding J.*, 5, 2–6.

EFFECT OF CARBON ON PHASE COMPOSITION OF WELD METAL OF WELDED JOINTS IN MARTENSITIC STEEL WITH 9 % Cr

V.Yu. SKULSKY and A.R. GAVRIK

E.O. Paton Electric Welding Institute, NASU, Kiev, Ukraine

The character of variations in phase composition of the 10Kh9MFB type weld metal depending upon its carbon content was analysed. It was found that single-phase martensitic structure of the welds could be provided at their carbon content of not less than 0.085 %. Decreasing the carbon content below the above limit leads to formation of δ -ferrite in structure of the welds.

Keywords: arc welding, tungsten electrode, filler, martensitic steel with 9 % Cr, weld metal, carbon, phase composition, formation of δ -ferrite

Arc welding of heat-resistant steel 10Kh9MFB is performed by using the welding consumables which provide alloying of the weld metal similar to that of the base metal. In manual arc welding with covered electrodes and in automatic submerged-arc welding, both welds and base metal have a martensitic structure. However, TIG welding (in argon atmosphere, with tungsten electrode and filler wire of the 10Kh9MFB

type) leads to a change in phase composition of the weld, i.e. formation of light regions of δ -ferrite in the martensitic metal. Characteristic features of δ -ferrite in this type of the metal are low hardness in the as-welded condition ($HV0.2-190-200$ for δ -ferrite, and approximately $HV 415$ for martensite), the same hardness and the absence of carbide precipitates in it after annealing, which is indicative of decarburisation of this phase and its insensitivity to hardening [1]. It is reported that formation of δ -ferrite in martensitic chromium steels and their welded joints causes decrease in high-temperature ductility and impact toughness, and sensitivity to cold cracking [2–5]. Although



the presence of up to 10–15 vol.% of ferrite in the martensitic metal was considered acceptable [2, 4], the results of relaxation tests of loaded welded joints in steel with 9 % Cr show that the presence of very thin interlayers of soft δ -ferrite in the martensitic welds leads to formation of cracks during heat treatment [6, 7]. To decrease the risk of cracking and improve mechanical properties of the weld metal, it is necessary to avoid formation of δ -ferrite in it, thus providing the homogeneous martensitic structure. The authors of study [8] advanced the same opinion.

As follows from the constitutional diagrams of iron-chromium systems [2], formation of δ -ferrite is strongly affected by changes in the carbon content, i.e. decrease in the carbon content is accompanied by increase in stability of δ -ferrite, which may lead to its higher content in the resulting structure of martensite. This effect takes place in TIG welding, which was experimentally established by the authors of the present study and is described in literature. For example, it is noted in [9] that the problem of TIG welding of steel P91 with 9 % Cr (of the 10Kh9MFB type) is an «intensive burning out of carbon» to a level of less than 0.08 %, and deterioration of properties of the welds. The mechanism of this phenomenon was not considered. However, it can be presumed that the cause of the loss of carbon in the weld may be related to its evaporation during concentrated overheating of the melt by the arc with a high current density, which is characteristic of the arc burning in inert gases, as well as to its partial oxidation due to oxygen impurities present in the shielding gas [10].

The purpose of this study was to determine the minimal carbon content of the weld metal in welding martensitic steel of the 10Kh9MFB type, at which the welds would contain no δ -ferrite.

The study considered the phenomenon of decrease in the carbon content of the weld metal in TIG welding. The TIG process was used to fill up the V-grooves 6 mm deep in 14 mm thick plates of steel P91 (X10CrMoVNb91 of the 10Kh9MFB type) by using filler rods of a similar chemical composition. Heat input q/v was varied approximately from 15 to 30.8 kJ/cm by varying the current from 120 to 250 A at a welding speed of 2.16–2.6 m/h. The contents of carbon and δ -ferrite in the welds were determined

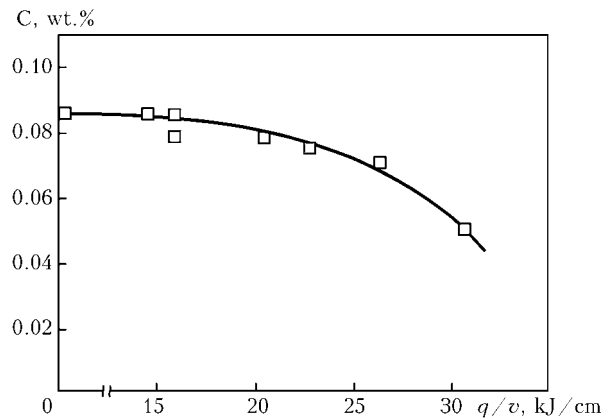


Figure 1. Variation in carbon content of the weld metal in TIG welding of steel of the 10Kh9MFB type

after welding. To better reveal the presence of δ -ferrite, the weld samples were subjected to high tempering. The content of the ferritic phase was evaluated by multi-frame panoramic photography of the microstructure in cross sections of the welds in a direction of secants from one end of the weld to the other, followed by counting the areas occupied by the ferritic regions in the tempered martensite matrix by using coordinate scales. The approximate content of ferrite in the welds was determined after averaging results of all the measurements.

It was found as a result of the experiments that increase in heat input during TIG welding leads to decrease in the carbon content of the weld metal (Figure 1). At $q/v \sim 14$ –15 kJ/cm the losses of carbon are insignificant, its residual content of the weld is about 0.087 %, which is hardly different from its initial concentration in filler metal. An intensive decrease in the carbon content takes place in welding at $q/v > 20$ kJ/cm. Process parameters with this heat input should be excluded. Parameters of TIG welding with a heat input of not higher than 13–15 kJ/cm can be considered acceptable in terms of limitation of substantial carbon losses.

Decrease in the carbon content leads to formation of δ -ferrite in the deposited metal. As shown by metallography, δ -ferrite is non-uniformly distributed in the welds. In one and the same weld it is possible to see the regions restricted by the microscope sight field, which contain either no δ -ferrite (or small amount of

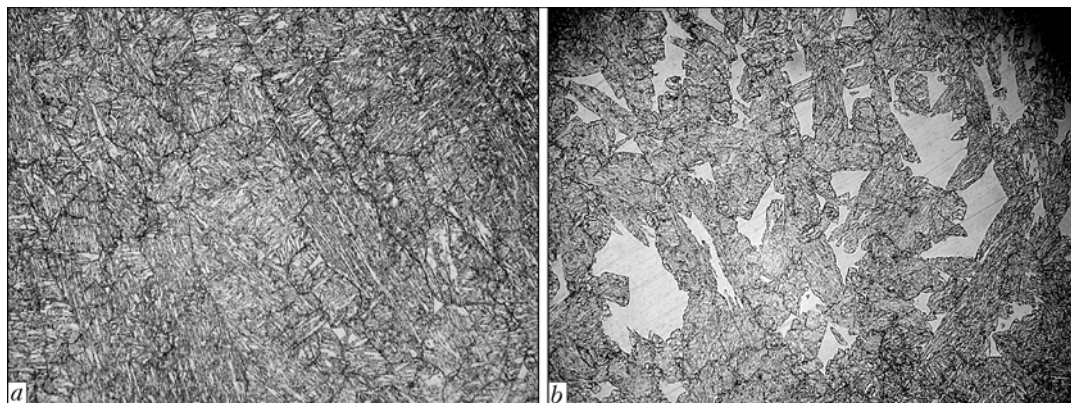


Figure 2. Microstructure of regions of the welds with different average contents of δ -ferrite: a — 0.86; b — 17.1 vol.% ($\times 200$)

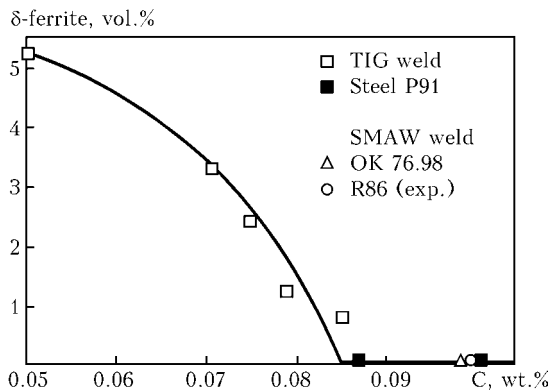


Figure 3. Effect of carbon on δ -ferrite content of martensitic metal with alloying system of the C-9Cr-Mo-V-Nb type

δ -ferrite) or its high local amounts (Figure 2). The ferrite regions grew in size with increase in the δ -ferrite content, which can also be seen in Figure 2. A high amount of ferrite usually formed in the upper part of the welds in cover beads, as well as within the active spot region, where the degree of decrease in the carbon content was likely to be maximal.

Figure 3 shows the results of evaluation of the content of δ -ferrite in the welds depending upon the carbon content. Additionally marked in the Figure are the carbon contents in the welds made with electrodes OK 76.98 (ESAB) and R86 (experimental electrodes produced by the E.O. Paton Electric Welding Institute), and in steel P91 (two different batches) having a single-phase martensitic structure. It follows from the dependence presented that the absence of δ -ferrite in the weld can be achieved at a carbon content of not less than 0.085 %.

Carbon exerts a dual effect on properties of the martensitic metal. In addition to compensation for the effect of ferritising elements and limitation of formation of δ -ferrite, carbon also acts as a main element that strengthens the martensite solid solution. Increasing the carbon content leads to growth of the degree of hardening and increase of the sensitivity of the welded joints to cold cracking. To ensure a satisfactory weldability, the maximal carbon content in multi-component martensitic steels, where the steels with 9 % Cr belong to, as well as in the weld metal is limited to about 0.12 %. Such steels are characterised by the sensitivity to hardening, which is one of the metallurgical factors for imparting them the required heat-resistant properties [2]. Therefore, to avoid cracking, it is necessary to use preliminary and concurrent heating to weld these steels. The minimal carbon content of the welds, as shown above, is determined from a condition of maintaining the homogeneous martensitic structure containing no δ -ferrite.

It should be noted that, in addition to carbon, nickel deliberately added in an amount of 0.4–1.0 %

[11], as well as manganese used as a deoxidiser, also prevent formation of δ -ferrite in metal with the C-9Cr-Mo-V-Nb alloying system. According to different data, carbon is 10–30 times more efficient than nickel, and 20–60 times more efficient than manganese in the degree of stabilisation of austenite and decrease in the δ -ferrite content of the chrome metal [2, 12]. Therefore, it is carbon that exerts the main effect on phase composition of the welds. In our experiments the nickel content was kept at a lower limit (approximately 0.4 %), which is typical for steel P91 being welded. To ensure the single-phase martensitic structure under conditions of the liquation heterogeneity developing in solidification of the weld metal, especially with a decreased carbon content, and provide a satisfactory impact toughness, the weld metal should be alloyed with nickel to a level close to its upper limit [13] (approximately 0.7–1.0 %).

It should be noted in conclusion that to avoid decrease in the carbon content of the welds in TIG welding of steel of the 10Kh9MFB type, it is necessary to use parameters with a heat input of about 13–15 kJ/cm. The condition for ensuring the single-phase martensitic structure of the weld metal with the C-9Cr-Mo-V-Nb alloying system is limitation of the maximal carbon content to approximately 0.085 %.

1. Skulsky, V.Yu. (2005) Metal structure in the fusion zone and HAZ of welded joints on high-chromium heat-resistant steels. *The Paton Welding J.*, **5**, 10–18.
2. Lanskaya, K.A. (1976) *High-chromium heat-resistant steels*. Moscow: Metallurgiya.
3. Zaruba, I.I., Kasatkin, B.S., Kakhovsky, N.I. et al. (1960) *CO₂ welding*. Kiev: Gostekhizdat Ukr. SSR.
4. Kakhovsky, N.I., Fartushny, V.G., Yushchenko, K.A. (1975) *Electric arc welding of steels*. Kiev: Naukova Dumka.
5. Yuferov, V.M. (1968) About technological ductility of stainless and heat-resistant steels. *Metallovedenie i Term. Obrab. Metallov*, **2**, 17–20.
6. Skulsky, V.Yu., Tsaryuk, A.K., Kuran, R.I. (2005) To the problem of adaptability to fabrication of heat-resistant steels with increased chromium content designed for construction of power plants of new generation of thermoelectric stations. In: *Proc. of 2nd Sci.-Pract. Seminar on Improving of Welded Joint Reliability in Assembly and Repair of Technological Equipment in Power Engineering* (Kiev, 6–8 December, 2005). Kiev: Ekotekhnologiya.
7. Skulsky, V.Yu., Tsaryuk, A.K., Moravetsky, S.I. (2009) Evaluation of susceptibility of welded joints of heat-resistant chromium martensitic steel to cracking at heat treatment. *The Paton Welding J.*, **1**, 5–9.
8. Zhang, Z., Farrar, J.S.M., Barnaes, A.M. (2001) Weld metals for P91 — tough enough? *IIW Doc. II-A-073-00, II-1428-01*.
9. Rosenbrok, L. (2001) A critical overview of the welding of P91 material. *Austral. Welding J.*, **46**(2nd Quarter), 5–8.
10. (1978) *Welding in machine building*: Refer. Book. Ed. by N.A. Olshansky. Moscow: Mashinostroenie.
11. Bergquist, E.-L. (1999) Consumables and welding modified 9Cr-1Mo steel. *Svetsaren*, **54**(1/2), 22–25.
12. Marshall, A.W., Farrar, J.C.M. (2001) Welding of ferritic and martensitic 11–14 % Cr steels. *Welding in the World*, **45**(5/6), 32–55.
13. Heuser, G. (1997) Consumables for welding in power machine building. *Avtomatich. Svarka*, **9**, 40–44, 47.



APPLICATION OF LASER-ARC CLADDING FOR FILLING UP NARROW CAVITIES IN ALUMINIUM ALLOY ITEMS

V. Yu. KHASKIN

E.O. Paton Electric Welding Institute, NASU, Kiev, Ukraine

Peculiarities of utilisation of hybrid laser-arc cladding for quality filling up of narrow cavities in items of aluminium alloys without preliminary machining are considered. Experiments on selection of process parameters are described. The expediency of application of this technology is shown.

Keywords: *hybrid laser-arc cladding, aluminium alloys, cladding parameters, laser radiation, metal-electrode arc, filler wire, engine piston, cladding technology*

Hybrid laser-arc cladding is applied to remove defects in cast products, repair cracks in machine and mechanism bodies, or restore parts worn-out during operation. Arc cladding involves the problem of quality filling up of lower parts of narrow cavities formed in products of aluminium alloys and steels without their preliminary machining. As a rule, machining is used in practice to remove, round or make blunt the corners in the lower part of products, which allows avoidance of porosity. Study [1] offers development of such techniques for hybrid cladding, which could eliminate the need of using preliminary machining through affecting the electric arc by laser radiation (e.g. by making it penetrate deep into a narrow cavity).

The cladding methods developed can be applied, for example, to restore pistons of internal combustion engines made from aluminium alloys. Diesel engines are often used under a maximal load and for a long time (diesel locomotive and marine engines). Such overloading conditions have a negative effect on engine components. Compression rings mounted on pistons break walls of the grooves, where they are located, during operation of an engine, thus leading to failure of pistons with time. This creates a permanent demand for reconditioning or repair of pistons for marine or diesel locomotive engines. Another problem is availability of spare parts (e.g. pistons) for cars produced in small volumes.

This poses the task of restoration, which can be tackled by different methods, the simplest one being arc cladding using the metal-electrode arc (e.g. [2]). However, this cladding method involves a number of problems: preliminary machining of the groove inside a piston is required, intensive spattering of the electrode metal and increased porosity of the deposited metal take place, and thermal parameters of arc cladding of aluminium materials cause formation of a coarse-grained structure of the deposited metal, which may lead to decrease in wear resistance of the clad pistons. The above problems can be handled by using the technology developed by the E.O. Paton Electric Welding Institute for two-arc cladding with tungsten

and metal electrodes [3]. This cladding method provides for successive and separate ignition of the tungsten- and metal-electrode arcs to form the common molten metal pool, which excludes their electromagnetic interaction, provides intensive stirring of the molten metal and its degassing, and makes it possible to produce the deposited metal with a fine-crystalline structure and uniform distribution of reinforcing intermetallic phases.

The method for cladding and hardening of pistons of internal combustion engines [3] can be considered most suitable for commercial application, although other methods are available as well, e.g. plasma hardening of grooves in car engine pistons [4] and electron beam restoration of pistons of internal combustion engines [5]. Based on the latter technology, the E.O. Paton Electric Welding Institute developed the method for electron beam hard-facing of pistons of internal combustion engine, which makes it possible to produce the hardened zone metal with hardness HV 150–180 [6, 7]. Hardness of the treated layer at a temperature of 100–360 °C is 2–3 times higher than that of the base metal of a piston, this providing a 1.5–2 times increase in service life of the piston group. However, this technology has a number of drawbacks, the main being the need to use electron beam chambers, which requires an extremely careful preparation of workpieces for hard-facing (first of all, cleaning them from contaminants). In addition, the need to degas a workpiece to be treated decreases the productivity of the hard-facing process. These drawbacks can be avoided by replacing the electron beam with the laser one.

Technical expediency of replacement of the electron beam technologies described in [5–7] with the laser analogues can be complemented by the possibility of cleaning the groove to be filled up by the laser beam without using traditional aggressive media [8]. However, from the economy standpoints (allowing for the price of a laser unit), this replacement causes certain doubts. In this connection, to solve the above problem, we suggest using the hybrid technology, in which the laser beam acts simultaneously with the metal-electrode arc. The use of the arc source will allow reduction of the laser power required for cladding at least by half [9], while the laser beam will

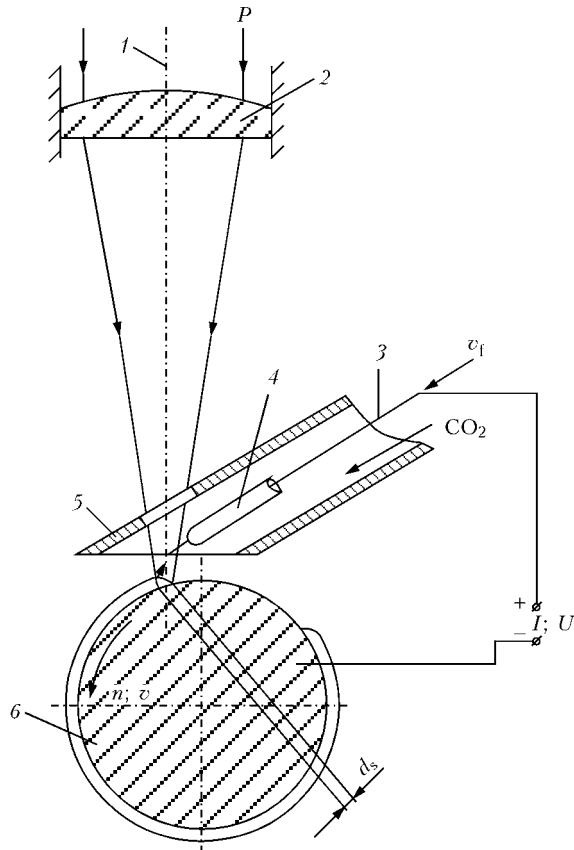


Figure 1. Schematic of the process of hybrid cladding of bodies of revolution: 1 — laser radiation; 2 — focusing lens; 3 — electrode (filler) wire; 4 — copper contact tube; 5 — shielding gas feed nozzle; 6 — sample; P — radiation power, kW; v_f — filler wire feed speed, m/h; n — sample rotation frequency, min^{-1} ; v — cladding speed, m/h; d_s — diameter of radiation focusing spot, mm; I — cladding current, A; U — voltage, V

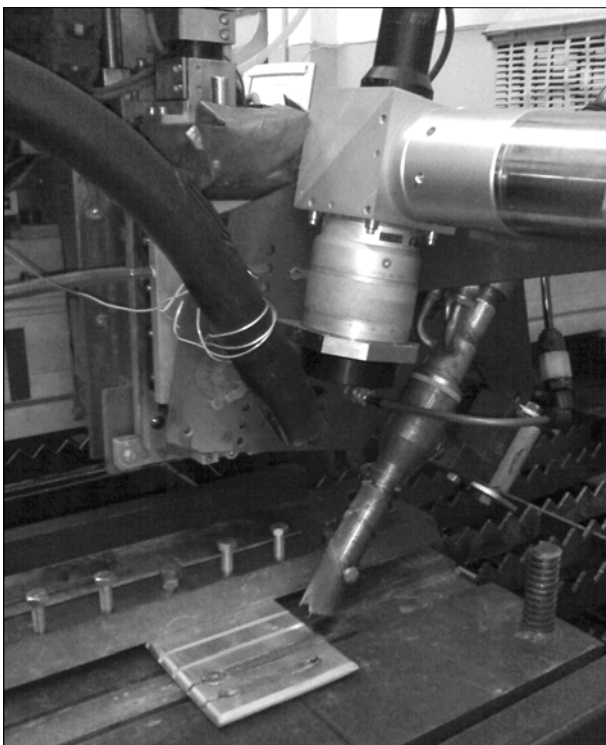


Figure 2. Rig based on three-coordinate manipulator for laser-arc cladding of flat aluminium simulation samples of piston grooves

make it possible to constrict the electric arc and lower it down to the bottom of the piston groove. As shown by preliminary studies, a high productivity of the cladding process is provided owing to its high speed [10].

Cladding parameters were preliminarily selected on aluminium samples with a smooth surface (without grooves), and finally selected on samples with narrow grooves to determine the possibility of using hybrid laser-arc cladding to fill up cavities without preliminary machining. Both cylindrical (according to the scheme shown in Figure 1) and flat samples were used for this selection. Rigs based on a lathe by using the CO_2 -laser radiation, as well as a three-coordinate manipulator with the Nd:YAG-laser radiation, the general view of which is shown in Figure 2, were used to conduct experiments. Both flat plates $200 \times 100 \times 10$ mm in size (including with cut-out slots 3 mm wide and 5 mm deep), which were clad by using a rig based on the manipulator, and beads 50–80 mm in diameter, which were clad by using a rig based on the lathe, were employed as samples for the experiments. Material of the samples was aluminium alloy AMg6. Cladding was performed with 1.2 mm diameter electrode (filler) wires SvAMg6 and SvAK5.

In cladding of the samples, the metal-electrode arc was powered from power unit TPS2700 (Fronius, Austria). The key difference of hybrid cladding from hybrid welding [1] consisted in the fact that laser radiation was focused on the surface of the clad sample into a spot with diameter $d_s = 2\text{--}3$ mm with defocusing $\Delta F = +(10\text{--}15)$ mm.

Lenses of potassium chloride single crystals with focus $F = 300$ mm were used in the experiments. In the case of hybrid cladding, power of the continuous-wave CO_2 -laser beam falling on a sample was 1.5 kW, and the maximal power of the pulsed Nd:YAG-laser at a pulse peak was $P_{\text{max}} = 3$ kW (average power $P_{\text{av}} = 2.3$ kW). Laser cladding was performed by using the pulsed Nd:YAG-laser with $P_{\text{av}} = 3$ kW (up to 4 kW at the pulse peak). The use of the pulsed radiation was caused by the need to eliminate the effect of formation of argon plasma, which absorbs laser radiation and has a negative influence on the cladding process. Argon and helium were used as a shielding gas for laser and hybrid cladding. Their flow rate was 8–10 l/min. The speed of laser and hybrid cladding was 60 m/h. Hybrid cladding of the aluminium alloy was performed in the pulsed mode at current $I = 200\text{--}230$ A and voltage $U = 22\text{--}24$ V. The metal-electrode arc was fed to a tailing part of the pool at a distance of up to 1–3 mm from axis of the laser beam. The angle of inclination of the contact tube feeding the wire to the axis of the laser beam was 25–35°.

Samples with the deposited aluminium alloy layers were studied from the transverse sections made at the beginning, in the centre and at the end of the deposited beads. Consider the results obtained in more detail.

Appearance of a sample of aluminium alloy AMg6 with the grooves filled up by cladding is shown in Figure 3. The first two grooves in it were filled up

by the arc cladding method, and the second two grooves --- by the hybrid method. The experiments showed that in the case of using wire SvAK5 the beads had a smoother surface, and the lower part of a groove was filled up better than in the case of using wire SvAMg6 (Figures 4 and 5). This can be explained by an increased spreading of the latter due to its high silicon content. Wire SvAK5 was employed to make the bead shown in Figure 5, *b*. The cladding parameters used to make this bead can be considered the best for the given experiments. However, the hybrid cladding method can provide a good formation of the beads and complete filling up of the lower part of the grooves even by using wire SvAMg6 (Figure 4). Increase of the cladding current allows improvement of fusion in the lower part of the groove (Figure 4, *b*, and 5, *d*). However, this causes inadmissible overheating of the sample. Note that the characteristic defect of arc cladding of narrow grooves without machining is a lack of fusion of the deposited metal with the base one in their lower parts (Figures 3, 4, *a*, and 5, *a*, *d*).

Laser cladding was carried out at the same process and wire feed speeds to compare and estimate the described results of hybrid cladding using identical materials. To perform laser cladding, it was necessary to increase the average power of pulsed radiation to 3 kW. Resulting structure of the deposited metal was much finer than in hybrid cladding. Comparison of the hybrid cladding method with the laser one showed a higher locality of heating with the second method. However, consumption of the laser radiation power in this case increases almost twice, and the cost of a running metre of cladding grows approximately as much. This is attributable to differences in thermal



Figure 3. Appearance of the beads deposited in grooves on a sample of alloy AMg6 ($\delta = 10$ mm) using wire SvAK5 ($d = 1.2$ mm): from left to right --- arc cladding at $I = 210$ A, $U = 23$ V, and $I = 250$ A, $U = 25$ V, two grooves --- hybrid cladding

processes, and in a degree of absorption of laser radiation between the above two cladding methods. In the case of hybrid cladding, saving of the laser radiation power is achieved due to its good absorption by the metal melted by the low-power electric arc. In laser cladding, the radiation power is additionally consumed for reflection from the melted wire and removal of heat from it.

It should be noted in assessment of quality of the deposited layers that with laser cladding using wire the characteristic defect is formation of pores, which can be eliminated by raising the laser radiation power. The least number of defects is fixed in the case of hybrid cladding. With this cladding method, the important point is deepening of the electric arc into a narrow cavity, which is directly proportional to density of the radiation power. If it is insufficient, po-

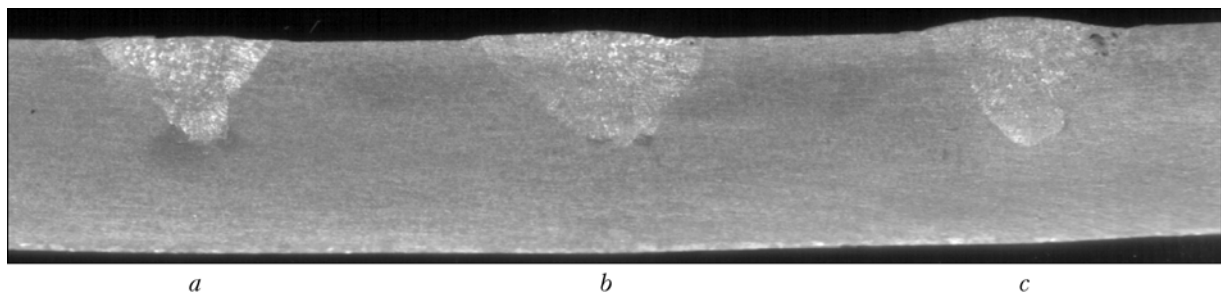


Figure 4. Macrosections of the beads deposited in grooves on a sample of alloy AMg6 ($\delta = 10$ mm) using electrode wire SvAMg6 ($d = 1.2$ mm) at a speed of 60 m/h in argon: *a*, *b* --- arc cladding at $I = 200$ A, $U = 22.5$ V, $v_f = 12.7$ m/min, and $I = 220$ A, $U = 23$ V, $v_f = 15$ m/min; *c* --- hybrid cladding at $P_{av} = 2.34$ kW ($P_{max} = 3$ kW), $I = 200$ A, $U = 22.5$ V, $v_f = 12.7$ m/min, respectively

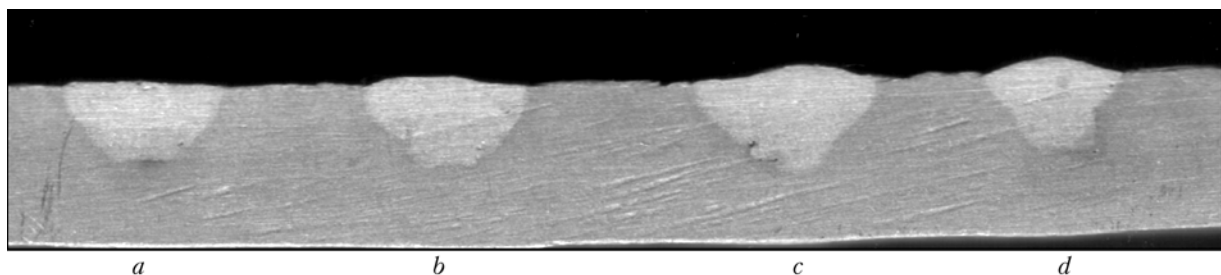


Figure 5. Macrosections of the beads deposited in grooves on a sample of alloy AMg6 ($\delta = 10$ mm) using electrode wire SvAK5 ($d = 1.2$ mm) at a speed of 60 m/h in argon: *a*, *d* --- arc cladding at $I = 206$ A, $U = 22.6$ V, $v_f = 12.7$ m/min, and $I = 226$ A, $U = 23.8$ V, $v_f = 15$ m/min; *b*, *c* --- hybrid cladding at $P_{av} = 2.34$ kW ($P_{max} = 3$ kW), $I = 200$ A, $U = 22.5$ V, $v_f = 12.7$ m/min, and $P_{av} = 2.34$ kW ($P_{max} = 3$ kW), $I = 210$ A, $U = 22.8$ V, $v_f = 13$ m/min, respectively



rosity and lacks of fusion in the lower part of the cavity filled up by cladding will take place. The simplest method for increasing the power density is to decrease defocusing ΔF . However, this is accompanied by growth of the degree of dilution of base and deposited metals, this making the cladding process similar to the welding process. The issue of optimisation of density of the laser power in hybrid cladding requires further investigations.

CONCLUSIONS

1. Quality filling up of narrow cavities in aluminium items without machining can be achieved by fixing the electric arc at the cavity bottom by using laser radiation. Laser-arc cladding makes it possible to eliminate such drawbacks characteristic of the arc process as porosity and lacks of fusion in the lower part of the cavities, and decrease overheating of workpieces.

2. Advantages of hybrid cladding are partial replacement of the laser radiation power with the metal-electrode arc power, and the fact that the liquid metal melted by the electric arc absorbs laser radiation much more intensively than the solid one. The latter leads to decrease in losses of the laser radiation power, compared with laser cladding.

3. In hybrid cladding, an excessive heat input may lead to distortion of a workpiece. Issues related to evaluation of hardness and wear resistance of the layers deposited by laser-arc cladding require further investigations.

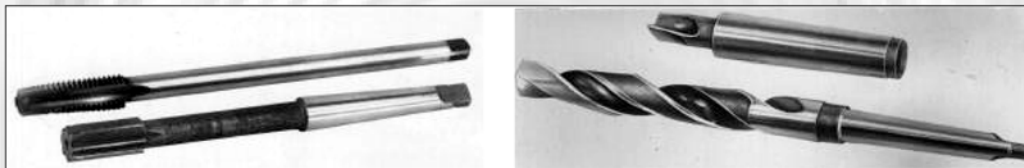
1. Shelyagin, V.D., Khaskin, V.Yu., Garashchuk, V.P. et al. (2002) Hybrid CO₂-laser and CO₂ consumable-arc welding. *The Paton Welding J.*, **10**, 35–37.
2. Zusin, V.Ya., Bajner, G.N., Chernoiyanov, V.N. (1982) Restoration of grooves in aluminium pistons of tractor engines by shielded-gas pulsed-arc cladding. *Svarochn. Proizvodstvo*, **11**, 37–38.
3. Voropaj, N.M., Lesnykh, V.V., Mishenkov, V.A. (1996) Twin-arc surfacing of aluminium pistons with combined consumable and nonconsumable electrodes. *Avtomatich. Svarka*, **6**, 21–25.
4. Chudinov, B.A., Zhmievsky, V.F. (2004) Strengthening of upper groove in internal combustion engine pistons at OJSC AVTOVAZ. In: *Proc. of 6th Int. Pract. Conf.-Exhibition (Toliatti, 13–16 April 2004)*. St.-Petersburg: Alfare, 89–90.
5. Bondarev, A.A. (1999) Technology for repair of worn-out pistons. *Svarshchik*, **6**, 17.
6. Bondarev, A.A. (2005) Technology for hard-facing using filler material in a zone of compression grooves in aluminium pistons. In: *Technologies. Materials. Equipment. Catalogue*. Kiev: PW1, 27–28.
7. Bondarev, A.A. (2005) Technology for repair and restoration of worn-out pistons and others machine parts and mechanisms. *Ibid.*, 28.
8. Vejko, V.P. (2001) Physical mechanisms of laser surface cleaning. *Izvestiya RAN. Series Physics*, **65**(4), 586–590.
9. Krivtsun, I.V., Shelyagin, V.D., Khaskin, V.Yu. et al. (2007) Hybrid laser-plasma welding of aluminium alloys. *The Paton Welding J.*, **5**, 36–40.
10. Shelyagin, V.D., Khaskin, V.Yu., Nabok, T.N. et al. (2005) Hybrid laser-arc welding of carbon steels and aluminium alloys. *Dopovidi NAN Ukrainy*, **7**, 97–102.

TECHNOLOGY AND EQUIPMENT FOR FLASH-BUTT WELDING OF CUTTING TOOLS

E.O. Paton Electric Welding Institute developed technology and equipment for flash-butt welding of tool steel to structural steel, in particular, high-speed steel of R6M5 grade to structural steels 45, 20Kh, 40Kh, etc., for making bimetal metal-cutting point tools (drills, taps, broaches, finger mills).

The developed technology guarantees producing sound flash-butt welded joints of cutting tools equivalent to the base metal.

The welding process is fully automated, has program control and a system for real time monitoring of welding parameters.



Samples of welded bimetal tools

The developed technology was the basis for designing specialized and upgrading all-purpose flash-butt welding machines K802, K793, K724A, K838, which allow welding tool billets of 7 to 8000 mm² cross-section. This equipment can be applied independently or as part of automated lines of tool manufacturing.

Purpose and application. Technologies and equipment for flash-butt welding of bimetal tools are designed for application in the tool and machine-tool construction industries.

Status and level of development. Developed technologies and equipment for their implementation correspond to the world standards and are protected by foreign patents and authors' certificates.

Forms of co-operation. To be determined during negotiations. Technology and equipment can be introduced, and all-purpose equipment can be upgraded on contract basis.

Contacts: Prof. Kuchuk-Yatsenko S.I.
E-mail: chvertko@paton.kiev.ua



DEVICE FOR IGNITING ARC OF DOUBLE-ANODE PLASMATRON

N.A. MAKARENKO¹, V.V. CHIGAREV², N.A. GRANOVSKY², A.A. BOGUTSKY¹ and A.M. KUSHCHY¹

¹Donbass State Machine Building Academy, Kramatorsk, Ukraine

²Priazovsky State Technical University, Mariupol, Ukraine

The device is suggested that contains energy storage capacitors of increased capacity, a thyristor key and a recharging capacitor, and two pulse transformers with serially connected primary windings. In contrast to usually used in practice devices the suggested device allows producing 5–6 igniting pulses of increased power within each half-period of the alternating current.

Keywords: double-anode plasmatron, plasma-MIG welding, pulse transformer, pulse energy, device for ignition, componenting

Processes of the plasma-MIG welding and surfacing are used in industry [1]. Possibility of adjustment within wide range of heat input into the items and high productivity in combination with a number of other advantages ensure good prospects for this process [2–4]. Plasma-MIG welding is used in manufacturing of items from copper [5] and aluminium [6] and in surfacing of tools and fittings-out [7, 8].

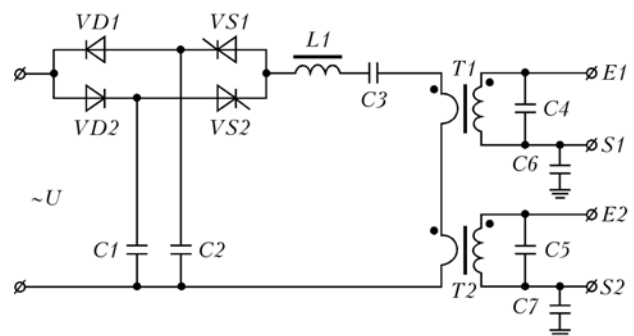
Plasma-MIG welding and surfacing of light metals is performed only on reverse polarity direct current of consumable and non-consumable electrodes. However, in manufacturing of items from other materials it is recommended in majority of cases to use reverse polarity. At reverse polarity a non-consumable rod electrode of the plasmatron functions as an anode due to which allowable current loads on it are significantly lower than in case of using straight polarity when a non-consumable electrode functions as a cathode [9]. At the same time in a number of cases (for example, in welding and surfacing of items from aluminium and aluminium-base alloys) it is necessary to ensure increased power of plasma arc, whereby it is advisable to use plasmatrons that have two non-consumable electrodes-anodes which have to be connected to two separate power sources thus increasing total plasma arc current without exceeding current allowable for a tungsten electrode.

At the beginning of the welding or surfacing process it is necessary to ensure ignition of the arc discharges from both anodes of the double-anode plasmatron [10], whereby it is necessary that both arcs excited simultaneously because at plasma-MIG process inside the plasmatron a consumable electrode is located which remains at excitation of one arc immovable, gets overheated by the plasma arc current, and melts inside the plasmatron which causes clogging of the plasmatron nozzle, its failure, and, as a result, impossibility of performing direct process of welding or surfacing. In connection with this an actual task is development of a device for igniting arc for a dou-

ble-anode plasmatron that ensures simultaneous ignition of arc discharges of both plasmatron anodes. As basis of the device, included into scheme of the double-electrode plasmatron for plasma-MIG welding and surfacing, a scheme of the UPD-1 device for excitation and stabilization of the arcing process, designed in the E.O. Paton EWI, was taken. In the device diodes and thyristors were included into the circuit of one of the outlets of the step-up transformer primary winding through the feed-through capacitor and constituted between each other two oppositely directed parallel rectifying circuits from serially connected diode and thyristor [11]. These devices are simple and reliable. Many UPD-1 devices have been operating in different installations for almost 30 years without any failures.

For ensuring simultaneous ignition of two arcs, an additional pulse transformer $T2$ was included into the circuit (Figure). Primary windings of the pulse transformers $T1$ and $T2$ were connected concordantly serially, and ends of secondary windings having the same signs were connected to non-consumable electrodes (anodes) of the plasmatron. It allowed avoiding occurrence of high voltage between the plasmatron anodes at the instant of the ignition pulse passage which prevented electrical break-down of the gap between the plasmatron anodes.

The device operates as follows. During one of the half-periods of the variable voltage U the capacitor $C1$ is charged through the diode $VD1$ (DL80), and



Device for igniting arc of double-anode plasmatron



during the next half-period the capacitor $C2$ is charged (through the diode $VD2$). So, before beginning of the device operation the capacitors $C1$ and $C2$ ($4 \mu\text{F}$, 450 V) are charged with the opposite polarity voltages. During next feeding of the control pulses on the thyristors $VS1$ and $VS2$ (TB series, 160 A , 22 C) the thyristors open in turn, whereby recharging of the capacitor $C3$ occurs ($4 \mu\text{F}$, 600 V) through prime windings of the transformers $T1$ and $T2$ in secondary windings of which are generated high-voltage pulses that ignite arcs of the plasmatron anodes. The capacitors $C4$ and $C5$ (1000 pF , 34 kV) are used for improving shape of the pulse that ignites the arc, and the capacitors $C6$ and $C7$ ($4 \mu\text{F}$, 400 V) --- for protection of the power sources connected to the plasmatron anodes against high voltage. The choke $L1$ limits rate of the current increase (di/dt) up to the value allowable for the thyristors $VS1$ and $VS2$.

During operation of the device the capacitors $C1$ and $C2$ respectively through the diodes $VD1$ and $VD2$ are charged in opposite polarity by the variable voltage U . As far as capacity of the capacitors $C1$ and $C2$ is 10 times higher than that of the capacitor $C3$, its recharging may be performed 5–6 times within one half-period of the supply voltage U . This allows increasing frequency of sequence and frequency of the ignition pulses up to 500–600 Hz while frequency of sequence of the UPD-1 device ignition pulses is 100 Hz.

For the purpose of increasing energy of the ignition pulses the device is powered with voltage 300 V , whereby energy of the high-voltage discharge in the each anode-plasma-shaping nozzle gap equals about 0.6 J .

The investigations have shown that increase of the power supply voltage causes increase of the di/dt value for the thyristors $VS1$ and $VS2$ and increase of the switching voltage surges on the thyristors which causes the need to use thyristors of the TB and TBI series, designed for current 160 A and having 22 class of voltage.

The tests demonstrated that the device reliably ignites auxiliary arcs of both plasmatron anodes (practically within one half-period of the power supply voltage U , i.e. within 0.01 s).

CONCLUSIONS

1. In the devices for igniting arc of the double-anode plasmatron for plasma-MIG welding and surfacing it is advisable to use two pulse transformers, primary windings of which are connected concordantly serially, whereby the ends of secondary windings of the same sign are connected to the plasmatron anodes.

2. Application of two separate energy storage capacitors of increased capacity charged with the opposite polarity voltages allows increasing frequency of the ignition pulses from 100 to 500–600 Hz.

3. Increase of energy of the ignition pulses due to increasing charging voltage of the energy storage capacitors requires for application of thyristors with high di/dt value and high class of voltage.

4. The developed scheme of the device for igniting arc of the double-anode plasmatron ensures reliable ignition of arcs of both plasmatron anodes within the time not more than 0.01 s .

1. (1978) *Welding in machine building*: Refer. Book. Vol. 1. Ed. by N.A. Olshansky. Moscow: Mashinostroenie.
2. Bakurskaya, M.A., Kolosova, N.A. (1984) Plasma-MIG process and its industrial application abroad. *Elektrotekh. Promyshlennost. Elektrosvarka*, **6**, 11–15.
3. Shchitsyn, Yu.B., Tytkin, Yu.M. (1985) Study of process of plasma consumable electrode welding of heat-resistant alloys. In: *Proc. of 2nd All-Union Conf. on Problems of Welding Technology of Thermostable, Refractory and Heat-Resistant High-Alloy Steels and Alloys*. Kiev: PWI.
4. Gvozdetzky, V.S., Makarenko, N.A. (2000) Plasma welding (Review). *The Paton Welding J.*, **12**, 24–28.
5. Venekers, R., Shevers, A.A. (1977) Plasma MIG welding of copper and copper alloys. *Welding and Metal Fabr.*, **45**(4), 227–235.
6. Essers, W.G., Willems, G.A. (1984) Plasma-MIG-Schweissen von Aluminium, Auftragschweissen und Zweielektroden-schweissen von Stahl. *DVS-Berichte*, **90**, 9–14.
7. Danilchenko, B.V., Makarenko, N.A. (1998) Plasma-arc surfacing with axial feed of consumable flux-cored wire. In: *Proc. of Int. Sci.-Techn. Conf. on Advanced Technique and Technology of Machine Building, Instrument Engineering and Welding Production*. Kiev: PWI, 322–325.
8. Kornienko, A.N., Makarenko, N.A., Kondrashov, K.A. (2003) Advantages of strengthening and recovery of press molds for glass by plasma-MIG surfacing method. In: *Proc. of Region. Sci.-Techn. Conf.* Vol. 1. Mariupol: PGU.
9. (1974) *Technology of electric welding of metals and alloys*. Ed. by B.E. Paton. Moscow: Mashinostroenie.
10. Makarenko, N.A. (2006) *Development of scientific and technological bases of plasma consumable and nonconsumable electrode welding and surfacing*: Syn. of Thesis for Dr. of Techn. Sci. Degree. Mariupol.
11. Shmakov, E.I., Fedotenkov, V.G., Kolesnik, G.F. et al. *Device for exciting and stabilizing of arcing process*. USSR author's cert. 567563. Int. Cl. B 23 K 9/06. Publ. 05.08.77.



ON THE ROLE OF CONTACT RESISTANCES IN ELECTROSLAG CLADDING PROCESS

K.A. TSYKULENKO

E.O. Paton Electric Welding Institute, NASU, Kiev, Ukraine

It is shown that when developing the technology of electroslag cladding without penetration in the current-carrying mould, as well as in designing new moulds, it is necessary to take into account the role of contact resistances. Slag melt temperature can be a criterion for determination of the required surface melting of the clad (welded) surface. However, the dependence should be established between it and temperature on the contact clad surface.

Keywords: *electroslag cladding, contact resistance, slag pool temperature, penetration*

Modern theory of electric contacts is still in the development stage. In this connection not all the physical phenomena occurring between the contacts have been completely studied and explained. The above theory is based on concepts related to the contact surface, contraction area and resistance, fogging films, contact pressure, contact difference of potentials, thermal effects and other statements characterizing the work of contacts of different kinds.

Welders have used such a property of electric contacts as increased (compared to electric resistance of materials of the parts being joined) electrical resistance, for a long time now. This primarily is resistance welding, which is often called contact welding, thus emphasizing the important role of electric contact between the parts being welded for this process.

In the case of electroslag processes such contacts are the surface of the electrode, which is immersed into the slag pool, limited by the mould surface, welded or clad surfaces of billets in the section of contact with the slag pool, as well as the interface of the slag and metal pools.

A large number of studies are devoted to investigation of the processes and phenomena occurring in the slag pool. They, however, practically did not consider the role of contact resistances. Attention was mainly given to phenomena occurring on the interfaces of the slag pool and surfaces of the electrode mould, supplying current to it. Investigations were conducted to study the issue of improvement of resistance of equipment (mould [1], non-consumable electrode [2, 3]) or improvement of the electroslag process effectiveness [4, 5]. Here such a phenomenon as alternating current rectification in the electroslag process [6–8], and features of current distribution in the slag pool [9] and mould [10], etc. were studied. Different mathematical models of heat distribution in the slag pool, electrode melting process, heat transfer through the slag pool surface do not allow for the potential difference arising on the interface of the slag–considered surface, and, therefore, also the additional heat evolution (see, for instance [11–15]). Only in [16] it

is noted that electrode heating in electroslag processes mainly occurs exactly due to electrode contact with the molten slag (it should be noted once more, that this is exactly due to contact). The electrode in the section extending beyond the contacts of the current-carrying device is heated by electric current passing through it, as well as heat evolution on the surface of contact with the slag pool and heat transfer from the slag pool heated by passing electric current. Electroslag welding (cladding) can be regarded to some extent, as resistance welding, in which the liquid conductor — the slag pool — acts as one of the contacting elements of the circuit.

Slag pool (as an element of the electric circuit) is regarded as an active inertia non-linear resistance, the value of which is considerably higher than that of the electrode or deposited metal. Therefore, the main amount of heat in the electroslag process evolves in the slag. At contact of dissimilar substances (in our case between the liquid slag and current-carrying metal surfaces) a double electric layer and a contact difference of potentials form on their interface. Alternating current passing through the circuit consisting of two or several conductors with different types of conductivity is partially or completely rectified owing to a difference in the energy conditions of passing through the interface between conductors in the positive and reverse direction [6, 17], with occurrence of thermal effects. Temperature in the section of contact of the consumable electrode–slag pool or slag pool–clad billet should have the highest value compared to temperature in other sections of the slag pool. So, in [11] an increased glowing of the slag is noted, which is indicative of the presence of a higher temperature on such a contact surface. Metal electric resistance rises with temperature, and that of molten slag quickly decreases. It has not yet been established how the contact resistance or temperature change here (or do they change at all). Because of a marked dependence of the slag electric resistance on temperature, the main part of the current flows through the most highly heated volume of the molten slag (by the classical schematic this volume is located between the electrode edge and molten metal pool surface).

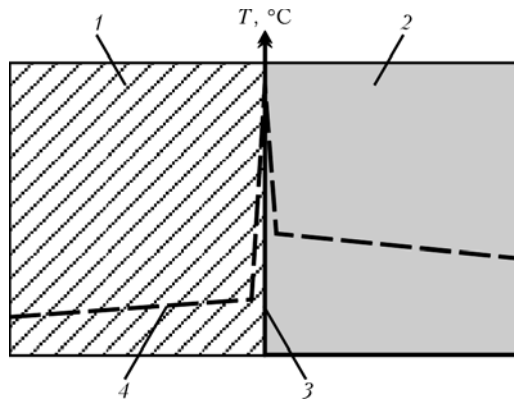


Figure 1. Assumed distribution of temperature at the interface of slag pool-clad billet in electroslag cladding: 1 — clad billet; 2 — slag pool; 3 — contact surface; 4 — temperature distribution

On the whole, it is believed that the hydrodynamic flows arising in the slag pool average its temperature over the volume. Considering the slag pool hydrodynamics, the contact between the slag pool and surface of the billet (electrode), can be regarded as a sliding surface contact, characterized by different electrokinetic, electrochemical and thermal phenomena, based on the classification accepted in the theory of electric contacts [18–20]. The process of heat transfer by such a contact is not sufficiently studied so far. The volume of slag overheated on the contact surfaces, compared to that of the entire slag pool, is negligible, and the heat input from is small. Apparently, that is why the contact resistances in electroslag processes were not given sufficient attention. Should then the presence of the double electric layer and increased electric resistance in the metal–slag pool contact be given greater attention in the welding and cladding technologies?

During development of the technology of electroslag cladding without penetration (the need for it and its capabilities are described in [21, 22]), it was found that surface melting of the clad surface can take place even with the use of a sufficiently low-melting flux. So, the experimental low-melting flux had the melting temperature markedly lower (by 250–300 °C)

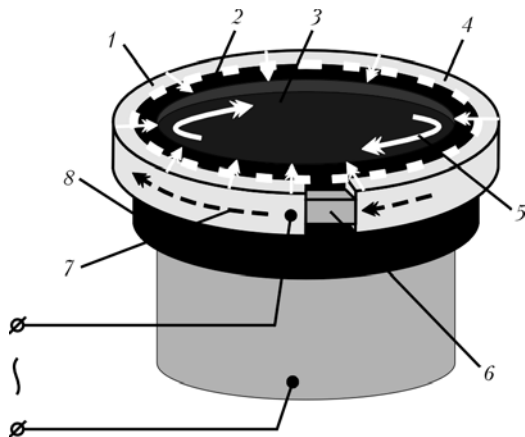


Figure 2. Schematic of current distribution through the elements of current-carrying mould in the electroslag process: 1 — copper current-carrying section; 2 — protective graphite (or steel) ring; 3 — slag pool; 4 — contact surface; 5 — insert; 6 — direction of slag pool rotation; 7 — current flowing along the current-carrying section; 8 — protective ring

than the material of the clad billet. Results of measurement during heating of the steel billets for cladding showed that its surface welding still occurred, even though the temperature of the slag pool in the gap between the mould wall and the clad surface is by 150 °C lower than the melting temperature of the billet. Under such cladding conditions, it cannot be due to formation of low-melting eutectics (as cladding was performed using metal similar to that of the clad billets), or phenomena occurring at contact-reaction brazing. Effect of surface melting is attributable to the influence of an increased electric resistance of the contact of the clad metal billet–slag pool. And although the additional heat evolving on the contact surface, is negligible (compared to heat content in the entire slag pool), at concentration in a small volume it results in fast heating and melting of the surface of the clad billet. It may be assumed that the nature of temperature distribution at the interface of the clad billet–slag pool at electroslag cladding has the form shown in Figure 1. Thus, during electroslag cladding the slag pool temperature cannot be a criterion of billet surface melting. The slag melt temperature can be an indication of surface melting only in the case, when dependencies are established between it and the temperature of the contact surface of the clad billet. Such dependencies will be, probably, different for each pair of slag melt–clad billet material. It is anticipated that the temperature of the clad billet contact surface can be evaluated by measuring the contact difference of potentials, similar to what is done for two solids at calculation of the temperature of heating of electric contacts and determination of the limit current value for a particular electric circuit.

The Table gives the values of potential difference U_i on contact pairs for parts from the above materials used in calculations of the electric contact heating temperature.

Development of the technology of electroslag cladding without penetration envisages application of current-carrying mould, the design of which largely determines the processes running in it. Here the role of contact resistances between the structure elements essentially affecting the melt hydrodynamics, should be noted. As is known [24], in the current-carrying mould an additional rotation of the slag pool in the horizontal plane is ensured. The upper copper current-carrying section with a break, as a rule, does not have any

Potential difference on contact pairs [23]

Material	U_i , V				
	Aluminium	Graphite	Brass	Copper	Steel
Aluminium	0.28	--	--	--	--
Graphite	3.00	3.0	--	--	--
Brass	0.63	2.4	0.54	--	--
Copper	0.65	3.0	0.60	0.65	--
Steel	1.40	1.6	2.10	3.00	2.5



direct contact with the slag pool, and is most often protected by a graphite ring to prevent electrochemical erosion. It would seem that the presence of such a ring from a material with a high electrical conductivity should eliminate the electric break in the circuit of the current-carrying section and lead to stopping of the slag pool rotation; this, however, does not happen. The difference of potentials of the copper-graphite pair is so high ($U_i = 3 \text{ V}$), that the main part of the current runs in the contour of the current-carrying section, thus leading to slag pool rotation (Figure 2). If the current-carrying section is closed by a copper ring or bridge ($U_i = 0.65 \text{ V}$), the slag pool rotation practically stops.

The speed of its rotation in the current-carrying mould is determined, primarily, but the value of current flowing in the mould upper section. In [25] it is proposed to control the speed of the melt rotation using special electric current conductors --- electrically-conducting inserts from different materials placed into the break of the current-carrying section of the mould. Owing to insulation inserts in the break of the current-carrying section, the speed of the slag pool rotation will be maximum.

Thus, the role of contact resistances should be taken into account in development of the technology of electroslag cladding without penetration in a current-carrying mould, as well as in design of new structures of the latter. The slag melt temperature can be a criterion for determination of melting of the clad (welded) surface. In this case, however, a relationship should be established between it and the temperature on the contact clad surface.

1. Artamonov, V.L., Medovar, B.I., Martyn, V.M. et al. (1972) To the problem of anode fracture in slag during ESR of current-carrying metallic elements. *Spets. Elektrometallurgiya*, Issue 17, 3-10.
2. Baglaj, V.M., Medovar, B.I., Latash, Yu.V. et al. (1971) To the problem of using steel cooled electrode in electroslag process. *Ibid.*, Issue 13, 53-54.
3. Dudko, D.A., Rublevsky, I.N. (1958) Influence of current type and polarity on metallurgical processes in electroslag welding. *Avtomatich. Svarka*, 3, 69-78.
4. Maksimovich, B.I. (1962) *Increase in efficiency of electroslag remelting of steels and alloys*: Syn. of the Thesis for Cand. of Techn. Sci. Degree. Kiev.
5. Kojima, Yu., Kato, M., Toyoda, T. et al. (1975) Study of the model of consumable electrode melting in ESR. *Elektroshlak. Pereplav*, Issue 3, 54-62.
6. Dudko, D.A., Rublevsky, I.N. (1962) To the problem of the nature of valve effect in electroslag process. *Avtomatich. Svarka*, 3, 40-48.
7. Lyuty, I.Yu., Latash, Yu.V., Nikulin, A.A. et al. (1973) About alternating current rectification in the electroslag process using graphite electrodes. *Spets. Elektrometallurgiya*, Issue 20, 29-36.
8. Mironchenko, V.L., Chernov, V.T., Shalomeev A.A. et al. (1976) About the mechanism of direct current component initiation in ESR. *Ibid.*, Issue 29, 8-14.
9. Stupak, L.M., Baglaj, V.M., Medovar, B.I. (1968) About current distribution in the slag pool during ESR. *Ibid.*, Issue 3, 42-46.
10. Arsenkin, V.T., Radchenko, V.G., Stepanov, P.I. (1974) About some peculiarities of current distribution in ESR mould. *Ibid.*, Issue 23, 46-52.
11. Mitchell, A., Shekeli, J., Elliot, J. (1974) Mathematical modelling of ESR process. *Elektroshlak. Pereplav*, Issue 2, 17-45.
12. Yoshi, S., Mitchell, A. (1973) Thermal processes in ESR. *Ibid.*, Issue 1, 168-179.
13. Omura, T., Wakabayashi, M., Hosoda, T. (1973) Analysis of heat transfer in ESR. *Ibid.*, 180-202.
14. Kato, M., Kojima, Ya., Inoye, M. et al. (1983) Electric resistance between consumable electrode and mould in electroslag process. *Ibid.*, Issue 7, 231-237.
15. Kato, M., Kojima, Ya., Inoue, M. et al. (1983) Distribution of electric potential between consumable electrode and mould in ESR process. *Ibid.*, 238-243.
16. Paton, B.E., Lebedev, V.K. (1966) *Electric equipment for arc and slag welding*. Moscow: Mashinostroenie.
17. Zilberman, G.E. (1970) *Electricity and magnetism*. Moscow: Nauka.
18. Holm, R. (1961) *Electric contacts*. Moscow: Inostr. Literatura.
19. Komarov, A.A., Yakovlev V.N. (2001) *Electric contacts*. Samara: SamIIT.
20. Kalashnikov, S.G. (2003) *Electricity*. Moscow: Fizmatlit.
21. Tsykulenko, K.A., Tsykulenko, A.K. (2001) Analysis of possibilities of electroslag cladding of dissimilar metals and alloys at small thickness of deposited layer. *Problemy Spets. Elektrometallurgii*, 3, 19-23.
22. Tsykulenko, K.A., Tsykulenko, A.K. (2001) To the problem of flux selection for electroslag cladding-brazing. *Ibid.*, 4, 3-6.
23. *ST 12.1.004-91 (Group T58)*: Building codes and rules. Introd. 01.07.92.
24. Ksyondzyk, G.V. (1975) Current-carrying mould providing rotation of slag pool. *Spets. Elektrometallurgiya*, Issue 27, 32-40.
25. Ksyondzyk, G.V., Frumin, I.I., Kuskov, Yu.M. *Current-carrying sectional mould*. USSR author's cert. 1085250. Int. Cl. 22 B 9/18. Publ. 30.03.82.



NEWS

NKMZ COMPANY TO MAGNITOGORSK METALLURGICAL WORKS

Novokramatorsk Machine-Building Plant (NKMZ company, Kramatorsk, Donetsk region) has fulfilled a big-volume contract that assumes radical re-design of the hot-rolling mill 2500 at Magnitogorsk Metallurgical Works.

Difficulties which experience Ural metallurgists in sales of the products during the crisis threaten financing of 11 big projects directed at development of the enterprise. However, the measures, taken by man-

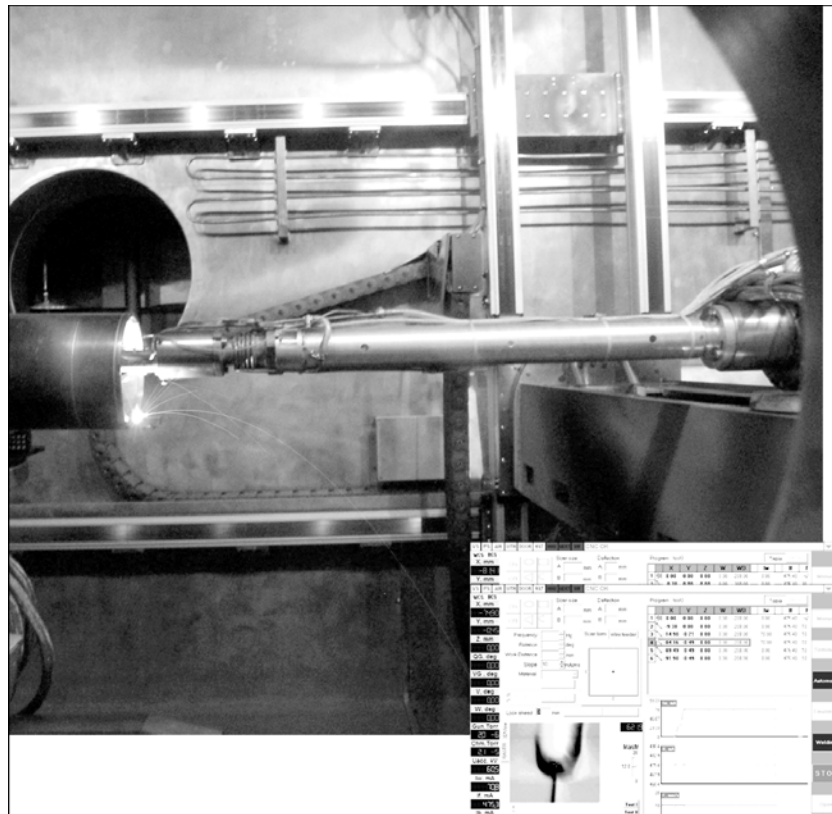
agement of Magnitogorsk Metallurgical Works, allowed it finding the formula, application of which will make it possible to fulfill main programs of technical re-equipment, including re-design of the mill 2500.

In first quarter of 2009 manufacturing of equipment for the hot-rolling mill 2500 at NKMZ company will be continued.

ELECTRON BEAM WELDING USING DEVIATED BEAM OF ELECTRONS

In the E.O. Paton Electric Welding Institute the equipment and technology for electron beam welding of items from steels and aluminium alloys using deviated at 90° beam of electrons has been developed. Such technology allows fulfilling welding and cosmetic «smoothing» of the welds in hard-to-reach places or on internal side of tubular structures of up to 1200 mm length. Due to this the need in labor consuming ma-

chining of root parts of the welds which occurs in welding performed on external side of an item is excluded. Technology of welding using a deviated beam of electrons envisages application of the computer equipment which allows controlling parameters of welding and real time imaging on the display screen of formation of the weld and melting of the edges to welded.





TECHNOLOGY FOR PRODUCTION OF SPIRALLY WELDED PIPES

In the E.O. Paton Electric Welding Institute of the NAS of Ukraine the technology for automatic production of spirally welded pipes has been developed and introduced. This technology implements a high-productivity method for production of electrically welded pipes of precise dimensions which may be used instead of all drawn and longitudinally welded pipes or pipes produced by coiling of separate cards.

Suggested method may be implemented in arc welding, hybrid technologies and in high-frequency welding at speed from 30 m/min and higher.

Per one shift on one welding line may be produced 1–2 km pipes from steels of the 08kp, St.3, 30KhGSA and 17GS grades, stainless steels and aluminium alloys.

Cost price of manufacturing pipes according to the suggested technology is about 0.6–1.8 UAH per running meter without taking into account cost of the metal.

Such technology is especially efficient at mass production of cylindrical parts of the cylinders for lique-



Sample of spirally welded pipe of 315 mm diameter with wall thickness 3 mm from 08kp steel after tests at internal pressure 8.2 MPa

fied gases and cylinders operating under pressure of the compressed gases, for example, cylinders for motor-vehicle transport, pneumatic systems and fire extinguishers.

DATABANK OF WELDING PARAMETERS

The databank contains information on parameters of CO₂, submerged-arc (with one or two wires) and inert-gas shielded welding of structural steels in different spatial positions depending upon the thickness of base metal, type of a welded joint, groove shape and welding wire diameter. Recommendations on the number of passes for welding the root, filling and decorative beads are given for a case of multipass welding. The recommended welding parameters provide quality weld formation and required amount of deposited metal to ensure structural strength of a welded joint. At the given development stage, the database contains more than two thousand entries of welding conditions.



Figure 1. Selection of welding method, type of welded joint, spatial position and groove shape



Figure 2. Information on CO₂ welding of butt joint

Application. The databank can be used at machine building enterprises for arrangement of computerised work place of a welding production engineer.

Contacts: Prof. Makhnenko V.I.
E-mail: d34@paton.kiev.ua

INTERNATIONAL CONFERENCE «WELDING AND RELATED TECHNOLOGIES INTO THE THIRD MILLENNIUM»

Representative International Conference «Welding and Related Technologies into the Third Millennium», organized by the National Academy of Sciences of Ukraine, E.O. Paton Electric Welding Institute, Intergovernmental Scientific Council on Welding and International Association «Welding», took place on November 24–26 in Kiev at the E.O. Paton Electric Welding Institute. The representatives of academic and branch research institutes, scientific, design and engineering centers, industrial enterprises and educational institutes, heads and managers of business structures, etc. participated in it. In addition to the PWI employee, more than 160 representatives from far foreign countries (Austria, Australia, Bulgaria, Brazil, Germany, Spain, Canada, CPR, Macedonia, Poland, Romania, Slovakia, USA, France, Switzerland, Japan) and former Soviet republics (Belarus, Georgia, Russia, Kazakhstan) took part in the Conference.

Program of the first day of the Conference included acquaintance of its participants with poster session (211 posters) according to five sections:

- technologies, materials, equipment for welding, brazing, surfacing and cutting (90 posters);
- strength, non-destructive testing, service life of welded joints and structures (76 papers);
- mathematical methods of modeling of welding processes (11 papers);
- technologies, materials and equipment for coating deposition (17 papers);
- special electrometallurgy (17 papers).

The acquaintance with posters took place in a spacious hall of the PWI research library, and was accompanied by lively discussions.

In the second and third day of the Conference 31 plenary papers presented by famous scientists and spe-

cialist and dedicated to topical problems of welding and related technologies were heard.

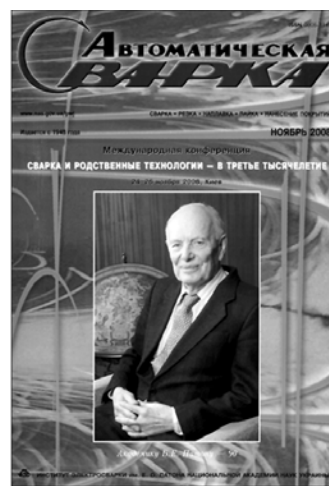
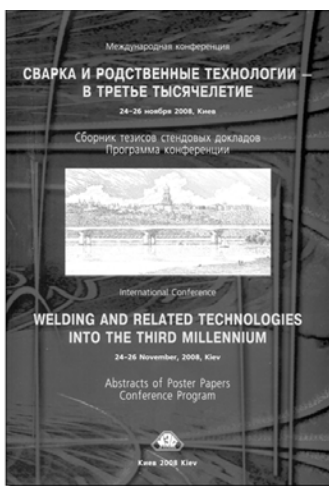
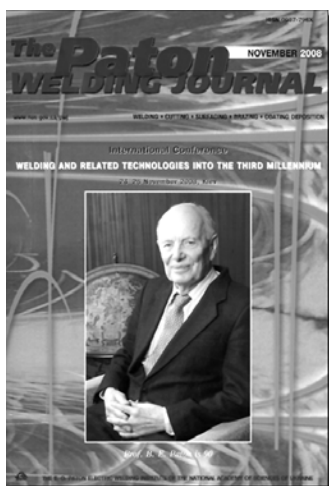
Among the speakers were Professors B.E. Paton, S.I. Kuchuk-Yatsenko, I.K. Pokhodnya, L.M. Lobanov, B.A. Movchan, K.A. Yushchenko, V.V. Panasyuk (Ukraine), I.V. Gorynin, N.P. Alyoshin, E.N. Kablov, Yu.V. Tsvetkov (Russia), and prominent scientists and specialists from Australia, Germany, Japan, China, Poland, Brazil, Romania, Bulgaria and Austria.

By the beginning of the Conference the plenary papers had been published in current issues of journals «Avtomaticeskaya Svarka» (Russian language) and «The Paton Welding Journal» (English language), and those of the poster session were published as a separate collection.

Besides, the meeting of the Bureau of Intergovernmental Scientific Council on Welding and Related Technologies took place on November 24. The representatives of the Republic of Belarus, Republic of Georgia, Republic of Kazakhstan, Russian Federation and Ukraine participated in the work. Mr. G. Hernandez (Spain), a chairman of the International Body of Accreditation at the International Institute of Welding and European Welding Federation, was invited to participate in the Bureau meeting. The key attention was given to the questions of standardization in the area of welding and organization of work on the quality control system in welding production. Also, some questions of organization were considered.

As a result of the comprehensive discussion on the considered problems the Bureau unanimously made the following decisions:

- 1) to consider formation of MTK-72 working group for preparation of unified catalog of terms and desig-





nations in welding production in Russian, Ukrainian and English languages as appropriate. The parties of agreement on scientific and technical cooperation are obliged to prepare proposals on staff from their countries;

2) to recommend, on the basis of the Authorized National Body of welding productions certification PATONCERT, to establish a methodical center for development of documentation on welding productions certifications in accordance with requirements of ISO 3834 standard series, by including into it representatives of the Republic of Belarus, Russian Federation, Ukraine and other countries-members of the agreement on technical and scientific cooperation;

3) to recommend to the parties of the agreement on scientific and technical cooperation to establish national centers for certification of welding productions, acting on behalf of the Authorized National Body of certification PATONCERT, according to companies certification system EWF ISO 3834.

Members of the Bureau of Intergovernmental Scientific Council on Welding and Related Technologies showed mutual interest in development of all-round relations of scientists and specialists of cooperating countries.

During the Conference, i.e. from 24 till 25 November, the meetings of the Council of International Association «Welding» (IAW) were held, at which the representatives of the E.O. Paton Electric Welding Institute, Mariupol STU (Ukraine); Volgograd STU (Russia); Welding Institute in Gliwice (Poland); Welding Institute «YuG» (Macedonia); KZU Holding Group (Bulgaria); Welders Society in Georgia, took part.

Managers of IAW reported on the work performed in a period of 2006–2008, marking out the main direction of the IAW activities, which were executed in a close cooperation with PWI: electric welding of soft live tissues and publishing activity.

The first area of the work was very successful in 2008. IAW organized commercial production of welding electrocoagulators at the «Schetmash» plant (Poltava region), which significantly improved their reliability. In August 2008, an American partner of IAW in a project on electric welding of soft live tissues — «Consortium Service Management Group» — obtained a permission of FDI for application of the technology for welding blood vessels in the USA, and a similar permission of CE Mark for the European Union countries.

Among the IAW tasks for 2009 under the soft live tissues welding, the IAW Council distinguished the following: further promotion of the technology in Ukraine, receiving certificates on the technology in Russia and Belarus.

Members of the IAW Council supported the IAW management efforts in of publishing activities, noting the importance of publishing proceedings of the conferences held by IAW.

The IAW Council unanimously extended the authorities of Prof. B. E. Paton as a Chairman of the IAW Council for a period of 2008–2011, and appointed A.T. Zelnichenko as a director of IAW.

*Prof. V.N. Lipodaev
Dr. A.T. Zelnichenko, PWI*

MEASURING SYSTEM FOR DETERMINATION OF RESIDUAL STRESSES IN ELEMENTS OF STRUCTURES USING THE ESPI METHOD



At the E.O. Paton Electric Welding Institute a compact measuring system and technology for determination of residual stresses, occurring in welded, brazed, cast and other metallic structures, have been developed. The developed system and technology can be also used for determination of stresses, caused in structures by applying the loads.

Residual stresses are determined on the basis of data about the value of in-plane displacements, measured by the method of electron speckle-interferometry in the vicinity of a blind hole. The in-plane displacements are the result of an elastic unloading of residual stresses after drilling of a blind hole.

The accuracy of determination of residual stresses is 10 % of value of yield strength of the material examined.

The measuring system consists of speckle-interferometer 1, CCD-camera 2, light guide 3, laser 4, computer with a board of pattern interference fringes figuring 5.

Proposals for co-operation. Measurement of residual stresses in elements of metallic structures, parts and sub-assemblies of machines. Manufacture of the measuring system and its delivery to the Customer, training of personnel.

Contacts: Prof. Lobanov L.M.
Tel.: (38044) 289 95 78

INTERNATIONAL FORUM ON NANOTECHNOLOGIES

The International Forum on Nanotechnologies «Rusnanotech», organized by state corporation «Russian Corporation of Nanotechnologies», took place in Central exhibition complex «Expocenter», Moscow, on December 3–5, 2008. This is the largest Russian annual exhibition in the area of nanotechnologies and nanomaterials.

The Forum plenary meeting was opened by S.B. Ivanov, Vice-Chairman of the Government of Russian Federation, Chairman of the Organizing Committee of the Forum on its preparation and holding, who read out a greeting of D.A. Medvedev, the President of Russian Federation, and addressed to those present with an opening speech. At the plenary meeting the presentations were made by the Minister of the Economic Development of Russian Federation E.S. Nabiullina, Director of the Russian Research Center «Kurchatov Institute» M.V. Kovalchuk («Nanotechnologies — the basis of new science-intensive economy of post-industrial society»), Paras Prasad, Executive Director of the Institute of Lasers, Photonics and Biophotonics (USA) («Nanotechnologies and Technical Challenges of the 21st century»), and Zh.I. Alfeyorov, Vice-President of RAS and laureate of the Nobel Prize («Semiconductor nanostructures — the basis of development of modern electronics and high-performance power engineering»). The speech by A.B. Chubajns, General Director of SC «Rosnanotech», completed the ceremonial part of the plenary meeting. Discussion «Business and Nanotechnologies» with participation of A.A. Mordashov (OJSC «Severstal»), M. D. Prokhorov (ONEK-SIM group), Uve Kruger (Oerlikon), Jong Min Kim (Samsung Electronics), Ouen Kemp (HP), V.V. Avdeev (Unikhimtek) and V.A. Bykov (NT-MDT) continued the meeting program.

9024 representatives of the world nanoindustry, entrepreneurs, statesmen and scientists took part in events of the Forum, among which there were 8354 participants from cities of Russian Federation and 670 participants from 32 foreign countries (Austria, Australia, Azerbaijan, Armenia, Belarus, Bulgaria, Belgium, Great Britain, Hungary, Germany, Denmark, Israel, Iran, Italy, Kazakhstan, Canada, China, Latvia, Lithuania, Malta, the Netherlands, Poland, Singapore, USA, Ukraine, Finland, France, Croatia, Czechia, Switzerland, Sweden, South Korea, Japan), including 4048 participants of a congress part of the Forum, 4212 visitors of exhibition and 559 persons working at booths. 205 representatives from the mass media described the Forum work. 236 persons took part in the programs of presentations and discussions

of a practical part of the Forum as negotiators, coordinators and speakers, from which 131 were from Russia and 105 were international representatives. 12 discussions were carried out, in which 127 representatives of Russian and international business took part. 109 presentations of products, technologies and companies — world leaders of the nanoindustry were made in 12 programs.

Scientific and technological sessions covered 18 main trends of development of nanotechnologies and nanomaterials: nanoelectronics, nanophotonics, nanodiagnosics, structural nanomaterials and high-purity materials, functional nanomaterials for power engineering, structural nanomaterials and nanomaterials with special properties, functional nanomaterials (catalysts, sorbents, membranes), chemistry and chemical technology of nanomaterials, nanomaterials for electronics, magnetic systems and optics, nanoelectromechanical systems, nanotechnology in power engineering, nanomechanics and nanoplasma, nanobiotechnology, biological molecular machines, nanotechnologies in medicine, nanotechnologies in oncology, mathematical modeling of nanotechnologies, training in the nanotechnologies area.

311 organizations from RF, Austria, Great Britain, Germany, Iran, Latvia, Lithuania, the Netherlands, USA, Finland, France, Sweden and Japan participated in the exhibition. The Forum demonstrated an increasing research and development potential of Russia in the area of nanotechnology, confirmed an inestimable role of knowledge exchange between foreign and Russian nanotechnologists for development of the nanoindustry in Russia, and provided the possibility to the Russian business to be directly acquainted with leading international and domestic developments in the area of nanotechnology and their authors. SC «Rosnanotech» instituted the International Prize in the area of nanotechnology, which was announced in the framework of Forum. The Prize for commercial application of scientific developments in the area of nanotechnologies will be awarded every year and presented to authors of specific scientific developments (not more than three persons). The total number of laureates in one year should not exceed three persons. Honorable diploma, Prize and Prize decoration will be presented to a head or authorized representative of a company that realized practical implementation of a given development. The value of the Prize in 2009 will make 3 mln roubles.

Prof. G.K. Kharchenko, PWI

RECONDITIONING ARC HARD-FACING OF WORN OUT TRAM RAILS

Technology and flux-cored wires of the austenitic (PP-AN202) and ferritic (PP-AN203) grades were developed for reconditioning hard-facing of tram rails made from steels M-75 and M-76 containing up to 0.82 % carbon. The technology requires no preheating or dismantling of rails from the track.

Hard-facing is performed by depositing horizontal beads. The quantity of the beads (from 5 to 15) depends upon the extent of wear. The first beads are deposited with self-shielding flux-cored ferritic wire PP-AN203, and the subsequent beads — with flux-cored wire PP-AN202 by the submerged arc method using flux AN-26P. This provides good bead formation, excellent detachability of the slag crust and absence of cracks and pores.

Deposited metal of all the layers (except for the first one) has tough austenitic structure with hardness *HRC* 22–25. Cold working increases its hardness to *HRC* 50–52, thus resulting in a substantial increase in wear resistance of the rails treated.

To realise this technology, the Research Centre DUGA-2 of the E.O. Paton Electric Welding Institute designed and manufactured hard-facing device UD-654. It has the form of a self-propelled carriage moving over the rails to be treated at a working and travel speed. Actuating mechanisms, control panel, as well as a reserve amount of wire and flux are located on the carriage. The welding circuit is powered from diesel generator. Not to prevent tram traffic, hard-facing should be performed during the night time in dry weather at a temperature not below +10 °C. The costs of reconditioning hard-facing are approximately 3 times lower than those of replacement of worn out rails by the new ones.

Application. Hard-facing of worn out rails without dismantling them from the track.

Proposals for co-operation. Application of the technology and equipment for hard-facing of tram rails at a customer's.

ARC HARD-FACING OF DRILL PIPE JOINTS

Available is the technology for hard-facing of joints in drill pipes with a nominal diameter of 104–177 mm. The technology provides for repairs of the joints in two stages. First hard-facing is performed with self-shielding flux-cored wire PP-AN198 to restore the nominal diameter of the pipes. Metal deposited with this wire has hardness *HB* 220–310 and mechanical properties at a level of those of base metal of the joints, i.e. steel 40KhMFA, according to GOST 4543–71. Then three wear-resistant belts having hardness *HRC* 42–52 are deposited over the nominal diameter using self-shielding flux-cored wire PP-AN199.

Machine U653 additionally equipped with carrying rollers and powered from the VDU-506 source is used for hard-facing. Other machines having similar parameters and operational capabilities can also be employed.

Application. Hard-facing of joints in drill pipes for oil and gas industry.

Proposals for co-operation. Application of the hard-facing technology at a customer's. Supply of flux-cored wire on a contract base.

ARC HARD-FACING OF HYDRAULIC PRESS RAMS

Available is the technology for high-productivity arc hard-facing using two flux-cored wires, allowing restoration of expensive hydraulic press rams and extension of their service life at a minimal cost (the cost of hard-facing is not in excess of 30 % of the cost of a new part).

Flux-cored wire PP-Np-12Kh14N3 was developed for hard-facing of such parts. The special feeding mechanism (nozzle) used with mass-produced surfacing machines was designed and manufactured for simultaneous feed of two flux-cored wires.

As proved by industrial tests, the hydraulic press rams with a deposited 12Kh14N3 layer has service life 3 times as long as that of the mass-produced rams, either non-deposited or deposited with solid wire of the Sv-20Kh13 type.

The E.O. Paton Electric Welding Institute can supply flux-cored wires and flux, as well as transfer «know-how» for the technology for two-electrode hard-facing of hydraulic press rams using two flux-cored wires.

Application. Repair and hardening of high-power hydraulic press rams at metallurgical and machine building enterprises.

Proposals for co-operation. Application of the technology and equipment for hard-facing of rams at a customer's.

ARC CLADDING OF ROLLERS OF SLAB CONTINUOUS CASTING MACHINES

Cladding consumables, procedure and technology were developed for treatment of rollers of slab continuous casting machines. Cladding is applied to restore geometric sizes of the rollers and extend their service life. An ingenious design of a working layer of the rollers was suggested, and the procedure and technology were developed for its deposition. The new procedure and technology allow a substantial reduction of residual stresses in the working layer of the rollers and, thus, increase in thermal stability of the deposited metal.

Flux-cored wires PP-Np-15Kh13 (mostly for rollers of less loaded horizontal regions) and PP-Np-12Kh13N2MFA (mostly for rollers of more loaded radius and curvilinear regions), as well as flux AN-26P or AN-26PU2, are employed as cladding consumables.

As proved by industrial tests, rollers with a deposited layer of a new design have life 1.5–2 times as long as that of new rollers made from steel 25Kh1M1F.

Application. Cladding of rollers of slab continuous casting machines at metallurgical works.

Proposals for co-operation. Application of the cladding technology at a customer's. Supply of flux-cored wire on a contract base.

ARC CLADDING OF HOT STEEL ROLLS

Technology and consumables were developed for arc cladding of hot steel rolls for different types of rolling mills. Arc cladding allows multiple and high-productivity deposition of a layer of high-alloy tool steel, free from cracks, pores and other defects, on rolls made from medium- and high-carbon low-alloy steels (up to 0.9 % C). The equipment developed (different types of roll cladding machine tools) enables deposition of a layer of required thickness in one or several passes with minimal allowance for machining on the surface of any configuration. This is very important for deposition of wear-resistant high-alloy steel. Cladding is performed with preheating, the temperature of which depends upon the roll material and weight. After cladding, a roll is slowly cooled in a thermostat or furnace.

The wide range of flux-cored wires developed by the E.O. Paton Electric Welding Institute particularly for deposition of rolls offers an optimal choice of compositions of deposited metal for each case on the basis of specific operational conditions of the rolls, character and intensity of their wear, workability of the deposited metal, price, etc.

Fluxes AN-20, AN-26, AN-60, AN-348, etc. are applied for cladding of the rolls. Strength of the treated rolls is 1.5–3 times as high as that of the non-treated ones, and it depends upon the type

of a rolling mill, stand, metal being rolled and other factors. Normally, the repeated claddings are 4–5, but can be larger in number. This provides a many times extension in service life of the rolls and reduction in their wear. In addition, cladding allows extension of intervals between regrindings and operation with maximal roll diameters, thus increasing productivity of the mills.

Electrode materials for cladding of rolls

Wire grade	Diameter, mm	Properties of deposited metal			Types of rolls
		Hardness <i>HRC</i>	Thermal stability*	Wear resistance*	
PP-Np-25Kh5FMS	3.6–6.0	42–46	3.0	2.5	Blooming-slabbing mill
PP-Np-35V9Kh3SF	3.6–6.0	46–52	1.5	3.0	Section rolling mill
PP-AN132	3.6–6.0	48–52	2.5	2.5	Plate and light-section rolling mill
PP-AN147	3.6–4.0	44–48	2.5	1.5	Skelp and plate rolling mill

*With respect to steel 30KhGSA the strength of which is taken as 1.

Application. Cladding of hot steel rolls.

Proposals for co-operation. Supply of flux-cored wire on a contract base, application of the cladding technology.

ARC CLADDING OF HYDRAULIC CYLINDER RODS

Flux-cored wire PP-Np-30Kh20MN and technology were developed for electric arc cladding of rods of hydraulic cylinders operating in various machines and mechanisms, such as supports of shaft heading machines, rock haulers, etc.

Hydraulic cylinder rods are made from steels of the type of 30Kh, and to protect their working surface from corrosion they are subjected to chromium plating. According to the offered technology, cladding of worn out rods can be performed after preliminary machining of their working surface or directly over the galvanic chromium coating.

The rods are deposited in one layer by the submerged arc method using flux AN-26P. The developed flux-cored wire provides deposited metal of the Fe–Cr–Ni–Mo alloying system, characterised by high corrosion resistance in the first deposited layer. Grinding of the treated surface ensures the required cleanness, and high corrosion resistance of the deposited layer allows avoiding of the chromium plating operation. Available is the experience in cladding rods with a diameter of 70 mm or more.

Application. Cladding of hydraulic cylinder rods.

Proposals for co-operation. Supply of flux-cored wire on a contract base, application of the cladding technology.

ELECTROSLAG CLADDING OF WORN OUT FORGING DIES

Offered is the method for repair of small- and medium-size dies by electrosag cladding.

Worn out die is installed into a mould, and the slag pool is induced on its surface using graphite electrodes. The die impressions are melted down to a depth required to remove fire cracks and other defects under the effect of heat released from the slag pool. Then a die steel chip is fed into the slag pool. While passing through the slag, the chip is heated, melted and fills up the pool formed in melting of the working surface of the die. The ESC process results in refining of the deposited metal. Thus, it is characterised by a lower content of sulphur (0.008–0.012 %) and non-metallic inclusions, compared with die steels made by open melting methods. If necessary, the deposited metal can be additionally alloyed and modified.

Field tests of the repaired dies showed that their strength was 1.5–4 times as high as that of dies made from conventional forged steel. Metal of the deposited layer is resistant to brittle fracture, and the fire crack network penetrates to a smaller depth, compared with forged dies, thus allowing the dies to be repaired by 3–4 fold gouging operations. Cost of the repaired dies is 2–3 times lower than that of the forges ones.

Installed power of the equipment for ESC of dies is 500 kW, water consumption is 30 m³/h, surface area of the region to be clad is 30 m², and maximal size of the die surface to be treated is 500 × 500 mm. Productivity of the ESC workshop is 1500 dies a year.

Application. Cladding of dies and die fixtures at enterprises of different industrial sectors.

Proposals for co-operation. Application of the cladding equipment and technology.

ANTICORROSION ELECTROSLAG STRIP CLADDING

Consumables and technologies were developed for high-productivity anticorrosion electros slag cladding using one or two electrode strips to treat casing parts of nuclear power generation equipment, oil hydrogen cracking vessels, hydraulic turbine blades, bimetal plates, etc.

Productivity of the cladding process using two electrode strips is 30–50 kg/h, and the content of base metal in the deposited one is 5–8 %, which provides the desirable operational properties even in the first deposited layer. These are the best indicators for the free-formation cladding processes.

The developed technology and consumables were field tested in cladding bimetal plates and parts of nuclear power generation equipment.

Application. High-productivity anticorrosion cladding of casing parts of nuclear power generation equipment, oil hydraulic cracking vessels, hydraulic turbine blades, bimetal plates, etc.

Proposals for co-operation. Application of the cladding technology at a customer's.

FLUX-CORED WIRES FOR SURFACING OF PARTS OPERATING UNDER DIFFERENT TYPES OF WEAR

Sanitary-hygienic evaluation was carried out, and compositions of earlier developed and new flux-cored wires intended for surfacing of parts operating under different types of wear were checked in view of increased requirements for environmental safety of surfacing operations.

Seventeen grades of surfacing flux-cored wires are commercially manufactured in compliance with TUU 05416923.024–97 and TUU 28.7.05416923.066–2002:

Wire grade	Shielding atmosphere, flux	Type of deposited metal ¹	Hardness HRC	Typical cladding objects
PP-AN105	Self-shielding	High-manganese austenitic steel	$\frac{20-25^2}{45-50}$	Railroad frogs, castings of steel G13
PP-AN130	Same	Heat-resistant tool steel	43–54	Steel rolls, hot forming dies, knives, etc.
PP-AN192	»	High-carbon chromium steel	54–63	Operating elements of road-building and agricultural machinery, etc.
PP-AN193	»	Tool maraging steel	$\frac{23-25^3}{50-55}$	Steel rolls, hot forming dies, knives, etc.
PP-AN196	»	Tool precipitation-hardening steel	$\frac{40-43^3}{50-54}$	Steel rolls, hot forming dies, etc.
PP-AN197	»	High-chromium cast iron	62–65	Operating elements of road-building and agricultural machinery
PP-AN198	»	Low-alloy steel (C ≤ 0.4 %)	20–30	Axles, shafts, crane wheels and other similar parts

Wire grade	Shielding atmosphere, flux	Type of deposited metal ¹	Hardness HRC	Typical cladding objects
PP-AN199	»	Low-carbon chromium steel	45–52	Bed rollers, brake pulleys, etc.
PP-AN203	»	Low-alloy steel (C ≤ 0.4 %)	18–25	Tram rails, sub-layers in cladding high-carbon steels
PP-AN132	AN-26	Heat-resistant tool steel	45–55	Steel rolls, hot forming dies, knives, etc.
PP-AN194	AN-348	Low-alloy steel (C ≤ 0.4 %)	20–30	Axles, shafts, crane wheels and other similar parts
PP-AN195	AN-26P	Tool precipitation-hardening steel	$\frac{23-25^3}{50-55}$	Steel rolls, hot forming dies, knives, etc.
PP-AN201	AN-26	High-chromium cast iron	45–52	Operating elements of road-building and agricultural machinery
PP-AN202	AN-26	High-manganese austenitic steel	$\frac{20-25^2}{40-55}$	Tram rails, sub-layers in cladding high-carbon steels
PP-Np-25Kh5MSGF	AN-20 AN-26	Heat-resistant tool steel	46–52	Steel rolls, hot forming dies, knives, etc.
PP-Np-30Kh2M2SGF	AN-20 AN-26	Heat-resistant tool steel	43–54	Same
PP-Np-35V9Kh3GSF	AN-20 AN-26	Heat-resistant tool steel	44–50	Same

¹Type of deposited metal according to the IIW classification.
²Numerator --- after cladding, denominator --- after cold working.
³Numerator --- after cladding, denominator --- after tempering.

Application. Repair and hardening of parts by the electric arc cladding methods for different industrial sectors.

Proposals for co-operation. Supply of flux-cored wires on a contract base.

Publications of the last years

- Kalensky, V.K., Chernyak, Ya.P., Ryabtsev, I.A. *Flux-cored wire for welding and surfacing of steel products*. Pat. 39646 C Ukraine. Publ. 15.09.03.
- Kondratiev, I.A., Ryabtsev, I.A., Chernyak, Ya.P. (2004) Study of properties of deposited metal of the maraging steel type. *The Paton Welding J.*, **10**, 12–14.
- Kuskov, Yu.M. (2004) Application of high-alloy high-speed steels for rolling mill rolls. *Stal*, **5**, 43–48.
- Kuskov, Yu.M. (2003) Special features of electroslag cladding with granular additives in current-conducting moulds. *Svarochn. Proizvodstvo*, **9**, 42–47.
- Kuskov, Yu.M., Kuzmenko, O.G., Lentuygov, I.P. (2004) Electroslag processing of metal wastes and application of the resulting semi-finished products in surfacing production. *Ibid.*, **10**, 58–61.
- Kuskov, Yu.M., Sarychev, I.S. (2004) Restoration electroslag cladding of cast iron rolls of mill 2000. *Ibid.*, **2**, 39–43.
- Kuzmenko, O.G. (2004) Behaviour of particles of a noncompact filler at air-slag interface in electroslag hardfacing. *The Paton Welding J.*, **10**, 8–11.
- Levchenko, O.G., Metlitsky, V.A., Ryabtsev, I.A. et al. (2003) Sanitary-hygienic evaluation of flux-cored wires for electric arc surfacing. *Ibid.*, **8**, 41–45.
- Osin, V.V., Ryabtsev, I.A. (2004) Effect of sulphur on properties of iron-base alloys and prospects of its application in surfacing materials. *Ibid.*, **10**, 18–21.
- Pereplyotchikov, E.F. (2004) Plasma-powder cladding of wear- and corrosion-resistant alloys in valve manufacturing. *Ibid.*, **10**, 31–37.
- Pereplyotchikov, E.F., Ryabtsev, I.A., Gordan, G.M. (2003) High-vanadium alloys for plasma-powder cladding of tools. *Ibid.*, **3**, 14–17.
- Pereplyotchikov, E.F., Ryabtsev, I.A., Vasiliev, V.G. et al. (2003) Structure and properties of high-alloy high-vanadium iron-base alloys for surfacing. *MiTOM*, **5**, 36–40.
- Pokhmursky, V.I., Student, M.M., Dovgunyk, V.M. et al. (2003) Structure and tribotechnical characteristics of coatings produced by electric arc metallizing using flux-cored wires. *The Paton Welding J.*, **8**, 12–16.
- Ryabtsev, I.A. (2005) Electrode materials for mechanized arc surfacing. *Ibid.*, **8**, 50–53.
- Ryabtsev, I.A. (2005) High-efficiency wide-band surfacing using electrode wires and strips (Review). *Ibid.*, **6**, 31–35.
- Ryabtsev, I.A. (2004) *Surfacing of machine parts and mechanisms*. Kiev: Ekotekhnologiya.
- Ryabtsev, I.A., Kondratiev, I.A., Kuskov, Yu.M. et al. (2003) Renovation surfacing technologies in metallurgy and machine-building. *Metallurgiya Mashinostroeniya*, **1**, 11–15.
- Ryabtsev, I.A., Kuskov, Yu.M., Kuzmenko, O.G. et al. (2003) Recycling of metal wastes using electroslag technologies. *Vestnik Mashinostroeniya*, **11**, 76–80.
- Ryabtsev, I.A., Kuskov, Yu.M., Ryabtsev, I.I. et al. (2004) Secondary hardening of deposited metal of the type of dispersion-hardening steel of Fe–C–Ni–Cr–Si–Al–Cu alloying system. *The Paton Welding J.*, **10**, 4–7.
- Ryabtsev, I.I., Kuskov, Yu.M. (2003) Prospects for utilisation of phosphorus in surfacing iron-base consumables. *Metallurgiya Mashinostroeniya*, **1**, 12–16.
- Ryabtsev, I.I., Kuskov, Yu.M., Grabin, V.F. et al. (2003) Tribotechnical characteristics of deposited metal of the Fe–Cr–Si–Mn–P alloying system. *Ibid.*, **6**, 20–24.

Dr. Ryabtsev I.A.

E-mail: ryabtsev@paton.kiev.ua

SUBSCRIPTION FOR «THE PATON WELDING JOURNAL»

If You are interested in making subscription directly via Editorial Board, fill, please, the coupon and send application by fax or e-mail.

The cost of annual subscription via Editorial Board is \$324.

Telephones and faxes of Editorial Board of «The Paton Welding Journal»:

Tel.: (38044) 287 6302, 271 2403, 529 2623

Fax: (38044) 528 3484, 528 0486, 529 2623.

«The Paton Welding Journal» can be also subscribed worldwide from catalogues of subscription agency EBSCO.

SUBSCRIPTION COUPON			
Address for journal delivery			
Term of subscription since	200	till	200
Name, initials	_____		
Affiliation	_____		
Position	_____		
Tel., Fax, E-mail	_____		



ADVERTISEMENT IN «THE PATON WELDING JOURNAL» (DISTRIBUTED ALL OVER THE WORLD)

«AVTOMATICHESKAYA SVARKA»

**RUSSIAN VERSION OF «THE PATON WELDING JOURNAL»
(DISTRIBUTED IN UKRAINE, RUSSIA AND OTHER CIS COUNTRIES)**

External cover, fully-colored:

- First page of cover (190×190 mm) – \$700
- Second page of cover (200×290 mm) – \$550
- Third page of cover (200×290 mm) – \$500
- Fourth page of cover (200×290 mm) – \$600

Internal cover, fully-colored:

- First page of cover (200×290 mm) – \$400
- Second page of cover (200×290 mm) – \$400
- Third page of cover (200×290 mm) – \$400
- Fourth page of cover (200×290 mm) – \$400

Internal insert:

- Fully-colored (200×290 mm) – \$340
- Fully-colored (double page A3) (400×290 mm) – \$570
- Fully-colored (200×145 mm) – \$170

- Article in the form of advertising is 50 % of the cost of advertising area
- When the sum of advertising contracts exceeds \$1000, a flexible system of discounts is envisaged

Technical requirement for the advertising materials:

- Size of journal after cutting is 200×290 mm
- In advertising layouts, the texts, logotypes and other elements should be located 5 mm from the module edge to prevent the loss of a part of information

All files in format IBM PC:

- Corell Draw, version up to 10.0
- Adobe Photoshop, version up to 7.0
- Quark, version up to 5.0
- Representations in format TIFF, color model CMYK, resolution 300 dpi
- Files should be added with a printed copy (makeups in WORD for are not accepted)